Supporting information

Sungeidines from a non-canonical enediyne biosynthetic pathway

Zhen Jie Low[1‡], Guang-Lei Ma[1‡], Hoa Thi Tran[1‡], Yike Zou[3‡], Juan Xiong[1,2], Limei Pang[1], Selbi Nuryyeva[3], Hong Ye[1], Jin-Feng Hu[2], K. N. Houk[3], Zhao-Xun Liang[1]*

[1]School of Biological Sciences, Nanyang Technological University, Singapore; [2]School of Pharmacy, Fudan University; China; [3]Department of Chemistry and Biochemistry, University of California at Los Angeles, USA.

Author contribution: ZJL and LP isolated the *Micromonospora* sp. MD118 strain and sequenced the genome. ZJL and HT optimized fermentation conditions, developed the CRISPR/Cas9 tool and performed gene knockout/overexpression. GLM, ZJL, JX isolated the compounds and characterized the structures. GLM and HT performed isotope labelling and ^{13}C NMR analysis. HY and JFH assisted with the structure elucidation. YZ, SN and KNH performed computational modeling and DFT calculations. GLM, ZJL, HT and ZXL wrote the manuscript with the assistance from other coauthors.

Content

General 4
Isolation of *Micromonospora sp.* MD118 from mangrove sediment....4
Complete genome sequencing....4
Gene deletion using the CRISPR/Cas9 method 4
Overexpression of transcriptional regulators 5
Cloning and overexpression of the sulfotransferase SgdX2 5
In vitro assay of enzymatic activity of the sulfotransferase SgdX2....6
Culture conditions 6
Analytic HPLC for metabolite profiling 6
Isolation of 1−9 from *Micromonospora* sp. MD118AE and Δ*sgdX2* mutant. 7
Detailed structural elucidation of 1−9. 8
^{13}C-labelled acetate feeding experiments. 11
Sungeidine C (3) and anthramicin (9) feeding experiment....11
DFT calculation[8,9]....12
Table S1. List of genes in *sgd* BGC and their proposed functions. The genes that are not found *dyn* BGC are shaded in light blue; whereas the genes from the minimal enediyne PKS gene cassette are shaded in yellow. 13
Table S2. List of Primers used in this study. 14
Table S3. List of Plasmids used in this study 15
Table S4. ^{1}H and ^{13}C NMR data (DMSO-d_6, δ ppm) for sungeidines A−E (**1**–**5**)[a] 16
Table S5. ^{1}H and ^{13}C NMR data (DMSO-d_6, δ ppm) for sungeidines F−H (**6**–**8**), and anthramicin (**9**)[a] 17
Table S6. ^{13}C NMR (100 MHz) assignment of [1-^{13}C]- and [2-^{13}C]-acetate and $^{1}J_{CC}$ of [1,2-$^{13}C_2$]-acetate labelled sungeidine F (**6**) 18
Scheme S1. Structures of **1**−**10**....19
Scheme S2. TOCSY/COSY, and HMBC correlations of **1**–**9**....19
Scheme S3. Key NOESY correlations in the computer-generated 3D drawing of **1**–**8**. 20
Scheme S4. ^{13}C-labelled structures of **6** and **9**....20
Scheme S5. Incorporation patterns of ^{13}C-labelled Sungeidine, Dynemicin, and Esperamicin. 20
Figure S1-1. ^{1}H NMR spectrum (700 MHz, in DMSO-d_6) of sungeidine A (**1**)....21

Figure S1-2. ^{13}C NMR spectrum (175 MHz, in DMSO-d_6) of sungeidine A (**1**).....21
Figure S1-3. HSQC NMR spectrum (700 MHz, in DMSO-d_6) of sungeidine A (**1**).....22
Figure S1-4. TOCSY NMR spectrum (700 MHz, in DMSO-d_6) of sungeidine A (**1**).....22
Figure S1-5. ^{1}H-^{1}H COSY NMR spectrum (700 MHz, in DMSO-d_6) of sungeidine A (**1**).....23
Figure S1-6. HMBC NMR spectrum (700 MHz, in DMSO-d_6) of sungeidine A (**1**).....23
Figure S1-7. NOESY NMR spectrum (700 MHz, in DMSO-d_6) of sungeidine A (**1**).....24
Figure S1-8. HRESIMS spectrum of sungeidine A (**1**).....24
Figure S2-1: ^{1}H NMR spectrum (700 MHz, in DMSO-d_6) of sungeidine B (**2**).....25
Figure S2-2: ^{13}C NMR spectrum (175 MHz, in DMSO-d_6) of sungeidine B (**2**).....25
Figure S2-3: HSQC NMR spectrum (700 MHz, in DMSO-d_6) of sungeidine B (**2**).....26
Figure S2-4: ^{1}H-^{1}H COSY NMR spectrum (700 MHz, in DMSO-d_6) of sungeidine B (**2**).....26
Figure S2-5: HMBC NMR spectrum (700 MHz, in DMSO-d_6) of sungeidine B (**2**).....27
Figure S2-6: NOESY NMR spectrum (700 MHz, in DMSO-d_6) of sungeidine B (**2**).....27
Figure S3-1. ^{1}H NMR spectrum (400 MHz, in DMSO-d_6) of sungeidine C (**3**).....28
Figure S3-2. ^{13}C NMR spectrum (100 MHz, in DMSO-d_6) of sungeidine C (**3**).....28
Figure S3-3. HSQC NMR spectrum (400 MHz, in DMSO-d_6) of sungeidine C (**3**).....29
Figure S3-4. ^{1}H-^{1}H COSY NMR spectrum (400 MHz, in DMSO-d_6) of sungeidine C (**3**).....29
Figure S3-5. HMBC NMR spectrum (400 MHz, in DMSO-d_6) of sungeidine C (**3**).....30
Figure S3-6. NOESY NMR spectrum (400 MHz, in DMSO-d_6) of sungeidine C (**3**).....30
Figure S4-1: ^{1}H NMR spectrum (600 MHz, in DMSO-d_6) of sungeidine D (**4**).....31
Figure S4-2: ^{13}C NMR spectrum (150 MHz, in DMSO-d_6) of sungeidine D (**4**).....31
Figure S4-3: HSQC NMR spectrum (600 MHz, in DMSO-d_6) of sungeidine D (**4**).....32
Figure S4-4: ^{1}H-^{1}H COSY NMR spectrum (600 MHz, in DMSO-d_6) of sungeidine D (**4**).....32
Figure S4-5: HMBC NMR spectrum (600 MHz, in DMSO-d_6) of sungeidine D (**4**).....33
Figure S4-6: NOESY NMR spectrum (600 MHz, in DMSO-d_6) of sungeidine D (**4**).....33
Figure S5-1: ^{1}H NMR spectrum (600 MHz, in DMSO-d_6) of sungeidine E (**5**).....34
Figure S5-2: ^{13}C NMR spectrum (150 MHz, in DMSO-d_6) of sungeidine E (**5**).....34
Figure S5-3: HSQC NMR spectrum (600 MHz, in DMSO-d_6) of sungeidine E (**5**).....35
Figure S5-4: ^{1}H-^{1}H COSY NMR spectrum (600 MHz, in DMSO-d_6) of sungeidine E (**5**).....35
Figure S5-5: HMBC NMR spectrum (600 MHz, in DMSO-d_6) of sungeidine E (**5**).....36
Figure S5-6: NOESY NMR spectrum (600 MHz, in DMSO-d_6) of sungeidine E (**5**).....36
Figure S6-1. ^{1}H NMR spectrum (400 MHz, in DMSO-d_6) of sungeidine F (**6**).....37
Figure S6-2. ^{13}C NMR spectrum (100 MHz, in DMSO-d_6) of sungeidine F (**6**).....37
Figure S6-3. HSQC NMR spectrum (400 MHz, in DMSO-d_6) of sungeidine F (**6**).....38
Figure S6-4. ^{1}H-^{1}H COSY NMR spectrum (400 MHz, in DMSO-d_6) of sungeidine F (**6**).....38
Figure S6-5. HMBC NMR spectrum (400 MHz, in DMSO-d_6) of sungeidine F (**6**).....39
Figure S6-6. NOESY NMR spectrum (400 MHz, in DMSO-d_6) of sungeidine F (**6**).....39
Figure S6-7. ^{1}H NMR spectra (400 MHz, in DMSO-d_6) of sungeidine F (**6**) labelled from [1-^{13}C]- and [2-^{13}C]-sodium acetate.....40
Figure S6-8. ^{13}C NMR spectra (100 MHz, in DMSO-d_6) of sungeidine F (**6**) labelled from [1-^{13}C]- and [2-^{13}C]-sodium acetate.....40
Figure S6-9. ^{1}H NMR spectrum (400 MHz, in DMSO-d_6) of sungeidine F (**6**) labelled from [1,2-$^{13}C_2$]-sodium acetate.....41
Figure S6-10. ^{13}C NMR spectrum (100 MHz, in DMSO-d_6) of sungeidine F (**6**) labelled from [1,2-$^{13}C_2$]-sodium acetate.....41
Figure S7-1. ^{1}H NMR spectrum (600 MHz, in DMSO-d_6) of sungeidine G (**7**).....42
Figure S7-2. ^{13}C NMR spectrum (150 MHz, in DMSO-d_6) of sungeidine G (**7**).....42
Figure S7-3. HSQC NMR spectrum (600 MHz, in DMSO-d_6) of sungeidine G (**7**).....43
Figure S7-4. ^{1}H-^{1}H COSY NMR spectrum (600 MHz, in DMSO-d_6) of sungeidine G (**7**).....43

Figure S7-5. HMBC NMR spectrum (600 MHz, in DMSO-d_6) of sungeidine G (**7**) 44
Figure S7-6. NOESY NMR spectrum (600 MHz, in DMSO-d_6) of sungeidine G (**7**) 44
Figure S8-1: ^{1}H NMR spectrum (400 MHz, in DMSO-d_6) of sungeidine H (**8**) 45
Figure S8-2: ^{13}C NMR spectrum (100 MHz, in DMSO-d_6) of sungeidine H (**8**) 45
Figure S8-3: HSQC NMR spectrum (400 MHz, in DMSO-d_6) of sungeidine H (**8**) 46
Figure S8-4: ^{1}H-^{1}H COSY NMR spectrum (400 MHz, in DMSO-d_6) of sungeidine H (**8**) 46
Figure S8-5: HMBC NMR spectrum (400 MHz, in DMSO-d_6) of sungeidine H (**8**) 47
Figure S8-6: NOESY NMR spectrum (400 MHz, in DMSO-d_6) of sungeidine H (**8**) 47
Figure S9-1: ^{1}H NMR spectrum (400 MHz, in DMSO-d_6) of anthramicin (**9**) 48
Figure S9-2: ^{13}C NMR spectrum (100 MHz, in DMSO-d_6) of anthramicin (**9**) 48
Figure S9-3: HSQC NMR spectrum (400 MHz, in DMSO-d_6) of anthramicin (**9**) 49
Figure S9-4: ^{1}H-^{1}H COSY NMR spectrum (400 MHz, in DMSO-d_6) of anthramicin (**9**) 49
Figure S9-5: HMBC NMR spectrum (400 MHz, in DMSO-d_6) of anthramicin (**9**) 50
Figure S9-6: NOESY NMR spectrum (400 MHz, in DMSO-d_6) of anthramicin (**9**) 50
Figure S9-7. ^{13}C NMR spectrum (100 MHz, in DMSO-d_6) of anthramicin (**9**) labelled from [1-^{13}C]- and [2-^{13}C]-sodium acetate. 51
Figure S9-8. HRESIMS and MS/MS spectra of anthramicin (**9**). 51
Figure S10: UV-vis spectra of **1**−**9**. 52
Figure S11: HRESIMS of **2**−**8**, and **6a**. 52
Figure S12. Experimental ECD spectra of **1**−**9.** 53
Figure S13: DFT optimized low energy conformations of **1** and **9** 53
Figure S14. Experimental and calculated ECD spectra of **1** (at B3LYP/def2tzvp/SMD(MeOH) level) and **9** (at B3LYP/def2tzvp/SMD(water) level). 54
Figure S15: XYZ coordinates of the optimized structures of **1** and **9** 54
Figure S16: Feeding of compound **9** into the MD118A and Δ*sgdX2* culture did not result in the production of sungeidines. The experimental conditions are described in the methods section. 56
Figure S17: SDS-PAGE analysis the expression and purification of SgdX2 using *E. coli* Rosetta (DE3). The DNA Marker is Thermo Scientific PageRuler Plus Prestained Protein Ladder #26619. 56
References 57

General

UV-Vis spectra were acquired on a Denovix spectrophotometer, and ECD spectra were recorded on a Chirascan™ circular dichroism spectrometer. IR spectra were recorded using a Thermo FT-IR spectrophotometer. Optical rotation values were measured using a Jasco P-1030 polarimeter. NMR spectra were collected on Bruker Avance NEO 400 MHz at 300 K, or Avance II 600/700 MHz with a cryoprobe at 298 K. Chemical shifts are expressed in δ (ppm) and referenced to the residual solvent signals. HRESIMS was performed on a Thermo LTQ XL spectrometer. Semipreparative HPLC was performed on a Shimadzu liquid chromatography system equipped with an ODS column (ACE: C18-HL, 250 mm × 10 mm, 5 μm), or an Agilent 1200 series LC system with an ODS column (Cosmosil: cholester, 250 mm × 10 mm, 5 μm). Column chromatography (CC) was performed using silica gel (230−400 mesh, Merck, Darmstadt, Germany), and Sephadex LH-20 (GE Healthcare Bio-Sciences AB, Uppsala, Sweden). All reagents were purchased from Sigma-Aldrich unless otherwise specified.

Isolation of *Micromonospora sp.* MD118 from mangrove sediment

Micromonospora sp. MD118 was isolated from a mangrove sediment sample, collected from the Sungei Buloh Wetland Reserve, Singapore. The sediment sample was rinsed and filtered, after being air dried. The serial diluted filtrates were then spread onto the modified Gauze's medium 2 agar (15 g/L bacto agar, 5 g/L peptone, 10 g/L glucose, 3 g/L tryptone, and 1 L sterile brackish water from Sungei Buloh Wetland Reserve) that was supplemented with 50 μg/mL cycloheximide, 10 μg/mL nalixidic acid, 10 μg/mL novobiocin and 50 μg/mL nystatin. Isolation plates were incubated for up to three weeks at 28 ^{o}C. Pure bacterial isolates were obtained after a few rounds of streaking and the strain was subsequently maintained in mannitol soy agar at 30 ^{o}C.

Complete genome sequencing

High quality genomic DNA was extracted using a modified genomic DNA extraction protocol. The complete genome sequence of *Micromonospora* sp. MD118 was obtained using Single Molecule Real Time (SMRT) sequencing technology (Pacific Biosciences, California, USA). Genome sequencing was done on a PacBio RS II platform. 1 SMRT cell was used and the sequencing run was performed 3 times. A read quality value of 84 was achieved with 86,939 zero-mode-waveguides (ZMWs), with average coverage value of 114.0. Mean polymerase read length was 15,610 bp with mean reads of inserts (ROI) read length value of 13,164 bp. A single contig of length 8,625,764 bases was obtained after assembly using CLC Genomics Workbench (CLC bio, Denmark). The DNA sequence for the sungeidine biosynthetic gene cluster (*sgd* BGC) has been deposited into NCBI GenBank (Accession number: MN296090). The genes within *sgd* BGC and their predicted functions are tabulated (Table S1).

Gene deletion using the CRISPR/Cas9 method

We previously successfully employed the pCRISPR-Cas9 vector for gene knockout and gene fusion in *Streptomyces*.[1] Although the pCRISPR-Cas9 vector can be used for gene knockout in *Micromonospora* strains, we found that plasmid-curing in *Micromonospora* sp. MD118A is very inefficient, considering that the strain retained the CRISPR plasmids after exposure to high temperature (37-39 ^{o}C) and several rounds of sub-culturing. To facilitate the identification of plasmid-free colonies, we introduced a counter-selective marker *cod*A*(sm)* into the pCRISPR-Cas9 vector to generate the vector pHZ-cod9 with the detailed plasmid cloning described

elsewhere (Low et al, manuscript submitted). The *cod*A*(sm)* gene encodes a cytosine deaminase mutant (D314A) that converts 5FC to 5FU, a toxic compound that can cause cell death.[2-5]

Counter-selection efficiency of the newly constructed pHZ-cod9 was tested by subjecting *Micromonospora* sp. MD118 containing pHZ-cod9 with serial concentrations of 5-FC. Low concentration of 5-FC (< 50 μg/mL) resulted in higher percentage of false positives (cells that contain plasmids). Effective working concentration of 5-FC was determined to be 200 μg/mL as lower concentration of 5-FC (<100 μg/mL) corresponded in higher percentage of false positives (plasmid bearing cells). Incubation of the plates with exconjugants that was exposed to 37 ^{o}C for 2-3 days prior to exposure 200 μg/mL of 5-FC yielded more colonies than a similar procedure performed without the additional 37 ^{o}C incubation step, suggesting that curing of pSG5 replicon bearing plasmid in *Micronomospora* sp. MD118 was retarded rather than completely non-existent.

The exconjugants were picked onto fresh MS agar plates containing 50 μg/mL apramycin and 25 μg/mL nalidixic acid. After incubating for 4 days at 30 ^{o}C, exconjugants were re-streaked onto MS agar that contain 50 μg/mL apramycin and 10 μg/mL thiostrepton for induction of Cas9 expression before incubation in GYM broth at 37 ^{o}C for 2−3 days to cure off plasmids. The true exconjugants were determined by PCR and spread onto agar plates containing 200 μg/mL 5-FC. Colonies that appeared after 4−5 days of incubation at 30 ^{o}C were spotted onto two types of agar plates with/without apramycin to identify true plasmid-free mutants.

We first tested the pHZ-cod9 plasmid by targeting the BGC that produces sioxanthin-related carotenoids in MD118. The phytoene synthase gene (*mmd2050*) was deleted by introducing a frameshift deletion of 460 bp to generate *Micromonospora* sp. MD118 Δ*mmd2050* knockout mutant. Diagnostic PCR was performed to establish deletion of 460 bp in *mmd2050*. This mutant strain was termed *Micromonospora* sp. MD118A and was used for subsequent genetic engineering experiments and compound production.

To demonstrate that sungeidines are produced by the *sgd* BGC, we targeted *sgdU15*, a conserved gene of the minimal enediyne PKS cassette for disruption. The *sgdU15* gene was disrupted through an in-frame deletion of 570 bp, generating the Δ*sgdU15* knockout mutant. Using the same method, we generated Δ*sgdX1*, Δ*sgdX2* single knockout mutants were generated by disrupting their corresponding genes through in-frame deletion of 222 bp and 462 bp, respectively, while Δ*sgdX3* mutant was constructed by deletion a 514 bp frame shift. All the primers and plasmids used in this study were summarized in Tables S2 and S3.

Overexpression of transcriptional regulators

A kasOp*-riboJ-RBS (from ΦC31 phage Tail Protein gene) cassette was inserted into a promoter-less integrative and conjugative plasmid, pSET152, to create pSK152. To construct *Micromonospora* sp. MD118AE, a *sgdR2* and *sgdR7* double gene overexpression mutant, plasmid pSK152-*sgdR2R7* was created. Using the genomic DNA of MD118 as template, *sgdR2* and *sgdR7* were PCR-amplified and the two PCR products were assembled into a *Not*I digested pSK152 to yield pSK152-*sgdR2R7*. The plasmid also contains a ribosomal binding site (RBS) sequence upstream of *sgdR7* to ensure its translation. The plasmid that contains the correct insert was validated by DNA sequencing and subsequently conjugated into *Micromonospora* sp. MD118A to create MD118AE.

Cloning and overexpression of the sulfotransferase SgdX2

The sgdX2 gene amplified from the genomic DNA of *Micromonospora* sp. MD118A was subcloned into the pET28b(+) vector and expressed using *E. coli* Rosetta. To produce the *N*-

terminal 6×His tagged SgdX2, 1% overnight culture of transformed *E. coli* Rosetta was fermented in 2.3 L LB medium using three 2L flasks. The fermentation medium was then supplemented with 50 μg/ml kanamycin and incubated at 37 °C, 200 rpm. 0.2 mM isopropyl 1-thio-β-D-galactopyranoside (IPTG) was added to induce protein expression when the OD_{600} reached 0.8. The *E. coli* cells was harvested after 18 hours (16 °C, 200 rpm). The cells were lysed in Tris buffer pH 7.4 (50 mM Tris, 50 mM NaCl, 5% glycerol, 0.5% Triton X100, 10 mM β-mercaptoethanol) by ultrasonication. After centrifugation, the supernatant was collected, followed by incubation with 2 ml Ni-NTA agarose (nickel nitrilotriacetic acid resin, Qiagen). The recombinant protein was then eluted using Tris buffer (50 mM Tris, 50 mM NaCl, 5% glycerol, 10 mM β-mercaptoethanol, 50-300 mM imidazole) and confirmed by SDS-PAGE gel visualization. The fractions containing the recombinant protein were concentrated using Vivaspin Turbo 5MWCO (Satorius) and desalted using PD-10 Desalting columns (GE Healthcare). A HEPES elution buffer (20 mM Hepes buffer, pH 7.5, 0.2 M NaCl, 5% (v/v) glycerol, 20 mM imidazole, pH 8.0, 5 mM DTT) was used to for the desalting column. The eluted protein was finally concentrated using Vivaspin Turbo 10K MWCO and stored at -80 °C after flash-freezing.

In vitro assay of enzymatic activity of the sulfotransferase SgdX2

The in vitro sulfotransferase enzymatic reaction was set up to include SgdX2, a sulfate donor 3′-phosphoadenosine 5′-phosphosulfate (PAPS) and the substrate sungeidine F (**6**).[6] The activity assay was carried out in 0.2 mL vials (30 μL reaction, 20 mM HEPES buffer, pH 7.5) that contains 0.4 mM PAPS, 0.2 mM sungeidine F (**6**), 5 μM sulfotransferase enzyme (SgdX2), 5% glycerol, 1.7 mM DTT. A control reaction was set up without adding SgdX2. The reaction mixture was incubated at 30 °C, and 5 μL aliquots were taken for HPLC and LC/MS analysis at different time points (1.0, 2.0, 3.0, 4.0, and 20 hr). The HPLC fractions that contains the sulfo-adduct (**6a**) was collected and dried using a GenVac evaporator for further analysis to reveal that the sample always contains a mixture of **6** and the sulfo-adduct, likely due to the spontaneous conversion of the sulfo-adduct **6a** to **6**.

Culture conditions

Spores of *Micromonospora* sp. MD118A and its mutants were plated on GYM agar plate (1% glucose, 0.5% yeast extract, 1% malt extract, 0.1% $CaCO_3$, 1.5% agar) and grown at 30 °C for 4-5 days. Mycelia on plates were then inoculated into 100 mL baffled flask with 25 mL GYM medium (1% glucose, 0.5% yeast extract, 1% malt extract, 0.1% $CaCO_3$) and cultured for 3−4 days at 30 °C and 170 rpm. The resulting seed culture was subsequently used to inoculate the production M5 medium (1% corn starch, 0.5% cotton seed flour, 0.005% $CuSO_4{\cdot}5H_2O$, 0.1% $CaCO_3$, 0.00005% Nal, pH 7.5 ± 0.2) at 5% (v/v) and cultured at 30 °C and 170 rpm for 8−10 days to obtain the fermented cultures (pH 7.2 ± 0.2). For small-scale production, the fermentation was performed in 250 mL baffled flasks containing 50 mL M5 medium; for large-scale, the fermentation was performed in 5 L baffled flasks containing 1.25 L M5 medium.

Analytic HPLC for metabolite profiling

After small-scale fermentation, the cell culture (100 mL) was rendered to centrifugation to separate the supernatant and biomass. The supernatant was extracted with an equal volume of EtOAc, while the biomass was extracted with MeOH (20 mL). The combined extracts were dried in vacuo and dissolved in MeOH (500 μL), which was analyzed using an Agilent1200 HPLC system equipped with an ODS column (Vision HT: 250 mm × 4.6 mm, 5 μm). Analysis was

performed using a linear gradient of CH_3CN in H_2O with 0.1% formic acid (0–5 min, 10–20%; 5–35 min, 20–70%; 35–50 min, 70–90%; 50–60 min, 90–100%) at a flow rate of 1.0 mL/min.

Isolation of 1−9 from *Micromonospora* sp. MD118AE and Δ*sgdX2* mutant.

To minimize the likelihood of artifact formation, all crude extracts were prepared without treatment by any acids or bases. The entire extraction and isolation processes were carried out at room temperature, and the water-bath temperature for evaporation was kept below 40 °C. All compounds isolated and characterized herein were identified as they occurred in the fermentation extract. For the large-scale fermentation (MD118AE or Δ*sgdX2*), sixteen 5.0 L baffled flasks, each containing 1.25 L of sodium iodide (3.3 μM) spiked production M5 medium, were inoculated with 60 mL of seed culture and incubated for 8−10 days at 28 °C and 250 rpm. The resulting cultures (20 L) were separated by centrifugation into supernatant and biomass, which was then extracted with EtOAc (1:1, v/v) and MeOH (3 × 2L), respectively. Extracts were combined and evaporated under vacuum to yield a concentrated crude, which was subsequently isolated by a separation strategy to obtain the sungeidines.

The compounds **1**, **2** and **9** from MD118AE, and **3**−**9** from Δ*sgdX2* mutant were obtained accordingly with their isolation procedures described below. For the MD118AE mutant, the extract (5.0 g) was fractionated by flash column chromatography (CC) on silica gel, eluted with a step gradient of hexane, EtOAc and MeOH (hexane/EtOAc/MeOH: 20\1\0, 5\1\0, 1\1\0, 0\1\0, 0\10\1, 0\1\1, 0\0\1) to obtain seven fractions (Fr. 1–Fr. 7). Further isolation was guided by HPLC analysis, which showed that sungeidines were mainly in Fr. 3 and Fr. 4. Fr. 3 was purified by repeated semi-preparative RP-HPLC [ACE ODS column, CH_3CN-H_2O (containing 0.1% formic acid, v/v) 40:60, v/v; flow rate, 4.7 mL/min] to afford compound **9** (anthramicin, 4.0 mg, t_R = 30.5 min). Fr. 4 was separated by CC on Sephadex LH-20 (MeOH) to generate Fr. 4A-4D. Fr. 4B was further purified by semi-preparative HPLC [Cosmosil cholester column, CH_3CN:H_2O (containing 0.1% formic acid, v/v) 65:35, v/v; flow rate, 3.0 mL/min] to furnish compounds **1** (sungeidine A, 2.0 mg, t_R = 16.2 min) and **2** (sungeidine B, 0.5 mg, t_R = 20.0 min). For the Δ*sgdX2* mutant, the crude extract (4.5 g) was applied to a flash CC over silica gel with the same gradient elution of hexane/EtOAc/MeOH mentioned above, to give Fr. A–G. HPLC analysis showed that sungeidines predominantly eluted in Fr. C-E. Purification of Fr. C by semi-preparative HPLC [ACE ODS column, CH_3CN:H_2O (containing 0.1% formic acid, v/v) 40:60, v/v; flow rate, 4.7 mL/min] afforded **9** (anthramicin, 5.2 mg, t_R = 30.5 min). Fr. D was chromatographed by Sephadex LH-20 (MeOH), followed by employing the semi-preparative HPLC with an ACE ODS column [CH_3CN:H_2O (containing 0.1% formic acid, v/v) 38:62, v/v; flow rate, 4.7 mL/min] to afford **8** (sungeidine H, 1.7 mg, t_R = 21.9 min), **6** (sungeidine F, 5.0 mg, t_R = 26.4 min), **5** (sungeidine E, 1.4 mg, t_R = 29.0 min) and **3** (sungeidine C,1.5 mg, t_R = 31.5 min). Compounds **7** (sungeidine G, 0.4 mg, t_R = 18.2 min) and **4** (sungeidine D, 1.0 mg, t_R = 27.3 min) were obtained from Fr. E by repeated semi-preparative HPLC [Cosmosil cholester column, CH_3CN:H_2O (containing 0.1% formic acid, v/v) 40:60, v/v; flow rate, 3.0 mL/min].

Sungeidine A (**1**): Violet amorphous powder; $[\alpha]_D^{20}$ +2872 (*c* 0.025, MeOH); UV (MeOH) λ_{max} (log ε) 229 (4.158), 292 (4.180), 418 (3.519), 535 (3.759), 570 (3.704) nm; IR (film) ν_{max}: 3390, 2928, 2858, 1667, 1622, 1574, 1451, 1343 and 1274 cm^{-1}; ^1H and ^{13}C NMR data, see Table S4; HRESIMS *m/z* 474.1173 $[M + H]^+$ (calcd for $C_{30}H_{20}NO_3S$, 474.1158).

Sungeidine B (**2**): Orange amorphous powder; $[\alpha]_D^{20}$ +190 (*c* 0.06, MeOH); UV (MeOH) λ_{max} (log ε) 241 (3.998), 281 (3.944), 402 (3.578), 494 (3.542), 523 (3.471) nm; IR (film) ν_{max}: 3397,

2920, 2854, 1658, 1629, 1555, 1460, 1359 and 1270 cm^{-1}; ^1H and ^{13}C NMR data, see Table S4; HRESIMS *m/z* 476.1304 $[M + H]^+$ (calcd for $C_{30}H_{22}NO_3S$, 476.1315).

Sungeidine C (**3**): Pale yellow amorphous powder; $[\alpha]_D^{20}$ +22 (*c* 0.1, DMSO); UV (MeOH) λ_{max} (log ε) 231 (4.034), 297 (4.001), 412 (3.893) nm; IR (film) ν_{max}: 3404, 2925, 2855, 1672, 1641, 1575, 1450, 1366 and 1263 cm^{-1}; ^1H and ^{13}C NMR data, see Table S4; HRESIMS *m/z* 510.1354 $[M + H]^+$ (calcd for $C_{30}H_{24}NO_5S$, 510.1370).

Sungeidine D (**4**): Pale yellow amorphous powder; $[\alpha]_D^{20}$ +67 (*c* 0.1, MeOH); UV (MeOH) λ_{max} (log ε) 232 (4.063), 296 (4.033), 414 (3.897) nm; IR (film) ν_{max}: 3410, 2926, 2850, 1673, 1640, 1574, 1452, 1366 and 1263 cm^{-1}; ^1H and ^{13}C NMR data, see Table S4; HRESIMS *m/z* 526.1302 $[M + H]^+$ (calcd for $C_{30}H_{24}NO_6S$, 526.1319).

Sungeidine E (**5**): Yellow amorphous powder; $[\alpha]_D^{20}$ +205 (*c* 0.1, MeOH); UV (MeOH) λ_{max} (log ε) 232 (4.034), 298 (4.003), 422 (3.925) nm; IR (film) ν_{max}: 3393, 2925, 2852, 1669, 1564, 1464, 1366 and 1233 cm^{-1}; ^1H and ^{13}C NMR data, see Table S4; HRESIMS *m/z* 494.1425 $[M + H]^+$ (calcd for $C_{30}H_{24}NO_4S$, 494.1421).

Sungeidine F (**6**): Yellow amorphous powder; $[\alpha]_D^{20}$ +1200 (*c* 0.1, MeOH); UV (MeOH) λ_{max} (log ε) 231 (4.637), 311 (4.591), 452 (4.520) nm; IR (film) ν_{max}: 3390, 2920, 2849, 1664, 1645, 1554, 1458, 1370 and 1228 cm^{-1}; ^1H and ^{13}C NMR data, see Table S5; HRESIMS *m/z* 492.1253 $[M + H]^+$ (calcd for $C_{30}H_{22}NO_4S$, 492.1264).

Sungeidine G (**7**): Yellow amorphous powder; $[\alpha]_D^{20}$ +598 (*c* 0.06, MeOH); UV (MeOH) λ_{max} (log ε) 226 (4.106), 305 (4.086), 454 (3.930) nm; IR (film) ν_{max}: 3383, 2923, 2851, 1710, 1654, 1553, 1456 and 1374 cm^{-1}; ^1H and ^{13}C NMR data, see Table S5; HRESIMS *m/z* 508.1191 $[M + H]^+$ (calcd for $C_{30}H_{22}NO_5S$, 508.1213).

Sungeidine H (**8**): Yellow amorphous powder; $[\alpha]_D^{20}$ +862 (*c* 0.1, MeOH); UV (MeOH) λ_{max} (log ε) 228 (4.444), 310 (4.385), 451 (4.295) nm; IR (film) ν_{max}: 3380, 2927, 2852, 1685, 1641, 1557, 1459, 1374 and 1225 cm^{-1}; ^1H and ^{13}C NMR data, see Table S5; HRESIMS *m/z* 508.1194 $[M + H]^+$ (calcd for $C_{30}H_{22}NO_5S$, 508.1213).

Anthramicin (**9**): Pale yellow amorphous powder; $[\alpha]_D^{20}$ –49 (*c* 0.1, DMSO); UV (MeOH) λ_{max} (log ε) 230 (3.813), 290 (4.147), 326 (3.633), 376 (3.387) nm; IR (film) ν_{max}: 3406, 3290, 2923, 1648, 1353 and 1320 cm^{-1}; ^1H and ^{13}C NMR data, see Table S5; HRESIMS *m/z* 396.9389 $[M + H]^+$ (calcd for $C_{15}H_{10}IO_3S$, 396.9390).

Detailed structural elucidation of 1−9.

The structures for **1**−**9** and their absolute configurations were established by extensive spectroscopic analyses (Schemes S2 and S3, Figures S1-S11) and experimental/calculated electronic circular dichroism (ECD) spectroscopy (Figures S12-S14). We described below how some of the key structural features for **1**−**9** were established.

For anthramicin (**9**), its molecular formula was established as $C_{15}H_9IO_3S$ based on its ^{13}C NMR data and the positive mode HRESIMS, which gave a *pseudo*-molecular ion at *m/z* 396.9389 ($[M + H]^+$, calcd for $C_{15}H_{10}IO_3S$, 396.9390, Δ = −0.3 ppm). The unexpected presence of iodine was also supported by the prominent fragmentation ions at *m/z* 252.0243 ($[M\text{-}H_2O\text{-}I]^+$) and 378.9284 ($[M\text{-}H_2O]^+$) in the MS/MS spectrum (Figure S9-8). This unique iodine- and sulfur-containing molecular formula $C_{15}H_9IO_3S$ of **9** was reminiscent of a thiolactone-fused iodoanthracene, 5-iodo-*2H*-anthra[9,1-*bc*]thiophen-2-one (**10**, $C_{15}H_7IOS$) reported recently by Townsend and coworkers as an intermediate in dynemicin biosynthesis.[7] The ^{13}C NMR data (Table S5) of **9**, in conjunction with the HSQC data, showed fifteen carbon resonances, comprising one carbonyl at δ_C 194.6, seven methines (two oxygenated at δ_C 73.9 and 71.2, and five aromatic at δ_C

139.0, 135.8, 126.3, 125.5 and 124.5) and seven quaternary carbons (including an iodine-bearing carbon at δ 107.8), which were also highly similar to those of **10**.[7] The only difference between **9** and **10** is that two aromatic methines in **10** were replaced by two oxygenated methines at C8 and C7. The difference of 34 Da indicated that the two additional oxygens should be presented as hydroxy groups, which was verified by two D_2O-exchangeable protons [δ_H 6.35 (br s, OH-8) and 5.54 (br s, OH-7)] observed in the ^{1}H NMR and absorption bands at 3406 and 3290 cm^{-1} in the FTIR spectrum. The key ^{1}H-^{1}H COSY correlation (Scheme S2) of H-7 (δ_H 4.41, br d, J = 9.2 Hz) with H-8 (δ_H 4.81, d, J = 9.2 Hz), along with a key HMBC correlation of H-8 with C-10 (δ_C 129.6), suggests the two hydroxyls were vicinal and located at C7 and C8. The *trans*-geometry of the vicinal diol was determined based on the larger coupling constant (J = 9.2 Hz) of H-7/H-8 (Table S5). The absolute configuration of **9** was then deduced based the ECD calculations using the Time-dependent density functional theory (TDDFT) method at B3LYP/def2tzvp/SMD(water) level.[8,9] The resulting simulated ECD spectrum of **9** was overlaid with the experimental one for comparison (Figures S12-S14), which suggested an absolute configuration of 7*R*,8*R* for compound **9**, as depicted in Scheme S1.

Sungeidine C (**3**) has a molecular formula $C_{30}H_{23}NO_5S$ based on a protonated molecular ion at *m/z* 510.1354 ([M + H]$^+$, calcd for $C_{30}H_{24}NO_5S$, 510.1370) in its HRESIMS and the ^{13}C NMR data. The ^{13}C NMR spectrum of **3** showed a total of thirty carbon resonances classified by HSQC NMR experiments as one methyl at δ_C 22.5, one methylene at δ_C 43.7, fifteen methines (two oxygenated at δ_C 71.0, 73.5), ten quaternary carbons, and three carbonyl groups at δ_C 195.4, 191.2 and 190.8 (Table S4). In the ^{1}H NMR spectrum, characteristic signals for two vicinal oxymethine groups [δ_H 4.72 (d, J = 8.8 Hz, H-15) and 4.34 (br d, J = 8.8 Hz, H-16)], five aromatic protons [δ_H 7.96 (s, H-20), 7.75 (d, J = 8.5 Hz, H-10), 6.71 (d, J = 8.5 Hz, H-9), 6.53 (br d, J = 9.8 Hz, H-18) and 6.03 (dd, J = 9.8, 2.0 Hz, H-17)] were observed. The above proton signals, together with their corresponding carbon resonances, are highly similar to those of **9.** This implied that compound **3** also contains a thiolactone-fused 1,2-dihydroxy-dihydroanthracene moiety (unit A), which was further confirmed by a detailed interpretation of 2D (^{1}H-^{1}H COSY, HSQC and HMBC) NMR data (Scheme S2). Among the remaining 15 carbon signals arising from unit B, six aromatic signals at δ_C 128.3 (C-23), 127.1 (C-24), 128.8 (C-25), 135.1 (C-26), 129.9 (C-27), and 137.6 (C-28), along with four aromatic protons resonating at δ_H 7.93 (d, J = 7.5 Hz, H-24), 7.50 (t, J = 7.5 Hz, H-25), 7.66 (t, J = 7.5 Hz, H-26) and 7.38 (d, J = 7.5 Hz, H-27)] in the ^{1}H NMR spectrum, were typical of an *ortho*-disubstituted aromatic ring. The remaining nine carbons of unit B was thereafter readily identified as a cyclohex-2-enone substituted with a methyl, a methylene, and a carbonyl group, based on the analysis of its 1D and 2D NMR data (Scheme S2). In particular, the key ^{1}H-^{1}H COSY correlations of H-3 (δ_H 3.55) with H-8 (δ_H 3.43), H-8 with H-7 (δ_H 3.85)/H_2-30 (δ_H 3.44), and the key HMBC correlations of H-3 with C-2 (δ_C 190.8)/C-5 (δ_C 122.0), Me-29 (δ_H 2.01) with C-3 (δ_C 53.4)/C-5 (δ_C 122.0) were observed. In addition, the key HMBC correlations of H-24 (δ_H 7.93) with C-2 (δ_C 190.8), and H-27 (δ_H 7.38) with C-7 (δ_C 50.2) suggest that the *ortho*-di-substituted aromatic ring is coupled to the cyclohexenone moiety at C-2 and C-7. The structure of units A and B were constructed accordingly ($C_{30}H_{22}O_5S$ out of the molecular formula $C_{30}H_{23}NO_5S$) and only a *N*H was unassigned. Units A and B are linked via a *N*-H group, as supported by a COSY correlation of H-30 (δ 3.44) with a broad triplet at δ 7.83 (N-H), which is not correlated to a carbon in the HSQC spectrum, and a key HMBC correlation of signal δ 7.83 with C-9 (105.9). Hence, the planar structure of **3** was determined to possess an anthrathiophenone unit conjugated with a unique [7.3.1.0^{2,7}]-tricyclic C_{15}-backbone. The relative configuration of **3** was established by analyses of the proton-proton coupling constants and NOESY data (Scheme S3). The broad singlet

of H-3 (δ_H 3.55, br s), H-7 (δ_H 3.85, br s), and the NOESY correlations of H-3 with Me-29, H-7 with *N*-H/H-27, suggested that H-3, H-7, and H-8 were all α-oriented, while the large *J* value (*J* = 8.8 Hz) between H-15 and H-16 indicated that they adopt the *trans*-configuration. The C-15 and C-16 in **3** was tentatively assigned to possess the same absolute configuration 15*R*,16*R* with those in anthramicin (**9**), from a biosynthetic perspective as described in main text. Sungeidine D (**4**) was assigned the molecular formula $C_{30}H_{23}NO_6S$ as determined from the ^{13}C NMR and HRESIMS (*m/z* 526.1302 $[M + H]^+$, calcd 526.1319) data. Its ^1H and ^{13}C NMR data (Table S4) resembled those of **3**, with the only difference being the presence of a 7-OH group in **4**, which was supported by the HMBC correlations (Scheme S2) of H-3 (δ_H 3.73)/H-5 (δ_H 5.79)/H-8 (δ_H 3.28) with C-7 (δ_C 75.3). Similar to **3**, the large $J_{H\text{-}15/H\text{-}16}$ value (8.8 Hz) and the small $J_{H\text{-}3/H\text{-}8}$ value (2.5 Hz) suggested that H-15 and H-16 were in *trans*-configuration, whereas H-3 and H-8 were α-oriented. The latter was further validated by the observed NOESY correlation of H-3 with H-8.

Sungeidine E (**5**) has the molecular formula of $C_{30}H_{23}NO_4S$ based on the $[M + H]^+$ ion at *m/z* 494.1425 (calcd. 494.1421) in the HRESIMS and ^{13}C NMR data. Its ^1H and ^{13}C NMR data (Table S4) are similar to those of **3**, the most noticeable difference being the presence of a methine group (δ_H 5.89, δ_C 61.1) rather than the C-2 carbonyl group in **3**. In addition, the distinct *N*-H proton signal in **3** was absent in **5**. The above evidence and its unsaturation degrees suggest an additional tetrahydrofuran ring formed by a linkage of C-2 with *N* atom in **5**, which was confirmed by the observed HMBC correlations of H-30 (δ_H 4.26)/H-24 (δ_H 7.24) with C-2 (δ_C 61.1). Therefore, the unit B in compound **5** was identified to be an unprecedented sterically congested [6,6,6,5]-tetracyclo C_{15}-backbone featuring a bridging phenylene coupled with 7-methyl-hexhydroisoindole-5-one. The small $J_{H\text{-}2/H\text{-}3}$ value (4.3 Hz) of doublet H-2, together with the NOESY correlations of Me-29 (δ_H 2.08) with H-2 (δ_H 5.89)/H-3 (δ_H 3.24), indicates H-2 and H-3 have the same α-orientation. Similar to **3** and **4**, the small coupling constants of H-3 (t, *J* = 4.3 Hz) and H-7 (d, *J* = 3.0 Hz) suggest that H-3, H-7, and H-8 were co-facial.

Sungeidine F (**6**) exhibited a *pesudo*-molecular ion at *m/z* 492.1253 ($[M + H]^+$, calcd for $C_{30}H_{22}NO_4S$, 492.1264), which corresponds to the molecular formula $C_{30}H_{21}NO_4S$, two hydrogens less than **5**. Comparison of the NMR data (Table S5) of **5** and **6** revealed their structural similarities, with the only difference being that two aromatic protons (H-20 and H-24) of **5** were absent in **6**, implying that a new C-C band should be formed between C-20 and C-24. This was confirmed by a detailed analysis of its 2D NMR experiment (Scheme S2), with the key HMBC correlations of H-25 (δ_H 6.91)/H-18 (δ_H 6.77) with C-20 (δ_C 131.9), and H-2 (δ_H 4.92) with C-24 (δ_C 135.7) observed. The H-2, H-3, H-7, and H-8 of **6** possessed similar splitting patterns and coupling constant as the corresponding protons in **5**, implying unit B in **5** and **6** share the same relative configuration. This conclusion is supported by the key NOESY correlations (Scheme S3) of H-2 with H-3 (δ_H 3.24), H-2 with Me-29 (δ_H 2.02), H-3 with Me-29, and H-7 (δ_H 3.54) with H-8 (δ_H 3.44). The *J* value (9.8 Hz) between H-15 and H-6 was indicative of their *trans*-configuration. Therefore, compound **6** was deduced to be an aromatic coupling product of **5** at C-20 and C-24, as shown in Scheme S1.

Sungeidines G (**7**) and H (**8**) have the same molecular formula $C_{30}H_{21}NO_5S$ based on their HRESIMS and ^{13}C NMR data. The NMR data of **7** and **8** were similar to those of **6**, except for one additional hydroxy group at C-27 in **7** and at C-7 in **8**, which was confirmed by the key HMBC correlation of H-25 (δ_H 6.73) with C-27 (δ_C 156.7) in **7**, and H-27 (δ_H 7.34)/H-3 (δ_H 3.40) with C-7 (δ_C 76.5) in **8**, respectively. The relative configurations of **7** and **8** were found to be consistent with that of **6** by analyses of the proton-proton coupling constants (Table S5) and NOESY spectrum (Scheme S3).

Sungeidine B (**2**) was found to possess a molecular formula $C_{30}H_{21}NO_3S$ as established by its HRESIMS (*m/z* 476.1304) and ^{13}C NMR data. The ^{1}H and ^{13}C NMR spectra of **2** are similar to that of **5**, expect two oxygenated methines in **5** replaced by two aromatic carbons (Figure S2). This indicates that **2** should be a dehydrated product of **5**, which was confirmed by the 1D and 2D NMR data, in particular the HMBC correlations of H-15 (δ_H 6.91) with C-13 (δ_C 123.6), and H-18 (δ_H 8.15) with C-16 (δ_C 157.8) (Scheme S2). The H-2, H-3, H-7, and H-8 in compound **2** display similar splitting pattern and coupling constants with those in compounds **5**−**7** (Tables S4 and S5), indicating they all possess the same relative configuration.

The molecular formula of sungeidine A (**1**) was established as $C_{30}H_{19}NO_3S$ based on the $[M + H]^+$ ion at *m/z* 474.1173 (calcd for $C_{30}H_{20}NO_3S$, 474.1158) in the HRESIMS and ^{13}C NMR data, 2 Da less than **2**. By a detailed inspection of its ^{1}H and ^{13}C NMR data (Table S4), sungeidine A was identified to be an aromatic coupling product of **2** via a direct linkage between C-20 and C-24, which was verified by the HMBC correlations of H-18 (δ_H 8.34)/H-25 (δ_H 7.06) with C-20 (δ_C 135.8), and H-2 (δ_H 5.01) with C-24 (δ_C 136.0). The relative configuration of **1** was confirmed based on the coupling constant and NOESY correlations. The small coupling constants observed for H-2 (d, J = 4.5 Hz), H-3 (t, J = 4.5 Hz), and H-7 (d, J = 2.8 Hz), together with the NOESY correlations of H-2/H-3, H-2/Me-29 (δ_H 2.01), H-7/H-27 (δ_H 7.18), H-7/H$_\beta$-30 (δ_H 4.35), H$_\alpha$-30 (δ_H 3.42)/H-8 (δ_H 3.48), and H$_\alpha$-30/H-9 (δ_H 6.71), suggested the H-2, H-3, H-7, and H-8 were all α-oriented, similar to those in **2** and **5**−**7**. To further determine the absolute configuration of enediyne moieties in sungeidines, an TDDFT-based ECD calculation was applied into the biogenetically final product **1**. Low energy conformations of **1** were optimized by DFT method at M06-2X/6-31G(d)/SMD(MeOH) level (Figure S13). The optimized structures were then subjected to TDDFT calculations at B3LYP/def2tzvp/SMD(MeOH) level. As a result, the calculated ECD spectrum of **1** was in a good match with the experimental one (Figures S12-S14), allowing the absolute configuration of **1** to be established as 2*R*, 3*R*, 7*R*, 8*S*.

^{13}C-labelled acetate feeding experiments.

To provide an insight into the biosynthetic origin of the C_{15} anthrathiophenone and C_{15} enediyne skeleton in sungeidines, three incorporation experiments (Scheme S4) with singly ([1-^{13}C]- or [2-^{13}C]-sodium acetate) and doubly ([1,2-$^{13}C_2$]-sodium acetate) ^{13}C-enriched acetate[10-13] were carried out with sungeidine F (**6**), which was produced in high yield by the Δ*sgdX2* mutant. [1-^{13}C]- and [2-^{13}C]-sodium acetate incorporated anthramicin (**9**) was also isolated and characterized rendered to ^{13}C NMR analysis. Briefly, 200 mg/L of [1-^{13}C]-, or [2-^{13}C], or [1,2-$^{13}C_2$]-sodium acetate, was added (at 24h-cultivation) to four flasks each containing 1.25 L culture of M5 medium. The incubation was conducted for 10−12 days at 28 °C and with the shaker set at 250 rpm. The purification of ^{13}C-labelled **6** were performed following the procedures described above. The ^{13}C-labelled patterns after incorporation of [1-^{13}C]-, [2-^{13}C], [1,2-$^{13}C_2$]-sodium acetate were determined from the respective ^{13}C NMR spectra and the results are summarized in Figure 3 (main text) and Scheme S4. The incorporation pattern of [1,2-$^{13}C_2$]-sodium acetate was confirmed by matching of $^{1}J_{CC}$ values as shown in Table S6, and signal intensity enhancements at the specific carbons in the model sungeidine F (**6**) were 1.3−3.5 folds. The [1-^{13}C]-, [2-^{13}C]-, and [1,2-$^{13}C_2$]-sodium acetate were purchased from Cambridge Isotope Laboratories, Inc.

Sungeidine C (3) and anthramicin (9) feeding experiment

For sungeidine C (**3**): spores of Δ*sgdU15* mutant was plated on GYM agar plate and grown at 30 ^{o}C for 4 days. Mycelia was then inoculated into 100 mL baffled flask with 25 mL GYM medium

and cultured for 3 days at 30 °C and 170 rpm. The resulting seed culture was subsequently used to inoculate 50 mL M5 medium supplemented with 20 µL of 10 mM stock solution of **3** in DMSO. Sterile DMSO was added to the control flasks. Similarly, 20 µL of 10 mM stock solution of anthramicin (**9**) in DMSO was supplemented with MD118A and Δ*sgdX2* mutants in M5 medium without NaI, respectively. After cultivation for 7 days, each crude extract was prepared and analysed by HPLC and HPLC-MS as mentioned above.

DFT calculation[8,9]

Because our effort to grow single crystals for determining the absolute configuration of **1** and **2** was futile, we relied on TDDFT-based calculated ECD method to deduce the stereochemistry of the chiral centers (Figures S12-S15). M06-2X/6-31G(d)/SMD(MeOH) (for **1**) and ωB97X-D/def2tzvp/SMD (water) (for **9**) methods were used for geometry optimizations and frequency calculations for each low energy conformation. Each optimized structure was then submitted for single point energy calculation using M06-2X functional with split-valence basis sets, SDD for iodine and 6-311++G(2d,p) for other elements, with the SMD solvation model of water (for **9)**, or at M06-2X/6-311++G(2d,p)/SMD(MeOH) level (for **1**). The resulting rotatory strength at the corresponding excitation energy of all low energy conformations were Boltzmann averaged based on their corresponding calculated Gibbs free energy to generate the simulated ECD spectra. The resulting simulated spectra were overlaid with the corresponding experimental spectrum for comparison. All the calculations were performed using Gaussian 09 program package[14] with the UltraFine integration grid.

Table S1. List of genes in *sgd* BGC and their proposed functions. The genes that are not found *dyn* BGC are shaded in light blue; whereas the genes from the minimal enediyne PKS gene cassette are shaded in yellow.

Gene	AA [a]	Closest homolog [source]	%Identity/ %Similarity	Predicted function	UniProt ID	Homologues in *dyn* BGCs*
sgdU21	189	Uncharacterized protein [*Micromonospora chaiyaphumensis*]	77/86	Hypothetical protein	A0A1C4W0Q8	*dyn21*
sgdU20	190	Uncharacterized protein [*Micromonospora* sp. CB01531]	47/57	Hypothetical protein	A0A1Q5BEB8	*dynU20*
sgd17	399	Uncharacterized protein (*Amycolatopsis coloradensis*]	48/58	Ketone reductase	A0A1R0KZ46	*orf17*
sgdR3	421	Protein with three transmembrane helices (*Saccharopolyspora shandongensis*)	61/72	AarF/ABC1/UbiB kinase family regulatory protein	A0A1H2QMM1	*dynR3*
sgd16	463	PBS lyase (*Amycolatopsis coloradensis*)	84/91	HEAT repeat-containing protein	A0A1R0KZ63	*orf16*
sgd15	214	Uncharacterized protein (*Streptomyces* sp. CB03234)	85/91	Hypothetical protein	A0A125SA03	*orf15*
sgdU16	286	Uncharacterized protein (*Amycolatopsis coloradensis*)	50/61	Enediyne self-sacrifice resistance protein	A0A1R0KZD6	*dynU16*
sgdU8	237	Transcriptional regulator, (*Micromonospora yangpuensis*)	57/70	HxlR-type regulator	A0A1C6UU66	*dynU8*
sgdX1	155	Uncharacterized protein (*Streptomyces* sp. RV15)	59/68	Hypothetical protein (OmdA-like domain)	A0A117RYF8	-
sgd14	347	Uncharacterized protein (*Streptomyces* sp. RV15)	75/84	Self-sacrifice resistance protein	A0A117RYI1	*orf14*
sgdE10	417	Cytochrome P450 (*Streptomyces* sp. RV15)	66/77	Cytochrome P450	A0A117RYX8	*dynE10*
sgdT5	328	ABC transporter (*Streptomyces* sp. RV15)	64/75	ABC transporter protein	A0A101UT78	*dynT5*
sgdT8	282	Transport permease protein (*Streptomyces* sp. RV15)	72/85	ABC-2 Transporter protein	A0A117RYB3	*dynT8*
sgdX2	253	Uncharacterized protein (*Streptomyces* sp. RV15)	53/73	Sulfotransferase	A0A101UT94	-
sgdX3	438	MBL fold metallo-hydrolase (*Streptomyces* sp. RV15)	57/72	Metallo-β-lactamase fold protein	A0A101UTE4	-
sgdE14	122	Uncharacterized protein (*Streptomyces* sp. RV15)	64/82	Resistance protein	A0A101UT77	*dynE14*
sgdX4	236	Uncharacterized protein (*Streptomyces* sp. RV15)	69/77	HAMP domain-containing translation initiation factor	A0A101UT83	-
sgdO6	295	Uncharacterized protein (*Streptomyces* sp. RV15)	52/65	O-methyltransferase	A0A101UT91	*dynO6*
sgd19	437	Cytochrome P450 (*Streptomyces* sp. RV15)	54/68	Cytochrome P450	A0A101UTD0	*orf19*
sgdR7	249	Transcriptional regulator [*Couchioplanes caeruleus*]	45/56	AraC-type regulator	A0A1K0FU55	*dynR7*
sgdR2	627	Transcriptional regulator (*Micromonospora citrea*)	45/58	AfsR/SARP-type regulator	A0A1C6VYX0	*dynR2*
sgdX5	341	Transposase (*Micromonospora cremea*)	57/72	IS630 family transposase	A0A1N5U972	-
sgdU15	353	Uncharacterized protein [*Couchioplanes caeruleus*]	50/57	UnbL (unknown conserved protein in enediyne biosynthesis)	A0A1K0FTV9	*dynU15*
sgdU14	626	DynU14 (*Micromonospora chersina*)	63/72	UnbV (unknown conserved protein in enediyne biosynthesis)	Q84HJ0	*dynU14*

sgdT3	313	Uncharacterized protein (*Micromonospora yangpuensis*)	66/77	UnbU (unknown conserved protein in enediyne biosynthesis)	A0A1C6UU53	*dynT3*
sgdE8	1901	Enediyne polyketide synthase [*Couchioplanes caeruleus*]	54/64	Iterative polyketide synthase	A0A1K0GXS2	*dynE8*
sgdE7	152	DynE7 (*Micromonospora chersina*)	65/74	Hot-dog fold thioesterase	Q84HI7	*dynE7*
sgdS6	224	Uncharacterized protein (*Micromonospora citrea*)	49/60	NADPH-dependent F420 oxidoreductase	A0A1C6W033	*dynS6*
sgdU6	308	Uncharacterized protein (*Micromonospora haikouensis*)	57/72	Putative transporter	A0A1C4Y6G0	*dynU6*

*Gene names are from Gao et al, *FEMS Microbial Lett*, 2008, 1-10.

Table S2. List of Primers used in this study.

Primer name	**Sequence (5'-3')**	**Function**
mmd2050 sgrna F	CATGCCATGGTGGTCGGATCGATTCGTCGCGTTTTAGAGCTAGAAATAGC	sgRNA amplification for sioxanthin BGC knock out (KO)
sgRNA R	ACGCCTACGTAAAAAAAGCACCGACTCGGTGCC	
ctg1-14sgrna F	CATGCCATGGCGCCTTGGTGTCCGGTTCCAGTTTTAGAGCTAGAAATAGC	sgRNA amplification for enediyne BGC *sgdX1* gene KO
sgRNA R	ACGCCTACGTAAAAAAAGCACCGACTCGGTGCC	
sulfo sgrna F	CATGCCATGGTCGGTCCGTCCCCGAAATGGGTTTTAGAGCTAGAAATAGC	sgRNA amplification for enediyne BGC *sgdX2* gene KO
sgRNA R	ACGCCTACGTAAAAAAAGCACCGACTCGGTGCC	
metallo sgrna F	CATGCCATGGAGAAGTCGCCGCAGCACAGGGTTTTAGAGCTAGAAATAGC	sgRNA amplification for enediyne BGC *sgdX3* gene KO
sgRNA R	ACGCCTACGTAAAAAAAGCACCGACTCGGTGCC	
ctg1-28 dynU15 sgrna F	CATGCCATGGCGACGTGGATCAGGTGGATGGTTTTAGAGCTAGAAATAGC	sgRNA amplification for enediyne BGC *sgdU15* gene KO
sgRNA R	ACGCCTACGTAAAAAAAGCACCGACTCGGTGCC	
sgRNA check R	ACCCCCCATTCAAGAACAGC	sgRNA sequencing
mmd2050 left F40	TCGTCGAAGGCACTAGAAGGAAGTTGCTCATCATGCCCGC	Homologous recombination template construction for pCRISPR-Cas9-*mmd2050*
mmd2050 left R40	GAAGTTGGTGAGCTGGAAGGGTCATAGGCAGCGGTCAGAT	
mmd2050 right F20	CCTTCCAGCTCACCAACTTC	
mmd2050 right R40	GGTCGATCCCCGCATATAGGGTGGATGTCGTCGTACCGAT	
ctg1-14 left F40	TCGTCGAAGGCACTAGAAGGTCAAGTAGCATGACAGCCGGAG	Homologous recombination template construction for pHZ-cod9-*sgdX1*
ctg1-14 left R40	CGGTGATCCAGGTGACGTACGCGTACGGCGTGTCGTTGAT	
ctg1-14 right R20	GTACGTCACCTGGATCACCG	
ctg1-14 right R40	GGTCGATCCCCGCATATAGGGATCAGCGTGAGTTTGTCGC	
sulfo left F40	TCGTCGAAGGCACTAGAAGGAAGGGAGAGGGCAAGTGACC	Homologous recombination template construction for pHZ-cod9-*sgdX2*
sulfo left R40	CACACCGAGGAACTTACACATGAGAATCTCCTTCGTGTGG	
sulfo right F20	TGTGTAAGTTCCTCGGTGTG	
sulfo right R40	GGTCGATCCCCGCATATAGGGTAGAAGTCGCCGCAGCACA	
metallo left F40	TCGTCGAAGGCACTAGAAGGCGGAGGCGAAGGTCATCCTG	Homologous recombination template construction for pCRISPR-

metallo left R40	CATCATCGCCACCACACCGTGAGGACGTGGTCGATGTGGC	Cas9-*sgdX3*
metallo right F20	ACGGTGTGGTGGCGATGATG	
metallo right R40	GGTCGATCCCCGCATATAGGGGATGATCGCACTGTTCGCC	
ctg1-28 dynU15 left F40	TCGTCGAAGGCACTAGAAGGAGGTGCTGGTGTCCACGCTG	Homologous recombination template construction for pCRISPR-Cas9-ctg1-28 *sgdU15*
ctg1-28 dynU15 left R40	AAGGCCACACCCTGACCGAGGTTGAAGCCGTCGAGGAAGG	
ctg1-28 dynU15 Right F20	CTCGGTCAGGGTGTGGCCTT	
ctg1-28 dynU15 right R40	GGTCGATCCCCGCATATAGGCTGCATCCGCATCACCGGGT	
pcrispr-cas9 seq F	TGAGGCTTGCAGGGAGTCAA	HDR template sequencing
pcrispr-cas9 seq R	CGTCGCTCTCTGGCAAAGCT	
phytoene synthase 2050 check F	GATCTCGGTGAGCGATTCGA	Validation of *mmd2050* gene deletion
phytoene synthase 2050 check R	CACCTCGTACTCGATCAGCT	
ctg1-14 check F	GGTGAGGGAGCACAGATGAG	Validation of *sgdX1* deletion
ctg1-14 check R	GTGGGAGTCAGGATCAGGTG	
sulfo check F	TACTTCAACGGCGTCTCACC	Validation of *sgdX2* gene deletion
sulfo check R	GAAGGCATCCTGGTCGTTGT	
metallo check F	TACAAGGGTGAGCTTCGCCG	Validation of *sgdX3* gene deletion
metallo check R	GCGGACGATGAACTGCGGAT	
dynU15 check F	CTCGCCGACTTCACGGTC	Validation of *sgdU15* deletion
dynU15 check R	GGATCAGAGCGACGCGAG	
md118 cluE 4330 F	CGACGACCTAGGGGTTTTGCGTGTTGCGTGCGGCAATTGT	PCR amplification of *sgdR2* (fragment 1) for pSK152-*sgdR2R7*
md118 cluE 4330 R	ATGGACACTCCTTACTTAGATCATAGGTTTGTTTCCCGACAGA	
md118 cluE 4329 F	TCTAAGTAAGGAGTGTCCATATGCCTGCCGTCCACGAAAC	PCR amplification of gene *sgdR7* (fragment 2) for pSK152-*sgdR2R7*
md118 cluE 4329 R	ACGAATTCGATATCGCGCGCTGGACCCGGTTCCACCGAC	
pSK152 integration check F	CCAGGTGCGAATAAGGGACA	Validation of pSK152-*sgdR2R7* integration in MD118
md118 integration check R	GTTCATCCACCTCGACCAGA	
pET28 sgdX2 F:	CATG CATATG GAGGTCATCGGCGTCGGC	PCR amplification of *sgdX2* for pET28b-sgdX2
pET28 sgdX2 R:	CATG CTCGAG TCAGCGGTTCTGGCCGG	

Table S3. List of Plasmids used in this study

Name	**Description**
pSET152	*ori* (pUC18), *lacZα*, *int* (ϕC31), *attP* (ϕC31), *oriT* (RP4), *aac(3)-IV*
pSK152	A pSET152 derivative with kasOp* and TAI(ϕC31) RBS separated by riboJ sequence
pCRISPR-Cas9	A conjugative and replicative, CRISPR/Cas9 plasmid for actinomycetes, *ApraR*

pHZ-cod9	A pCRISPR-Cas9 derivative with *codA(sm),* gene for counter selection
pSK152-*sgdR2R7*	pSK152 with *sgdR2* and *sgdR7* under control of synthetic promoter-RBS cassette [kasOp*-Rj-TAI(ϕC31) RBS]
pCRISPR-Cas9- *mmd2050*	pCRISPR-Cas9 plasmid for generating *Δmmd2050*
pHZ-cod9-*sgdU15*	pHZ-cod9 plasmid derivative for generating *ΔsgdU15*
pHZ-cod9-*sgdX1*	pHZ-cod9 plasmid derivative for generating *ΔsgdX1*
pHZ-cod9-*sgdX2*	pHZ-cod9 plasmid derivative for generating *ΔsgdX2*
pHZ-cod9-*sgdX3*	pHZ-cod9 plasmid derivative for generating *ΔsgdX3*
pET28b-sgdX2	The overexpression plasmid for sgdX2 *in E. Coli* Rosetta

Table S4. ^{1}H and ^{13}C NMR data (DMSO-d_6, δ ppm) for sungeidines A−E (**1**–**5**)[a]

No.	sungeidine A (**1**)		sungeidine B (**2**)[b]		sungeidine C (**3**)		sungeidine D (**4**)		sungeidine E (**5**)	
	δ_H (*J* in Hz)	δ_C	δ_H (*J* in Hz)	δ_C	δ_H (*J* in Hz)	δ_C	δ_H (*J* in Hz)	δ_C	δ_H (*J* in Hz)	δ_C
1	--	--	--	--	7.83 (t, 4.2)	--	7.87 (t, overlapped)	--	--	--
2	5.01 (d, 4.5)	57.7	6.06 (d, 4.5)	61.0	--	190.8	--	190.5	5.89 (d, 4.3)	61.1
3	3.31 (t, 4.5)	44.1	3.30 (t, 4.5)	44.3	3.55 (br s)	53.4	3.73 (d, 2.5)	55.4	3.24 (t, 4.3)	44.5
4	--	157.8	--	158.0	--	159.4	--	159.5	--	158.0
5	5.94 (br s)	125.1	5.72 (br s)	125.1	5.69 (br s)	122.0	5.79 (d, 1.3)	122.1	5.70 (br s)	125.0
6	--	197.3	--	198.4	--	195.4	--	--	--	--
7	3.60 (d, 2.8)	51.8	3.64 (d, 3.1)	53.5	3.85 (br s)	50.2	--	75.3	3.58 (d, 3.0)	53.5
8	3.48 (m)	40.0	3.46 (m)	40.4	3.43 (m)	41.4	3.28 (m)	47.9	3.40 (m)	40.1
9	6.71 (d, 8.2)	106.6	7.33 (d, 8.5)	108.4	6.71 (d, 8.5)	105.9	6.72 (d, 8.5)	105.6	7.36 (d, 8.5)	112.3
10	7.93 (d, 8.2)	129.4	8.02 (d, 8.5)	129.6	7.75 (d, 8.5)	127.7	7.78 (d, 8.5)	127.8	7.84 (d, 8.5)	126.3
11	--	116.6	--	116.0	--	117.0	--	116.9	--	118.7
12	--	132.3	--	132.0	--	135.3	--	135.0	--	136.5
13	--	121.7	--	123.6	--	130.0	--	130.0	--	129.8
14	--	130.1	--	128.7	--	132.5	--	132.4	--	132.2
15	7.01 (d, 2.1)	103.0	6.91 (d, 2.0)	102.2	4.72 (d, 8.8)	73.5	4.72 (d, 8.8)	73.5	4.70 (d, 8.8)	73.5
16	--	157.8	--	157.8	4.34 (br d, 8.8)	71.0	4.34 (br d, 8.8)	71.0	4.35 (br d, 8.8)	71.0
17	7.16 (dd, 9.2, 2.1)	119.8	7.14 (dd, 9.2, 2.0)	120.0	6.03 (dd, 9.8, 2.0)	132.8	6.03 (dd, 9.8, 2.6)	132.8	5.98 (dd, 10.0, 2.5)	132.2
18	8.34 (d, 9.2)	131.8	8.15 (d, 9.2)	133.2	6.53 (br d, 9.8)	126.8	6.53 (dd, 9.8, 1.6)	126.8	6.68 (dd, 10.0, 1.8)	127.4
19	--	123.7	--	126.3	--	131.1	--	131.2	--	130.7
20	--	135.8	9.02 (s)	125.3	7.96 (s)	117.5	7.92 (s)	117.5	8.06 (s)	121.4
21	--	117.9	--	117.6	--	118.5	--	118.6	--	120.2
22	--	152.1	--	151.3	--	150.8	--	150.9	--	150.3
23	--	133.4	--	134.2	--	128.3	--	129.9	--	134.4

24	--	136.0	7.41 (dd, 7.5, 1.5)	128.2	7.93 (d, 7.5)	127.1	7.88 (d, 7.5)	126.6	7.24 (d, 7.5)	128.0
25	7.06 (d, 7.5)	131.4	7.15 (td, 7.5, 1.5)	127.7	7.50 (t, 7.5)	128.8	7.50 (td, 7.5, 1.5)	128.9	7.13 (t, 7.5)	127.7
26	7.19 (dd, 7.5, 7.5)	127.6	7.17 (td, 7.5, 1.5)	128.2	7.66 (t, 7.5)	135.1	7.73 (br t, 7.5)	135.3	7.16 (t, 7.5)	128.2
27	7.18 (d, 7.5)	128.5	7.13 (dd, 7.5, 1.5)	129.2	7.38 (d, 7.5)	129.9	7.72 (d, 7.5)	126.5	7.11 (d, 7.5)	129.1
28	--	130.5	--	132.7	--	137.6	--	141.1	--	132.7
29	2.01 (br s)	23.0	2.09 (br s)	23.0	2.01 (br s)	22.5	1.99 (br s)	22.4	2.08 (br s)	23.0
30	4.35 (dd, 12.0, 6.2) 3.42 (br d, 12.0)	53.0	4.61 (dd, 11.5, 6.6) 4.17 (br d, 11.5)	55.7	3.44 (m)	43.7	3.80 (br d, 12.0) 3.22 (m)	41.3	4.26 (dd, 11.5, 6.4) 3.90 (br d, 11.5)	55.1
31	--	186.7	--	187.1	--	191.2	--	191.3	--	191.1
15-OH	--	--	--	--	5.94 (br s)	--	5.96 (br s)	--	5.97 (br s)	
16-OH	--	--	--	--	5.36 (br s)	--	5.38 (br s)	--	5.33 (br s)	

[a] Assignments were made by a combination of 1D and 2D NMR experiments. [b] Carbon data of the amount-limited compounds were collected mainly based on the HSQC and HMBC NMR experiments due to the extremely weak signal intensity in their ^{13}C NMR spectra.

Table S5. ^{1}H and ^{13}C NMR data (DMSO-d_6, δ ppm) for sungeidines F−H (**6**–**8**), and anthramicin (**9**)[a]

No.	sungeidine F (**6**)		sungeidine G (**7**)[b]		sungeidine H (**8**)		anthramicin (**9**)	
	δ_H (J in Hz)	δ_C	δ_H (J in Hz)	δ_C	δ_H (J in Hz)	δ_C	δ_H (J in Hz)	δ_C
1	--	--	--	--	--	--	--	107.8
2	4.92 (d, 4.2)	57.2	4.82 (d, 4.4)	57.3	4.96 (d, 4.4)	57.1	--	130.3
3	3.24 (t, 4.2)	44.3	3.13 (t, 4.4)	44.0	3.40 (dd, overlapped)	47.3	7.58 (s)	125.5
4	--	157.9	--	155.8	--	157.9	--	135.9
5	5.91 (br s)	125.0	5.86 (br s)	125.3	6.02 (br s)	125.2	6.76 (dd, 10.0, 1.6)	126.3
6	--	197.4	--	196.5	--	197.2	6.12 (dd, 10.0, 2.2)	135.8
7	3.54 (br s)	52.0	3.65 (d, 3.0)	47.0	--	76.5	4.41 (br d, 9.2)	71.2
8	3.44 (m)	40.0	3.38 (m)	40.3	3.20 (t, 6.0)	47.7	4.81 (d, 9.2)	73.9
9	6.88 (d, 8.2)	111.3	6.85 (d, 8.5)	110.8	6.95 (d, 8.5)	111.4	--	134.0
10	7.77 (d, 8.2)	125.7	7.76 (d, 8.5)	125.4	7.78 (d, 8.5)	125.6	--	129.6
11	--	117.5	--	117.7	--	117.6	--	132.8
12	--	136.5	--	136.7	--	136.5	--	132.8
13	--	127.0	--	126.2	--	127.0	7.75 (d, 7.6)	124.5
14	--	133.7	--	133.4	--	133.6	8.35 (d, 7.6)	139.0
15	4.77 (d, 9.8)	74.7	4.75 (d, 9.8)	74.8	4.77 (d, 9.8)	74.7	--	194.6
16	4.53 (br d, 9.8)	71.2	4.50 (br d, 9.8)	71.4	4.53 (br d, 9.8)	71.2		
17	6.03 (br d, 10.0)	133.1	5.98 (dd, 10.0, 1.8)	132.2	6.03 (dd, 10.0, 2.0)	133.1		
18	6.77 (dd, 10.0, 1.8)	125.6	6.75 (dd, 10.0, 2.0)	125.6	6.78 (dd, 10.0, 2.2)	125.5		
19	--	127.0	--	126.3	--	127.0		
20	--	131.9	--	132.7	--	132.1		
21	--	119.5	--	119.6	--	119.4		

22	--	151.0	--	151.0	--	151.1			
23	--	133.3	--	134.3	--	132.0			
24	--	135.7	--	126.2	--	134.7			
25	6.91 (d, 7.5)	131.0	6.73 (d, 8.4)	132.2	6.91 (d, 7.5)	131.4			
26	7.18 (dd, 7.5, 7.5)	127.4	6.70 (d, 8.4)	114.7	7.21 (t, 7.5)	127.5			
27	7.11 (d, 7.5)	128.3	--	156.7	7.34 (d, 7.5)	125.8			
28	--	130.5	--	115.1	--	135.2			
29	2.02 (br s)	23.0	1.98 (br s)	22.8	2.02 (br s)	22.9			
30	4.30 (dd, 11.6, 6.0)	52.5	4.27 (dd, 11.6, 6.3)	52.4	4.23 (dd, 11.8, 6.0)	49.2			
	3.28 (br d, 11.6)		3.26 (br d, 11.6)		3.50 (br d, 11.8)				
31	--	191.7	--	191.7	--	191.7			
8/15-OH	6.26 (br s)	--	6.29 (br s)		6.26 (br s)		6.35 (br s)	--	
7/16-OH	5.50 (br s)	--	5.54 (br s)		5.49 (br s)		5.54 (br s)	--	

[a] Assignments were made by a combination of 1D and 2D NMR experiments. [b] Carbon data of the amount-limited compounds were collected mainly based on the HSQC and HMBC NMR experiments due to the extremely weak signal intensity in their ^{13}C NMR spectra.

Table S6. ^{13}C NMR (100 MHz) assignment of [1-^{13}C]- and [2-^{13}C]-acetate and $^{1}J_{CC}$ of [1,2-$^{13}C_2$]-acetate labelled sungeidine F (**6**)

No.	δ_C (ppm)	[1-^{13}C]-acetate (relative intensity)	[2-^{13}C]-acetate (relative intensity)	$^{1}J_{CC}$ (Hz)	No.	δ_C (ppm)	[1-^{13}C]-acetate (relative intensity)	[2-^{13}C]-acetate (relative intensity)	$^{1}J_{CC}$ (Hz)
2	57.2	1.8	1	42.1	17	133.1	1.3	1	65.4
3	44.3	1	3.4	28.0	18	125.6	1	3.3	65.4
4	157.9	1.3	1	40.7	19	127.0	1.3	1	66.0
5	125.0	1	3.4	52.5	20	131.9	1	3.0	66.0
6	197.4	1.5	1	52.5	21	119.5	1.5	1	60.6
7	52.0	1	3.1	38.4	22	151.0	1	3.0	60.6
8	40.0	overlapped	overlapped	28.0	23	133.3	1	3.4	42.1
9	111.3	1.5	1	59.6	24	135.7	1.6	1	58.1
10	125.7	1	3.2	59.6	25	131.0	1	3.5	58.1
11	117.5	1.3	1	59.8	26	127.4	1.8	1	55.5
12	136.5	1	3.0	59.8	27	128.3	1	3.4	55.5
13	127.0	1.3	1	71.5	28	130.5	1.8	1	38.4
14	133.7	1	3.0	71.5	29	23.0	1	2.8	40.7
15	74.7	1.4	1	40.8	30	52.5	1	3.6	s
16	71.2	1	3.4	40.8	31	191.7	1	2.8	s

Scheme S1. Structures of **1**−**10**.

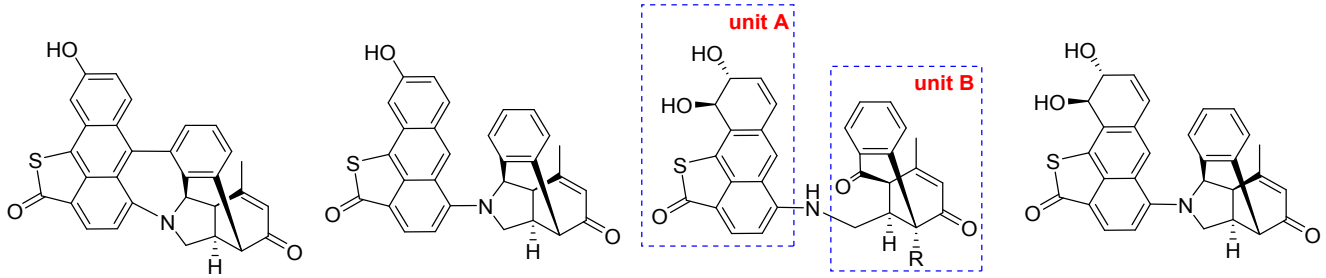

Sungeidine A (1)

Sungeidine B (2)

Sungeidine C (3): R = H
Sungeidine D (4): R = OH

Sungeidine E (5)

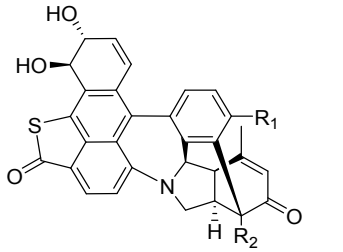

Sungeidine F (6): R_1 = H, R_2 = H
Sungeidine G (7): R_1 = OH, R_2 = H
Sungeidine H (8): R_1 = H, R_2 = OH

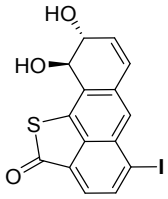

Anthramicin (9)

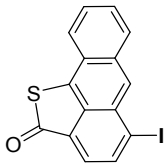

10 reported by Townsend

Scheme S2. TOCSY/COSY, and HMBC correlations of **1**–**9**.

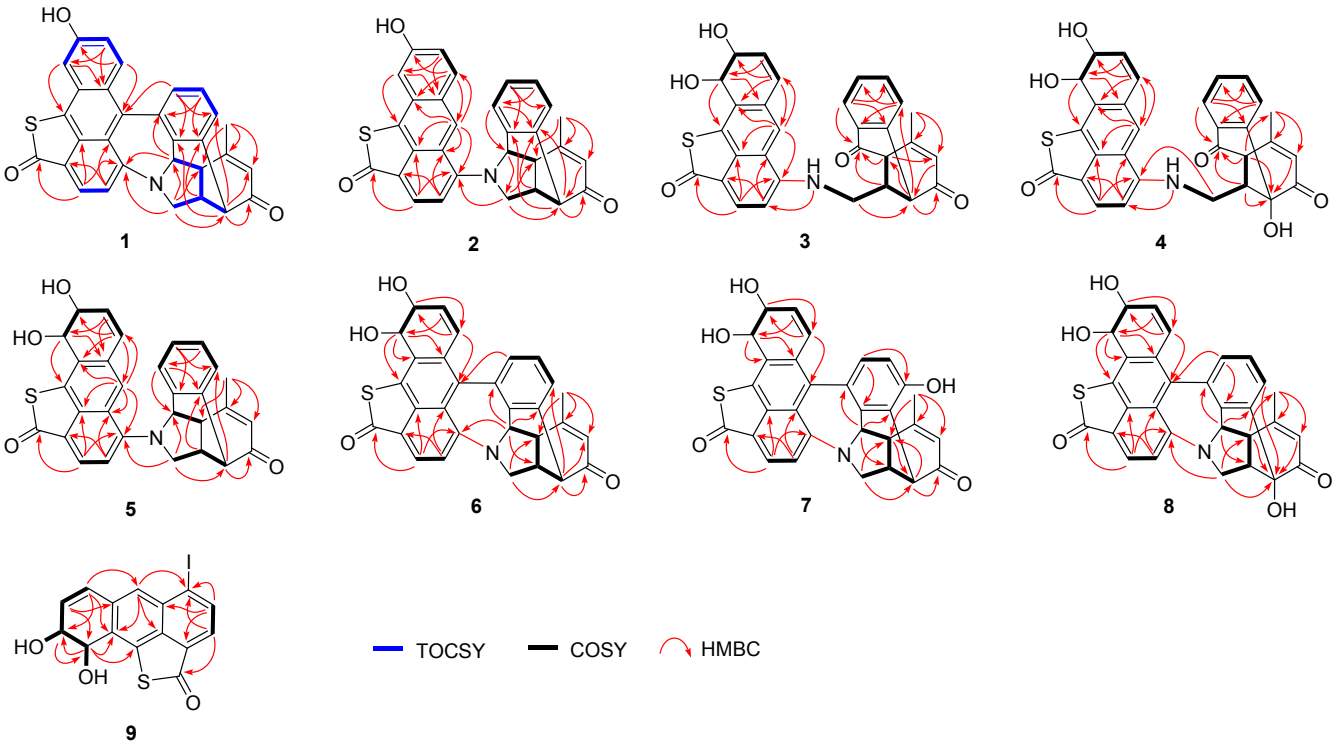

Scheme S3. Key NOESY correlations in the computer-generated 3D drawing of **1**–**8**.

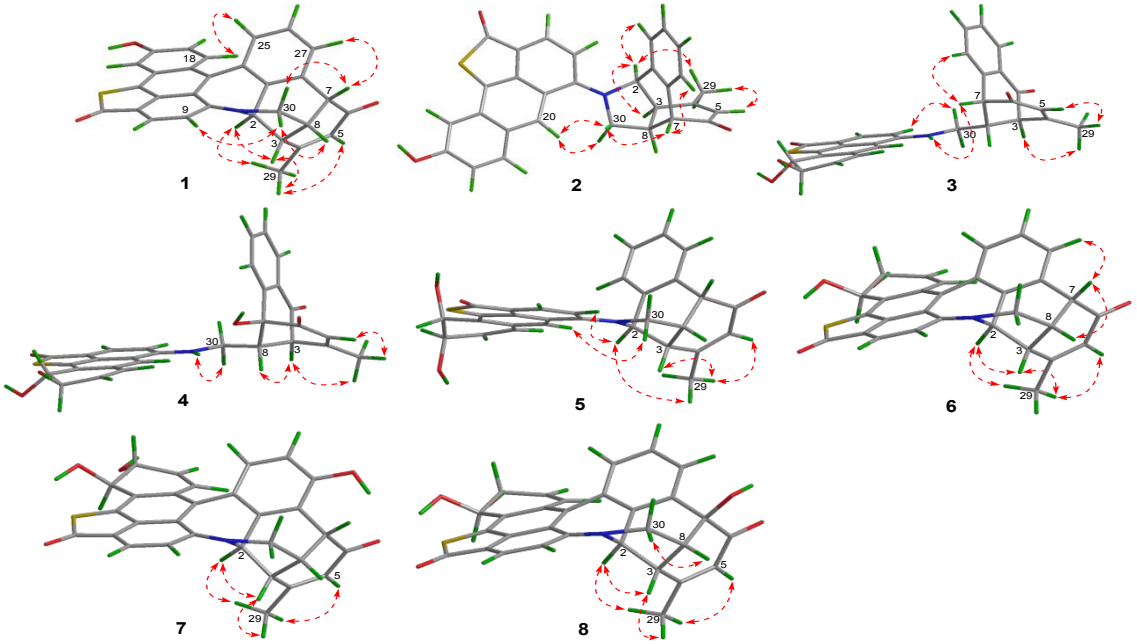

Scheme S4. ^{13}C-labelled structures of **6** and **9**.

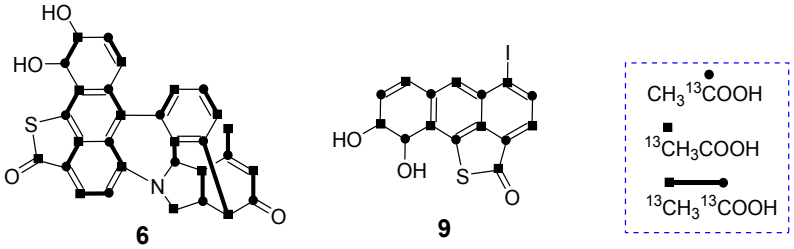

Scheme S5. Incorporation patterns of ^{13}C-labelled Sungeidine, Dynemicin, and Esperamicin.

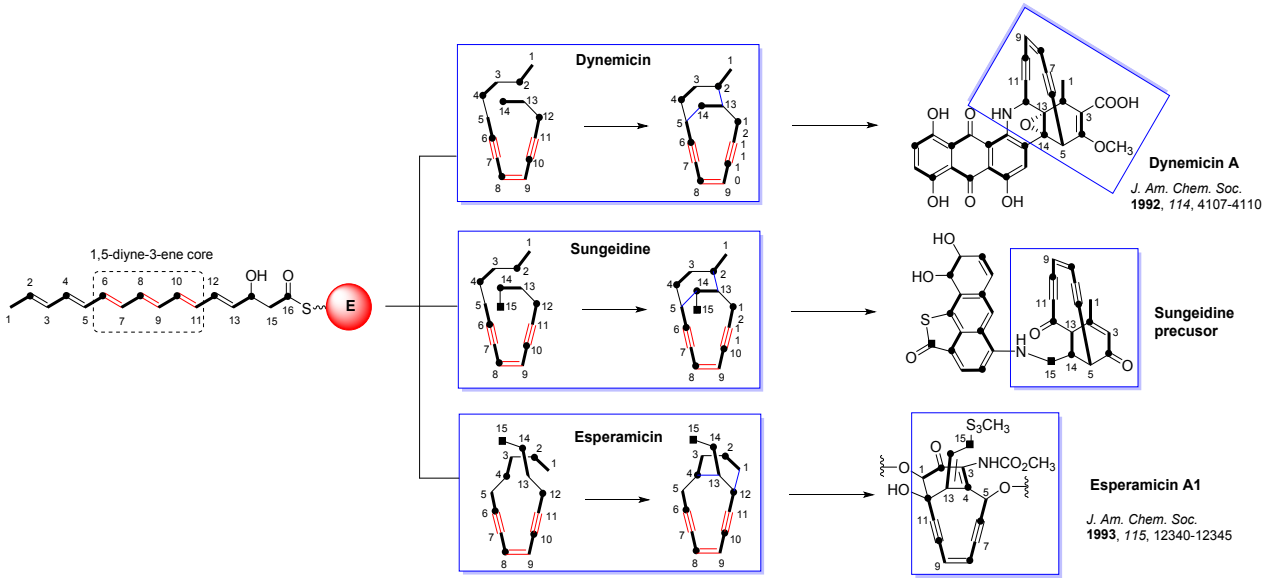

Figure S1-1. ^{1}H NMR spectrum (700 MHz, in DMSO-d_6) of sungeidine A (**1**).

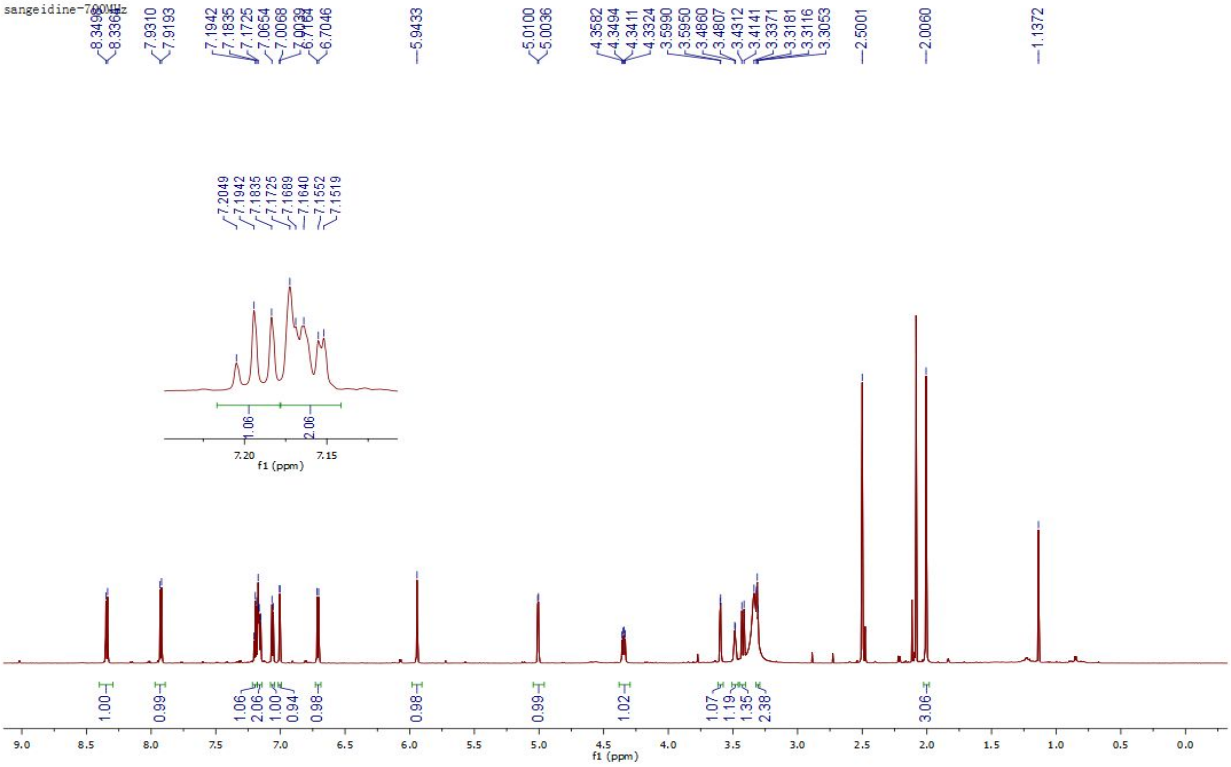

Figure S1-2. ^{13}C NMR spectrum (175 MHz, in DMSO-d_6) of sungeidine A (**1**).

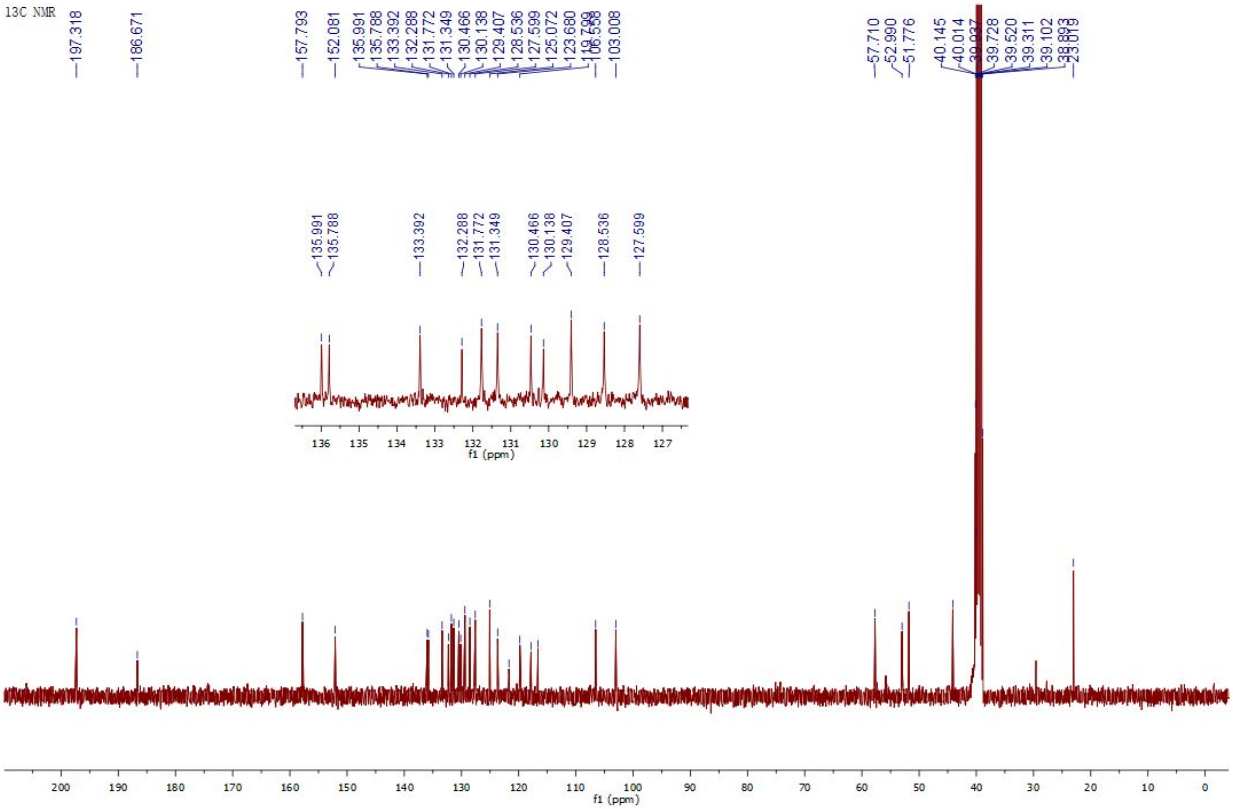

Figure S1-3. HSQC NMR spectrum (700 MHz, in DMSO-d_6) of sungeidine A (**1**).

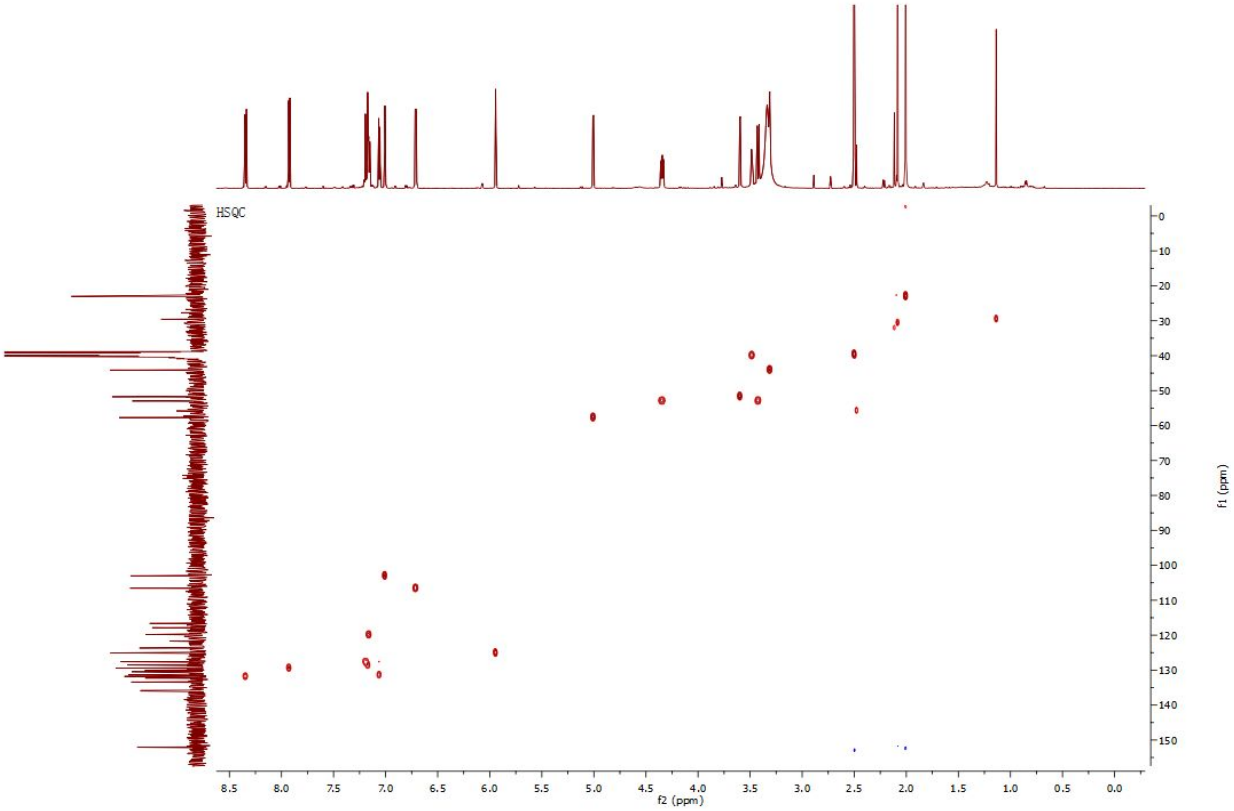

Figure S1-4. TOCSY NMR spectrum (700 MHz, in DMSO-d_6) of sungeidine A (**1**).

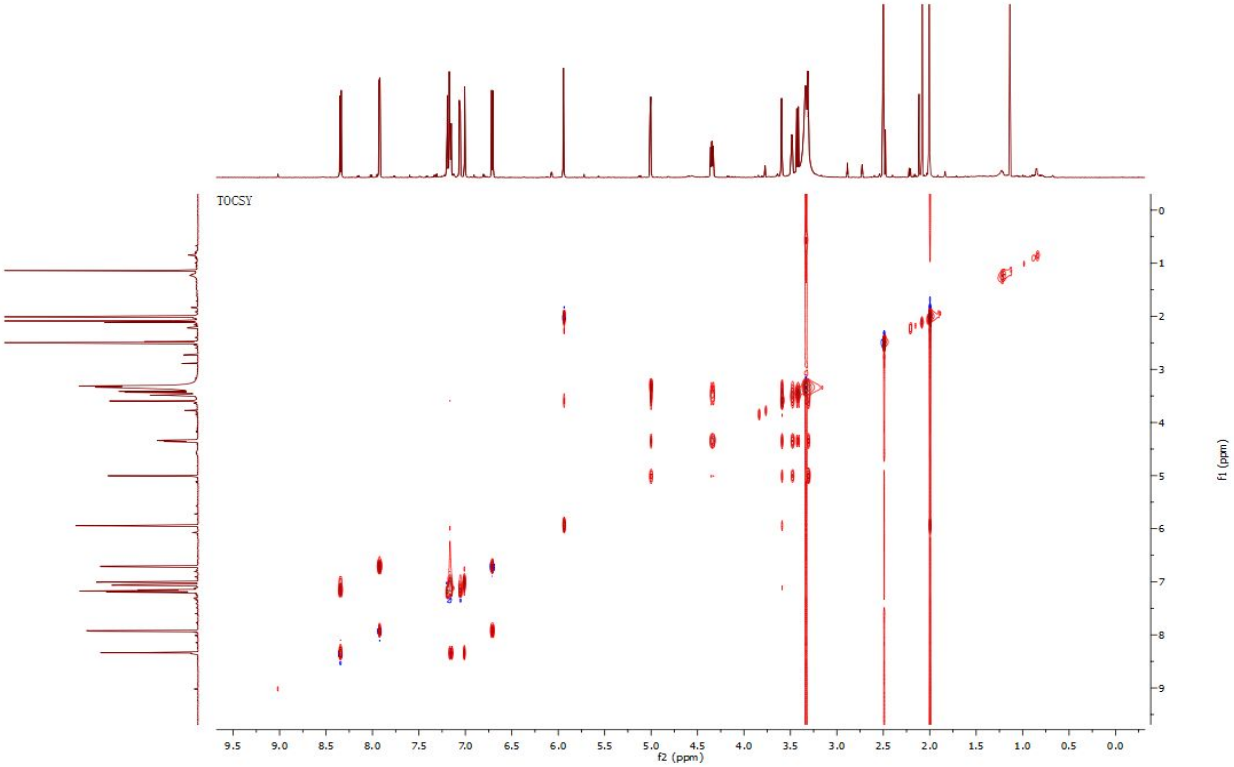

Figure S1-5. ^{1}H-^{1}H COSY NMR spectrum (700 MHz, in DMSO-d_6) of sungeidine A (**1**).

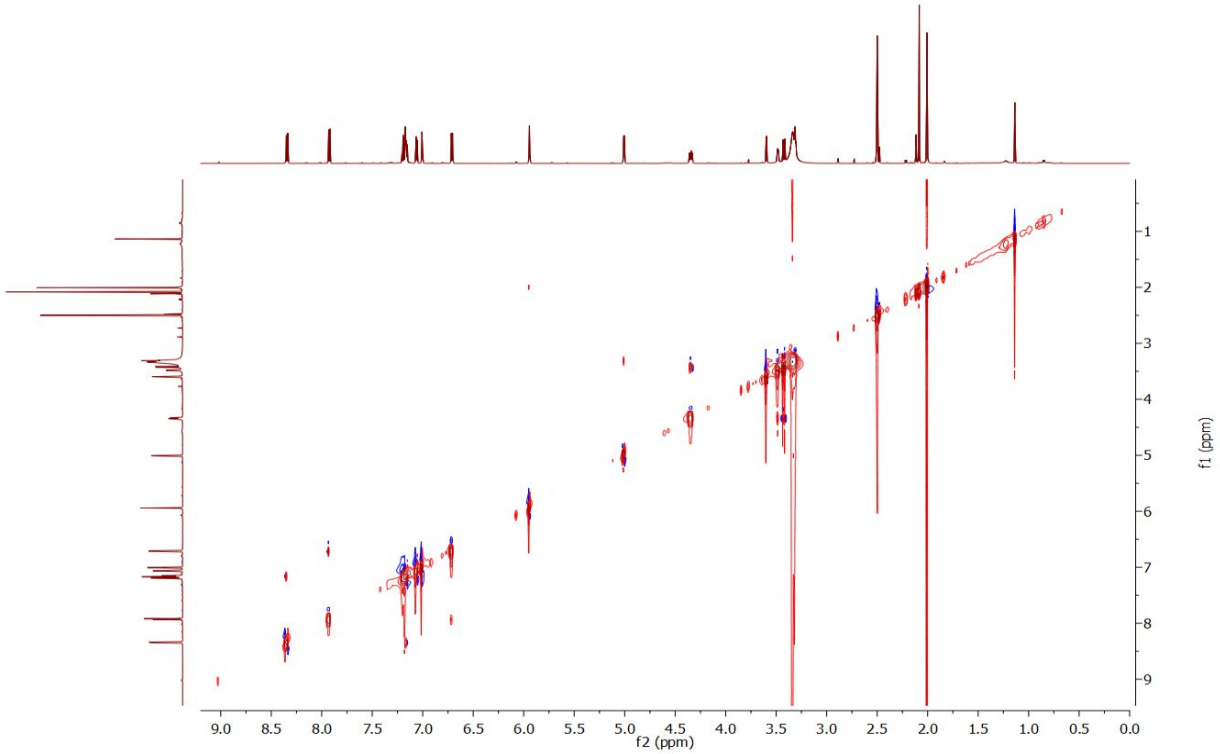

Figure S1-6. HMBC NMR spectrum (700 MHz, in DMSO-d_6) of sungeidine A (**1**).

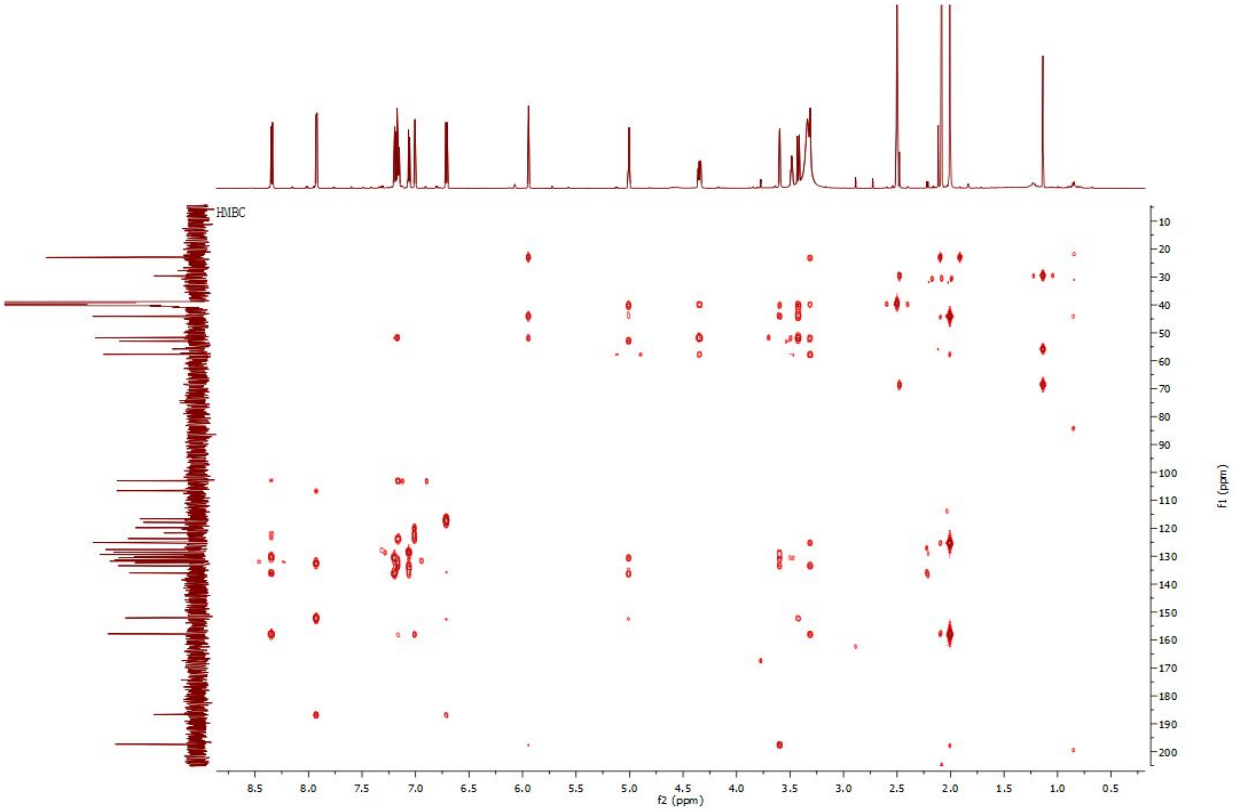

Figure S1-7. NOESY NMR spectrum (700 MHz, in DMSO-d_6) of sungeidine A (**1**).

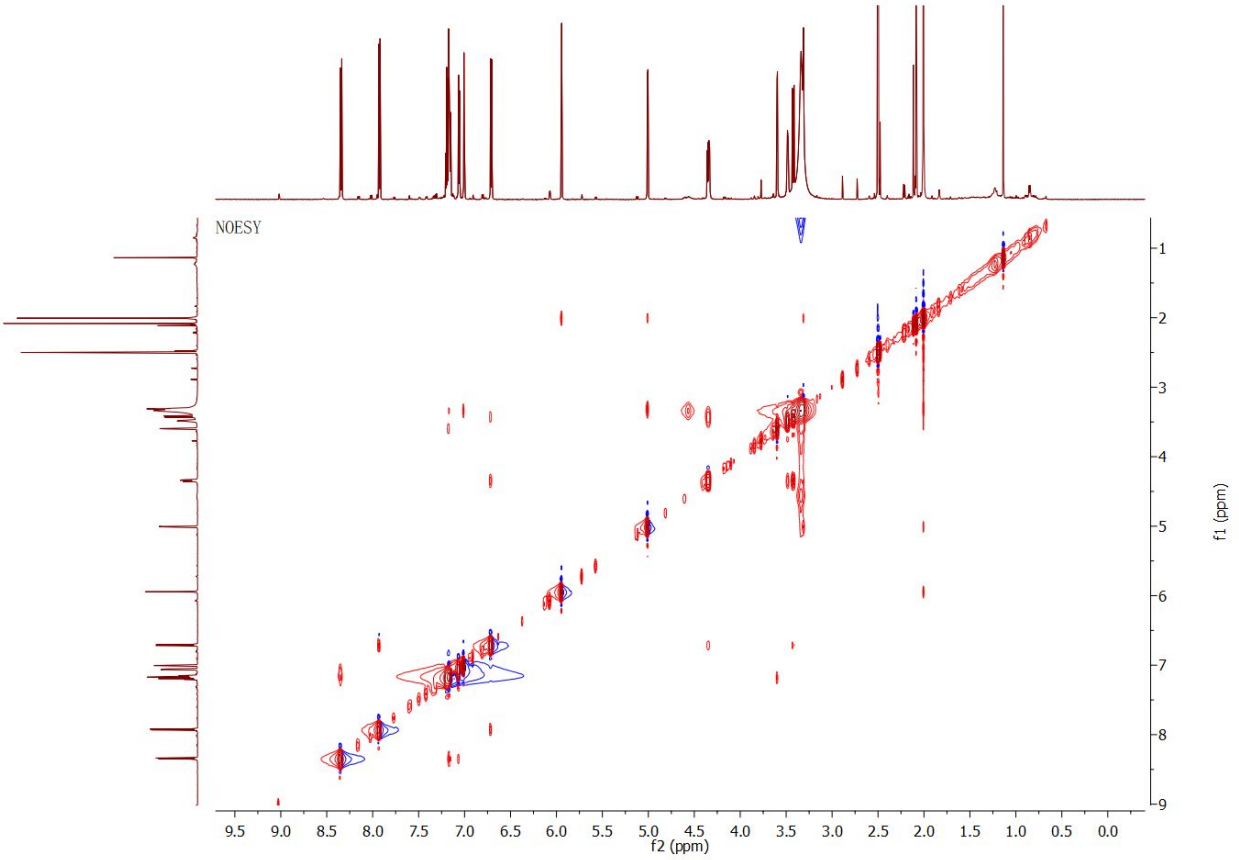

Figure S1-8. HRESIMS spectrum of sungeidine A (**1**).

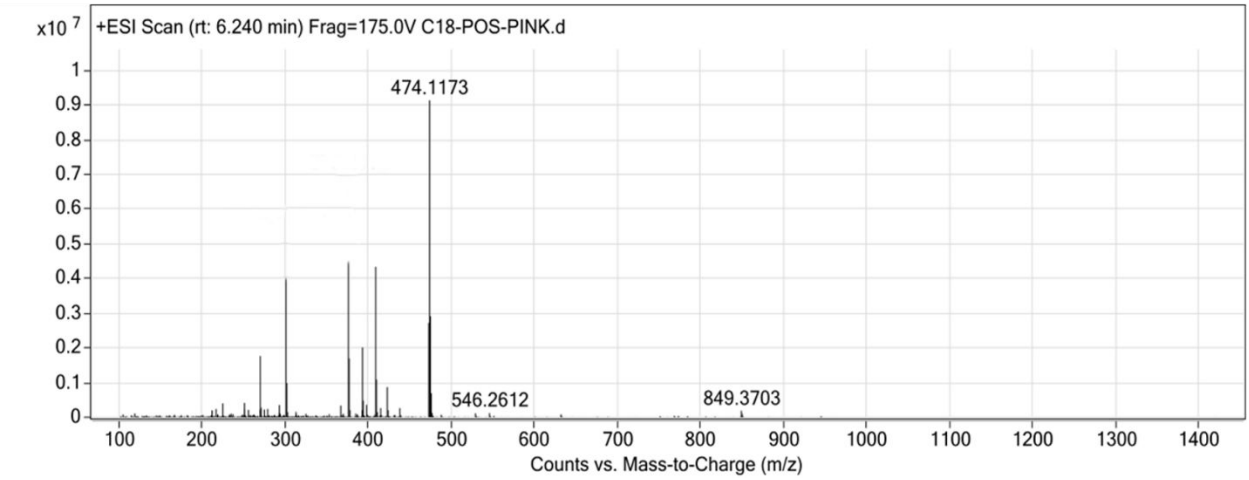

Figure S2-1: ^{1}H NMR spectrum (700 MHz, in DMSO-d_6) of sungeidine B (**2**)

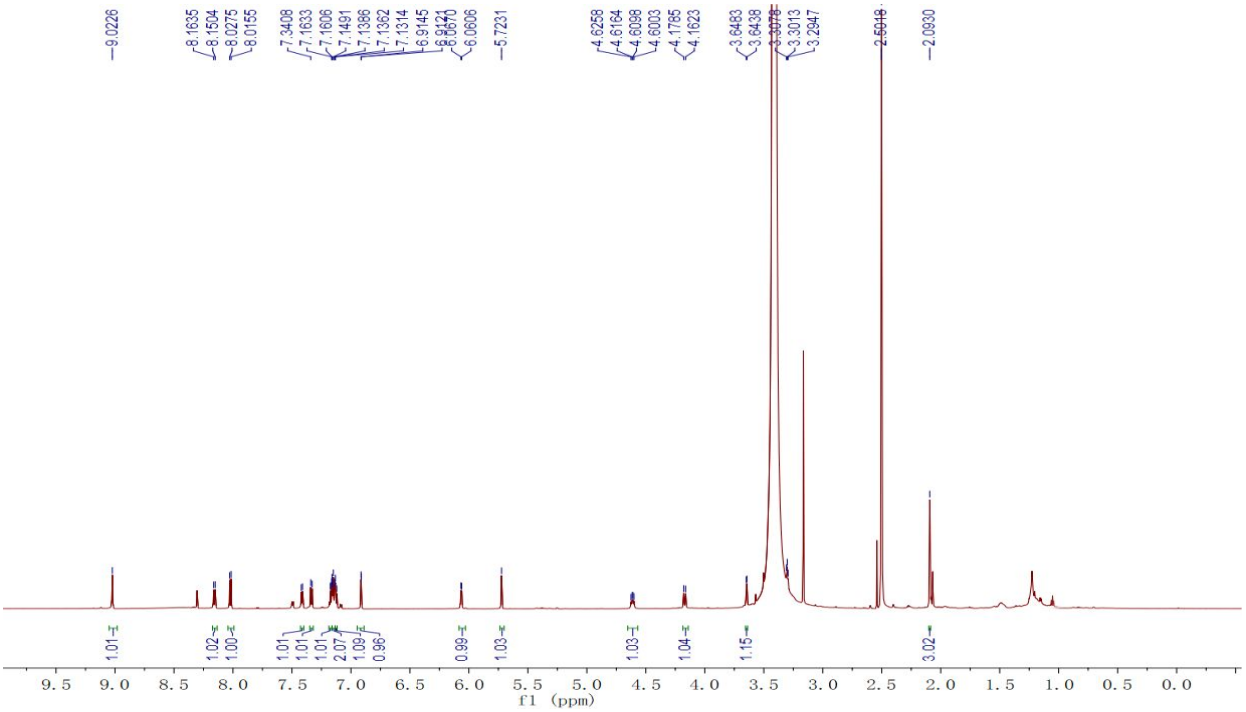

Figure S2-2: ^{13}C NMR spectrum (175 MHz, in DMSO-d_6) of sungeidine B (**2**)

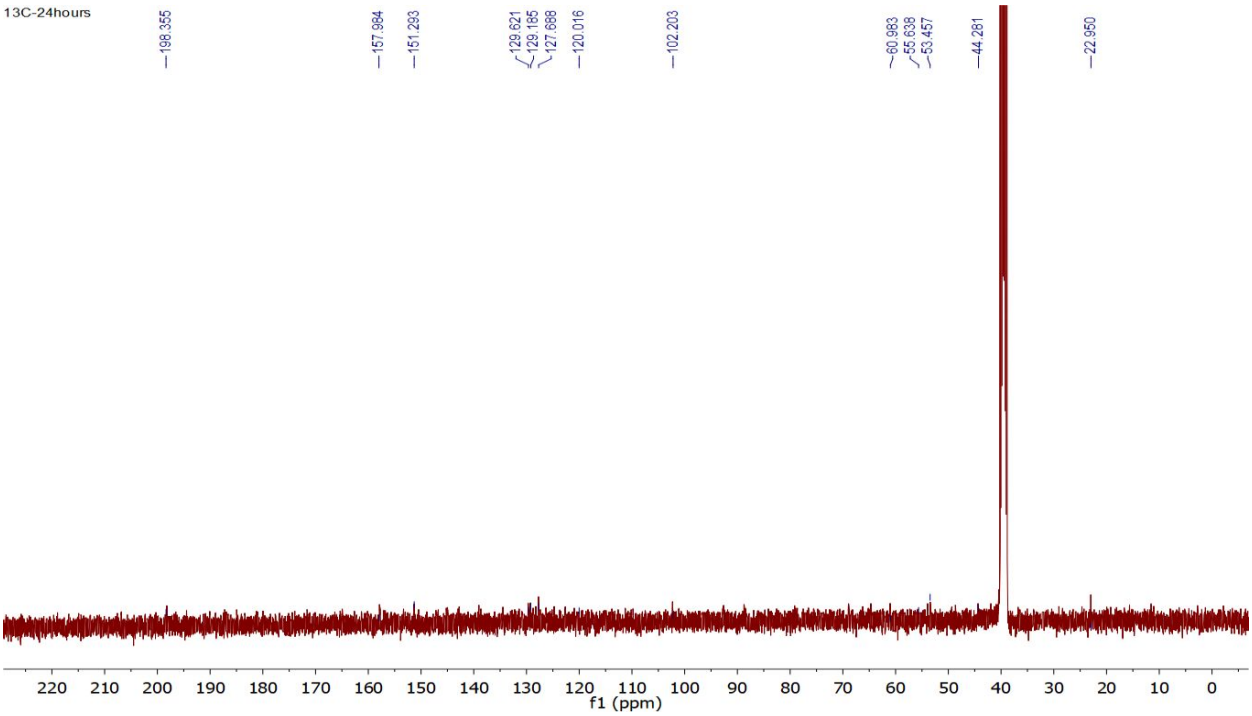

The ^{13}C NMR assignment of tiny amount **2** (0.5 mg) was achieved mainly based on the HSQC and HMBC data analyses, since the acquired ^{13}C signals (24 hr) were extremely weak.

Figure S2-3: HSQC NMR spectrum (700 MHz, in DMSO-d_6) of sungeidine B (**2**)

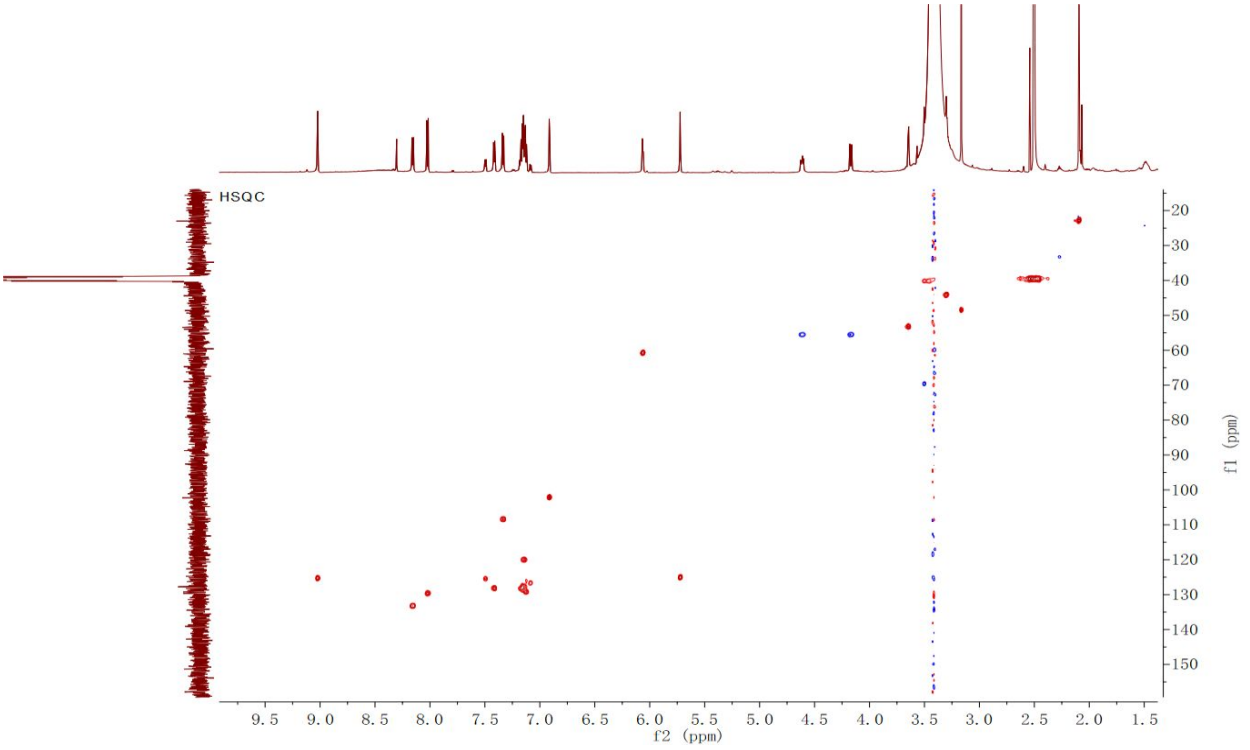

Figure S2-4: ^{1}H-^{1}H COSY NMR spectrum (700 MHz, in DMSO-d_6) of sungeidine B (**2**)

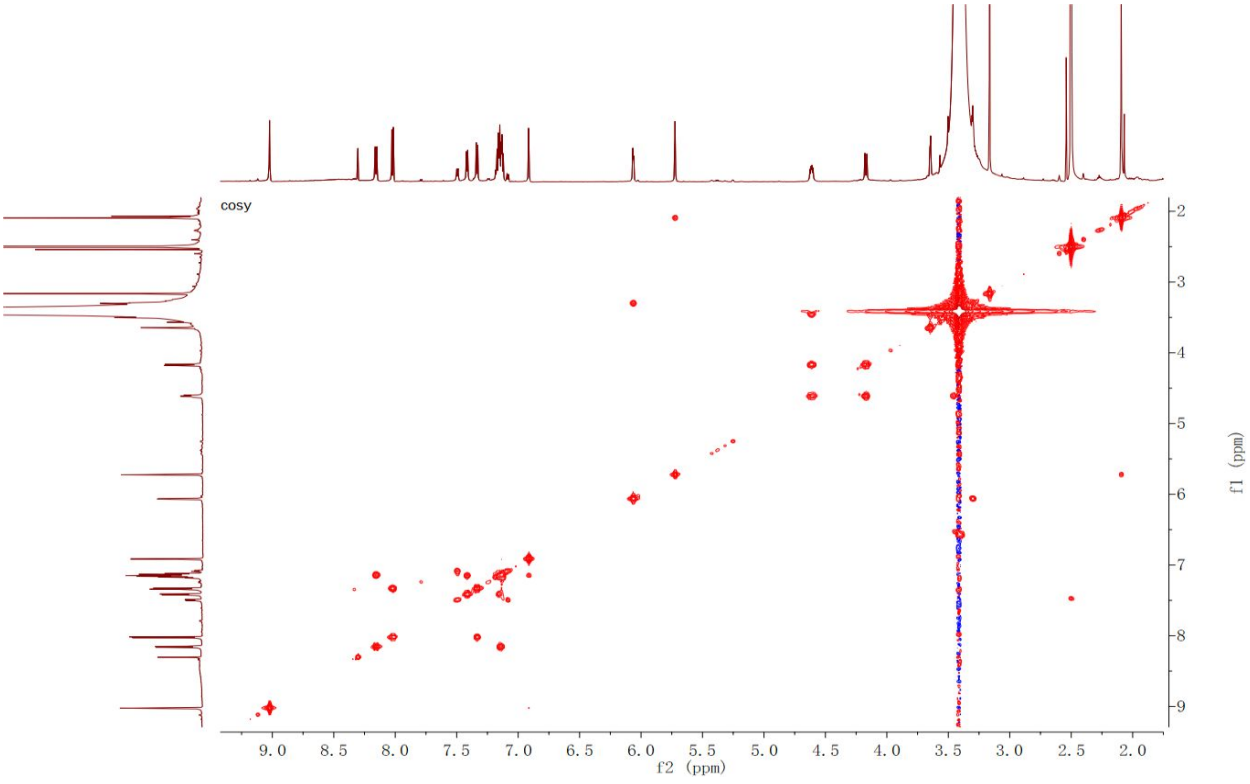

Figure S2-5: HMBC NMR spectrum (700 MHz, in DMSO-d_6) of sungeidine B (**2**)

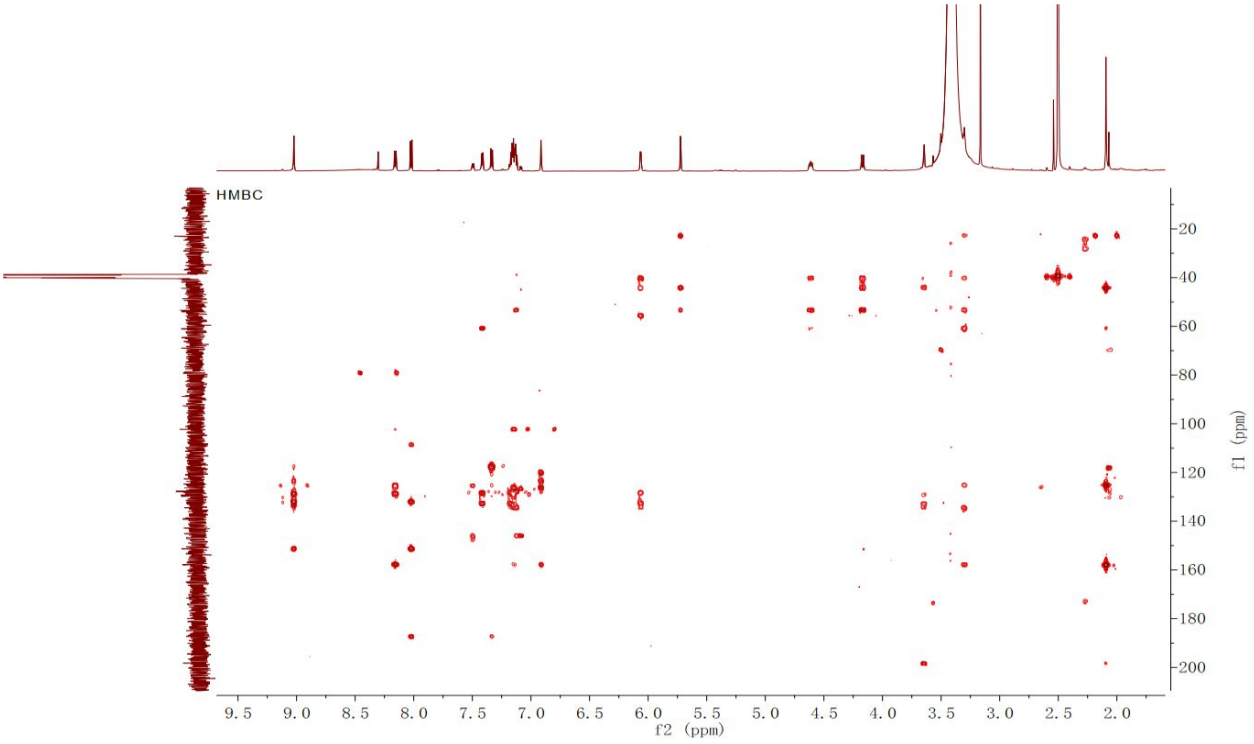

Figure S2-6: NOESY NMR spectrum (700 MHz, in DMSO-d_6) of sungeidine B (**2**)

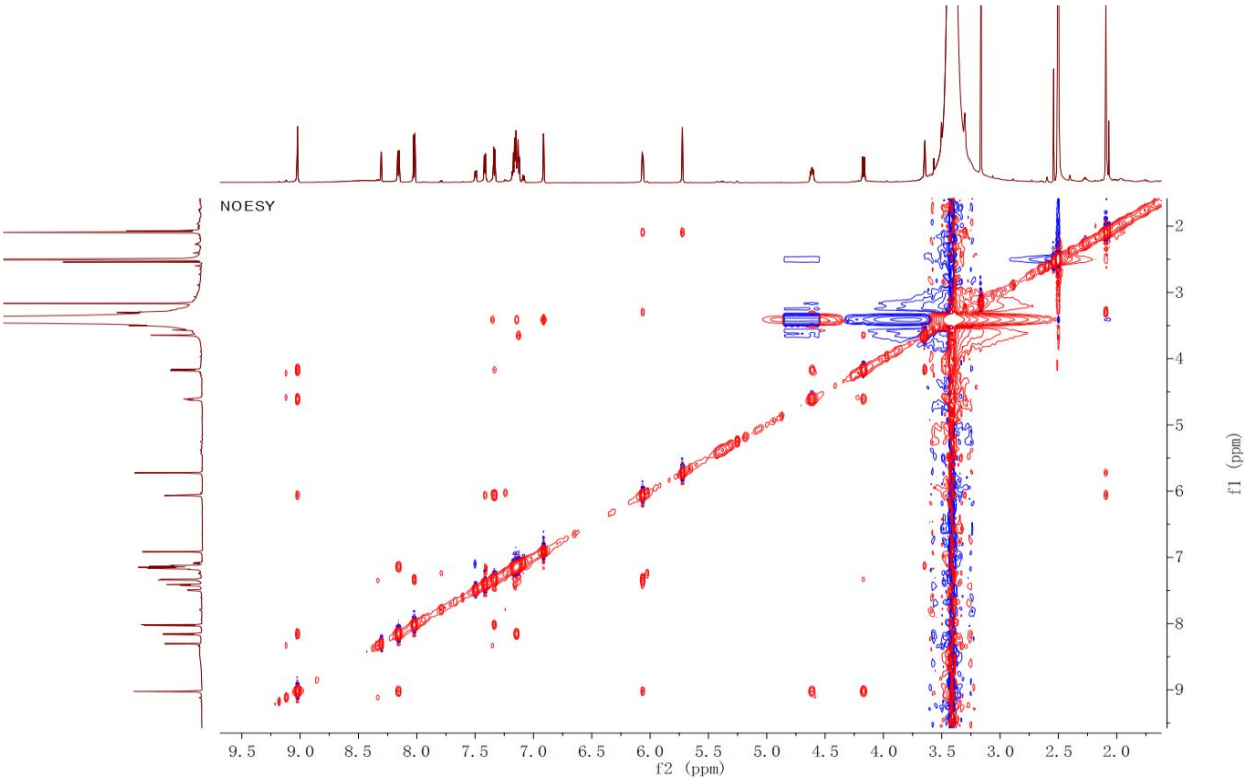

Figure S3-1. ^{1}H NMR spectrum (400 MHz, in DMSO-d_6) of sungeidine C (**3**)

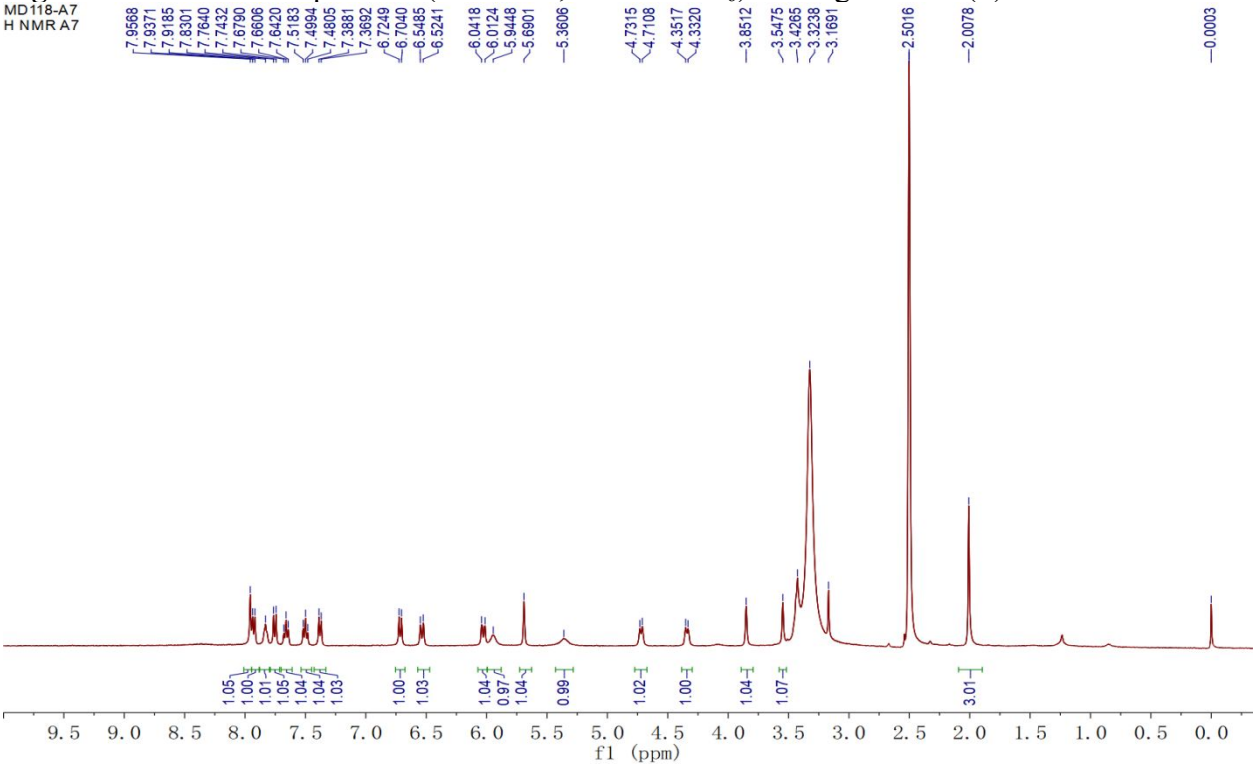

Figure S3-2. ^{13}C NMR spectrum (100 MHz, in DMSO-d_6) of sungeidine C (**3**)

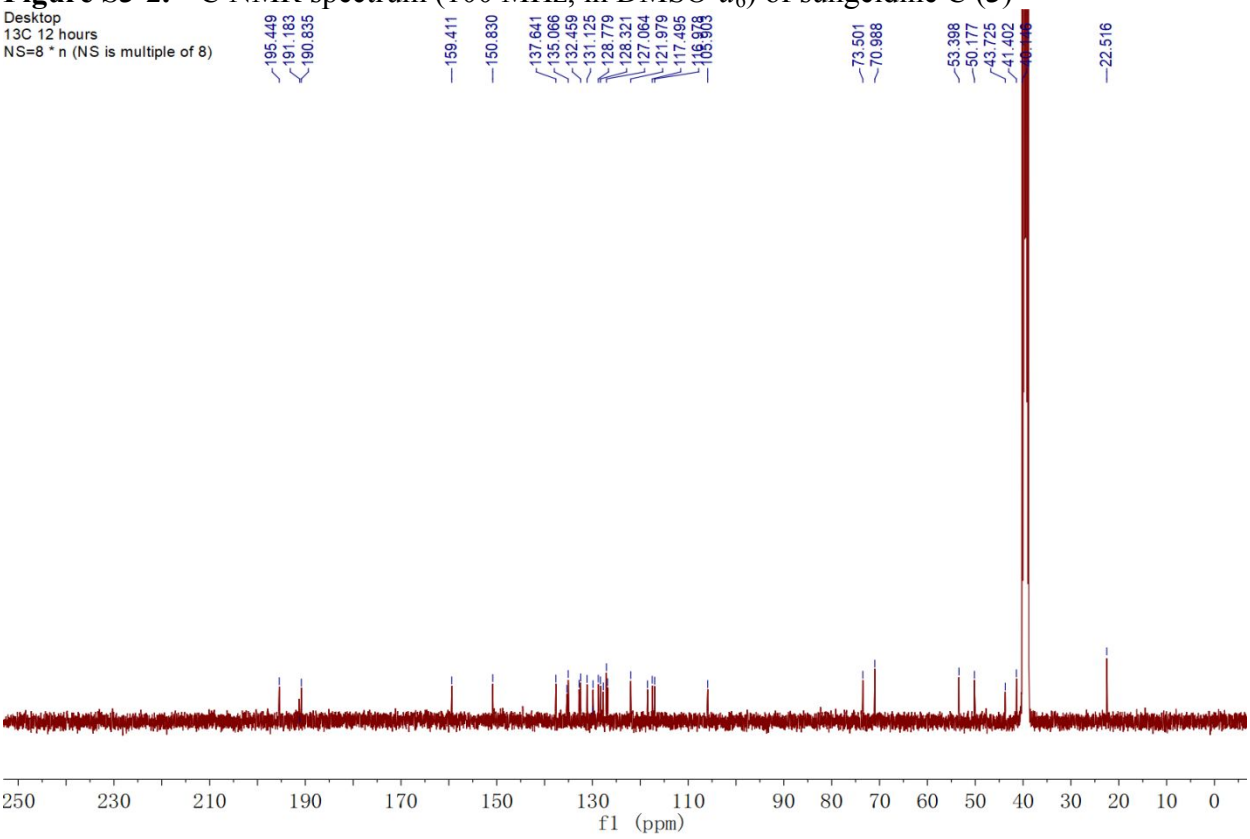

Figure S3-3. HSQC NMR spectrum (400 MHz, in DMSO-d_6) of sungeidine C (**3**)

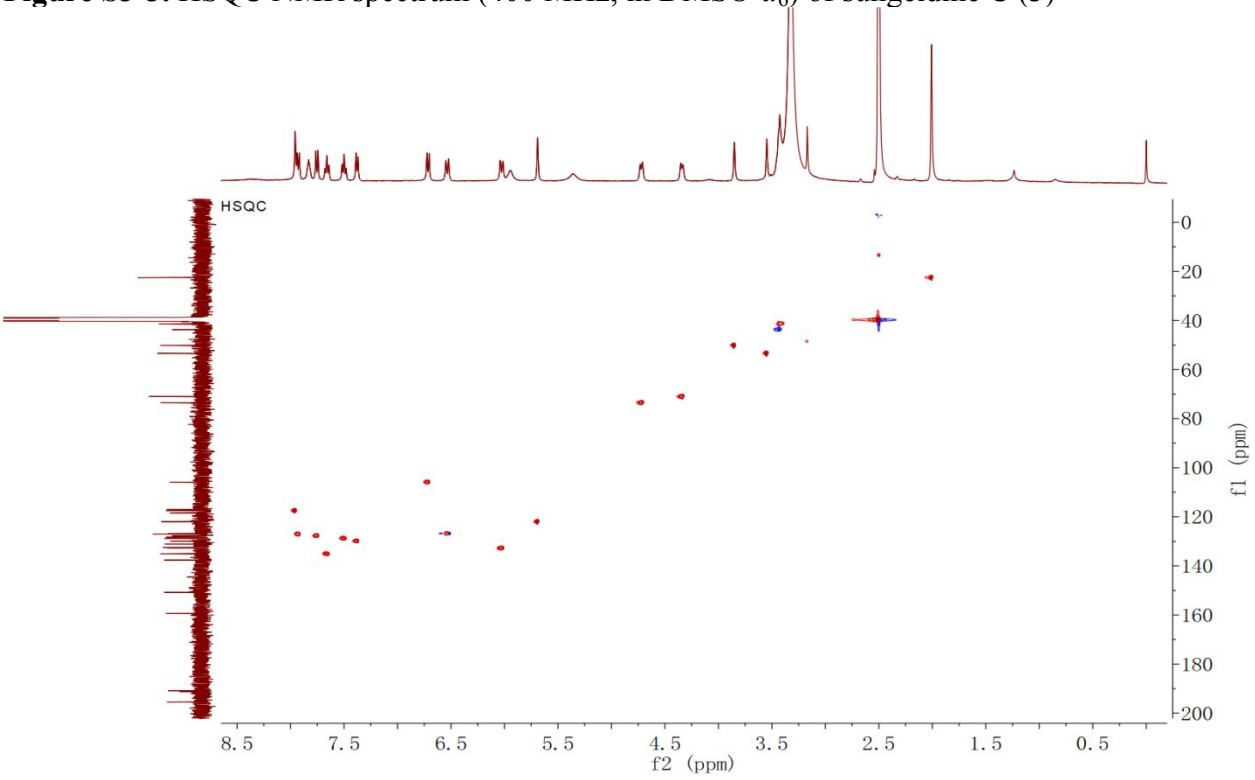

Figure S3-4. ^{1}H-^{1}H COSY NMR spectrum (400 MHz, in DMSO-d_6) of sungeidine C (**3**)

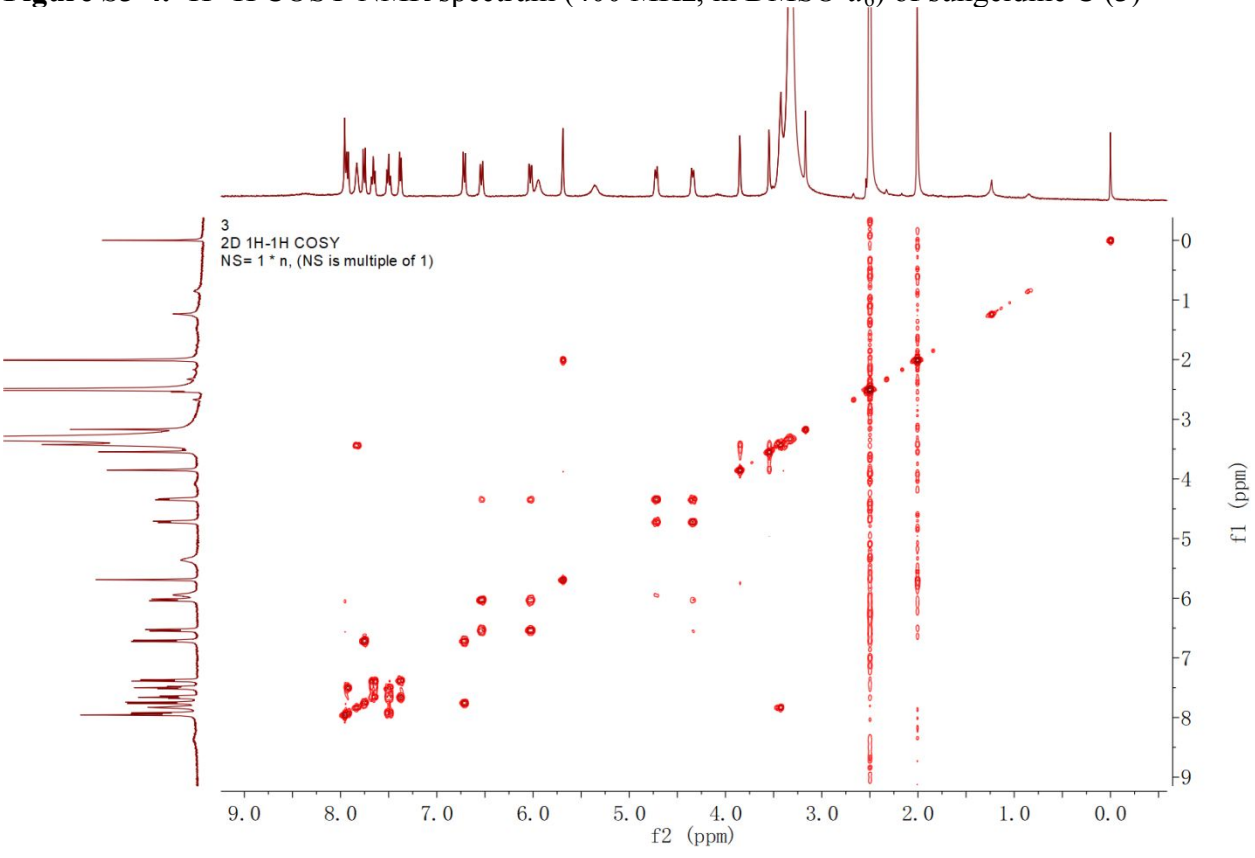

Figure S3-5. HMBC NMR spectrum (400 MHz, in DMSO-d_6) of sungeidine C (**3**)

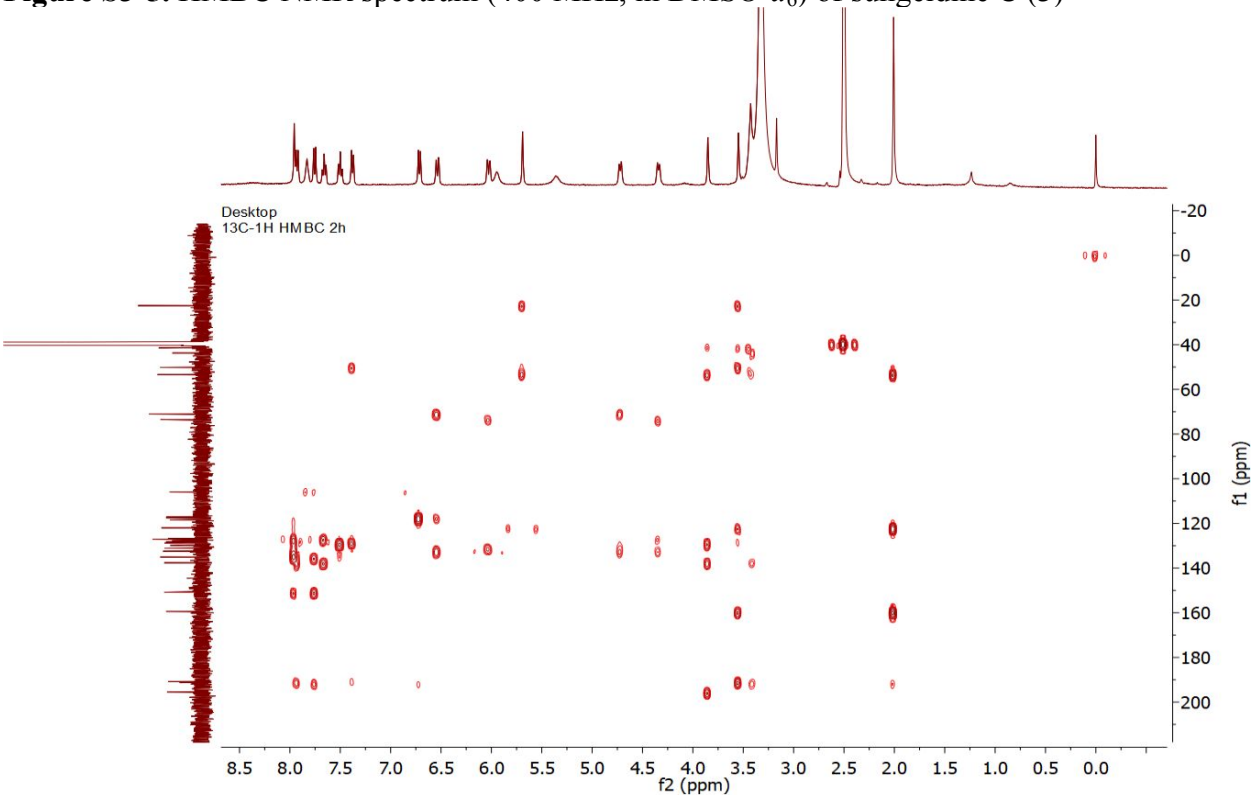

Figure S3-6. NOESY NMR spectrum (400 MHz, in DMSO-d_6) of sungeidine C (**3**)

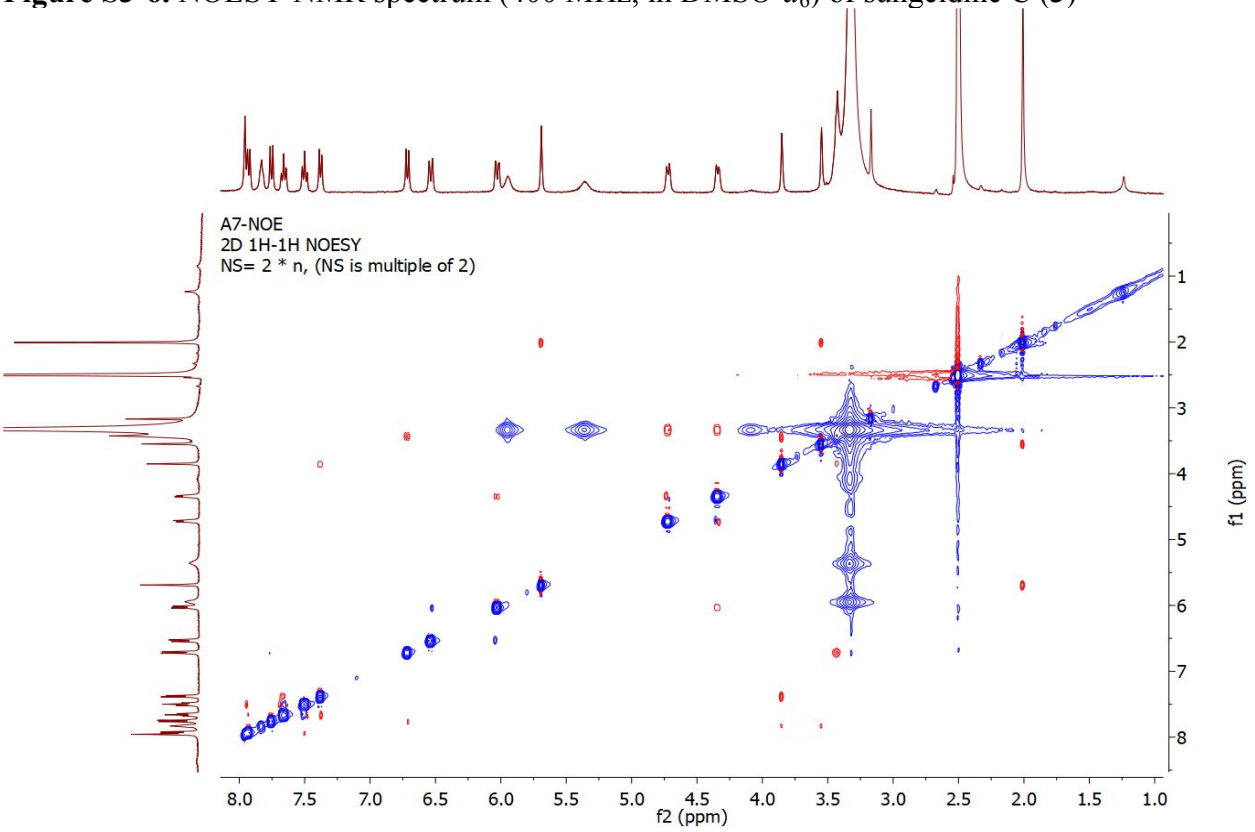

Figure S4-1: ^{1}H NMR spectrum (600 MHz, in DMSO-d_6) of sungeidine D (**4**)

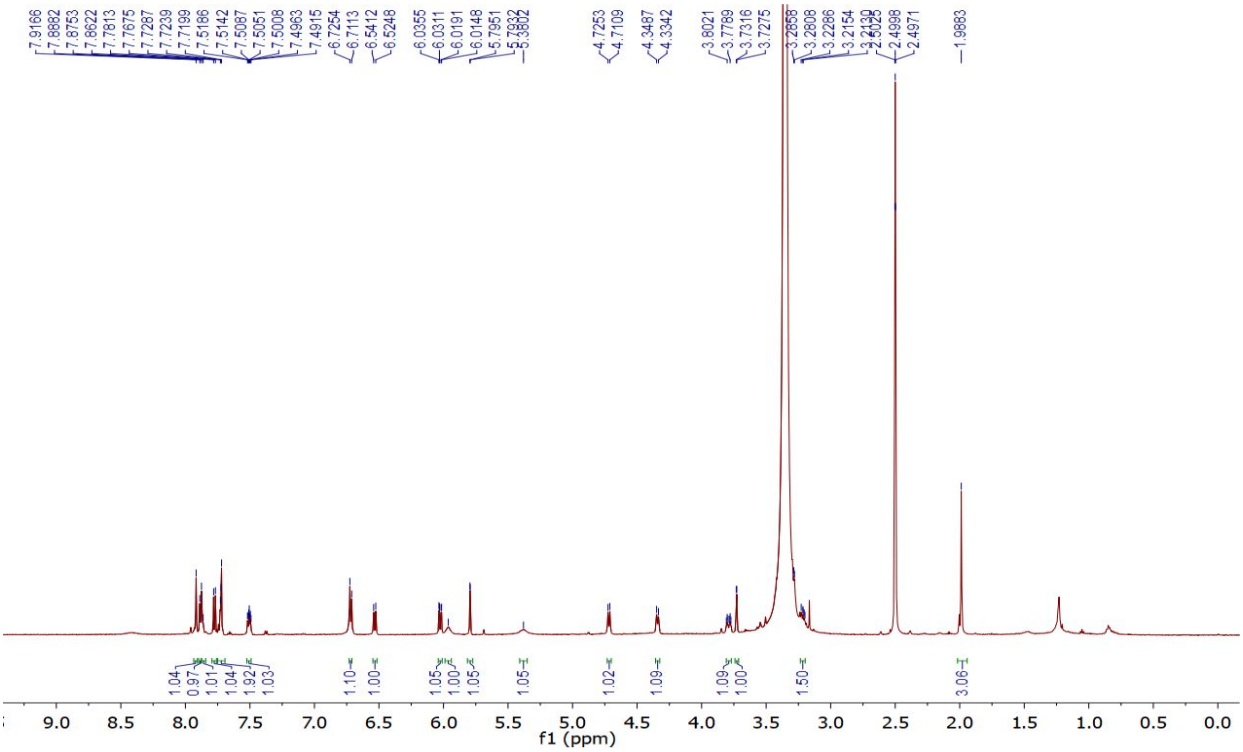

Figure S4-2: ^{13}C NMR spectrum (150 MHz, in DMSO-d_6) of sungeidine D (**4**)

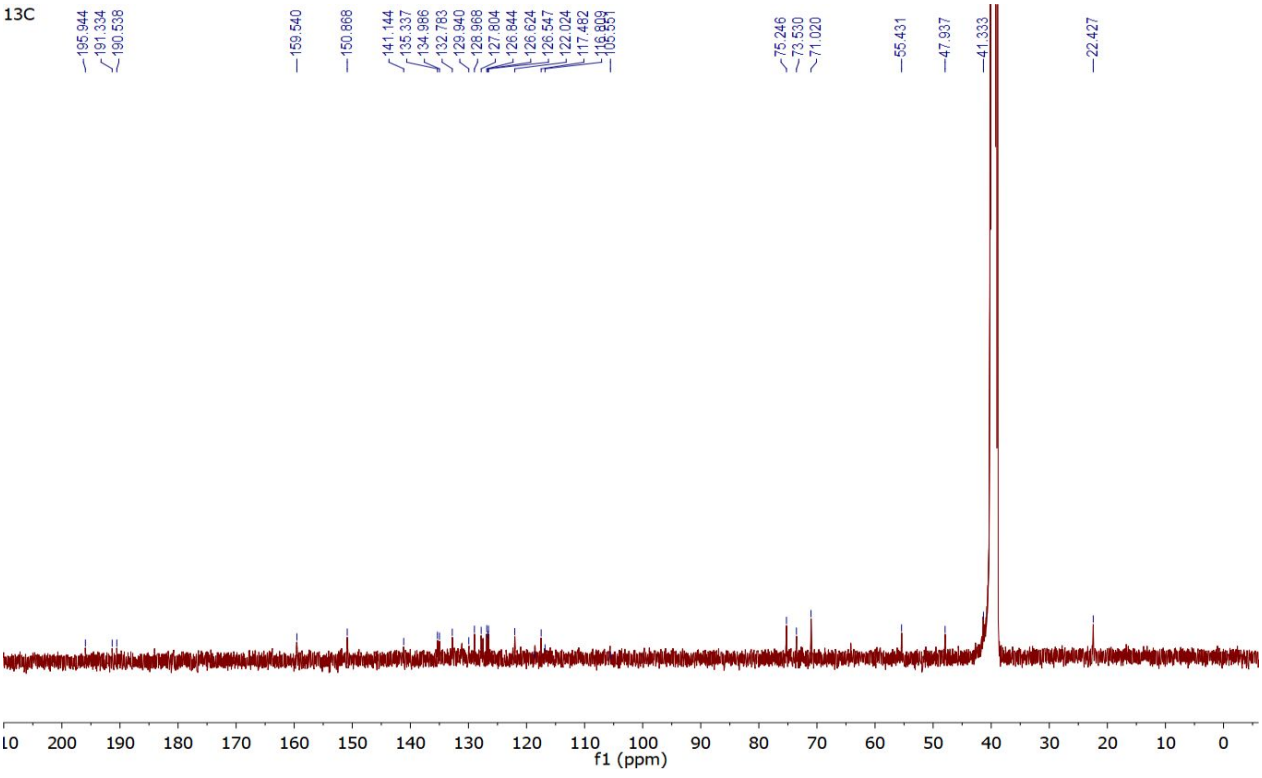

Figure S4-3: HSQC NMR spectrum (600 MHz, in DMSO-d_6) of sungeidine D (**4**)

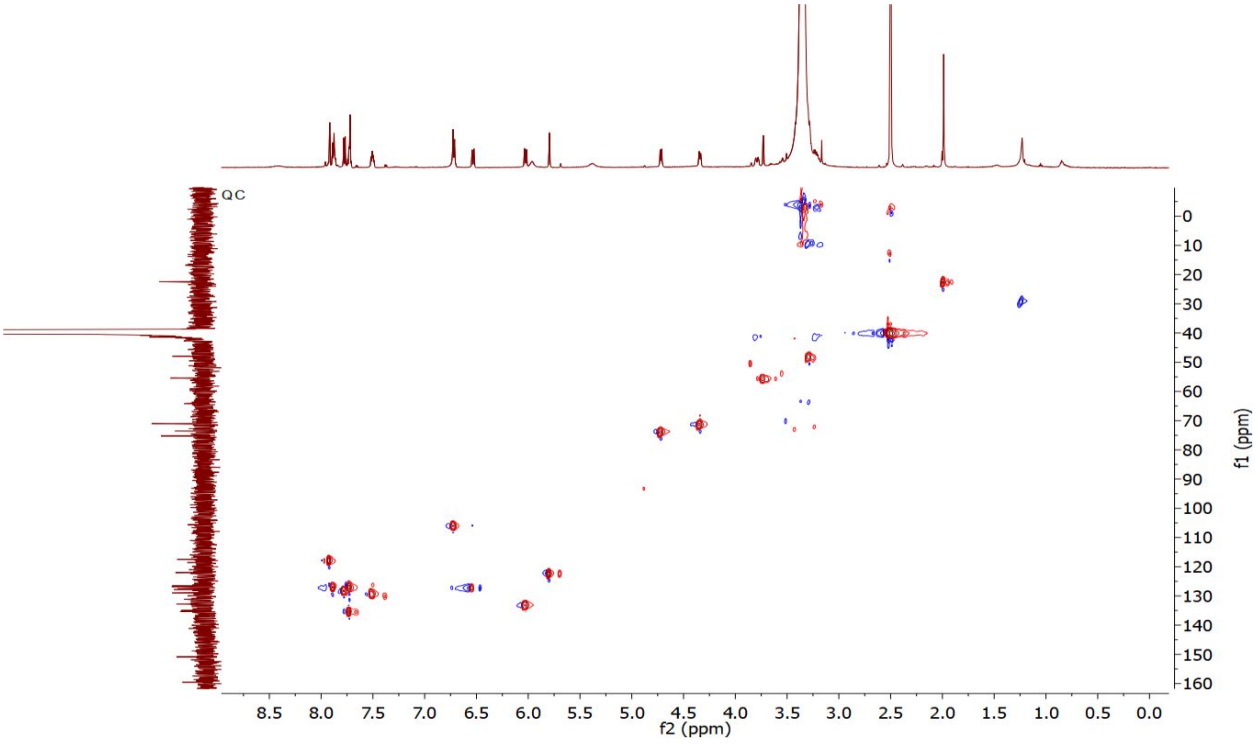

Figure S4-4: ^{1}H-^{1}H COSY NMR spectrum (600 MHz, in DMSO-d_6) of sungeidine D (**4**)

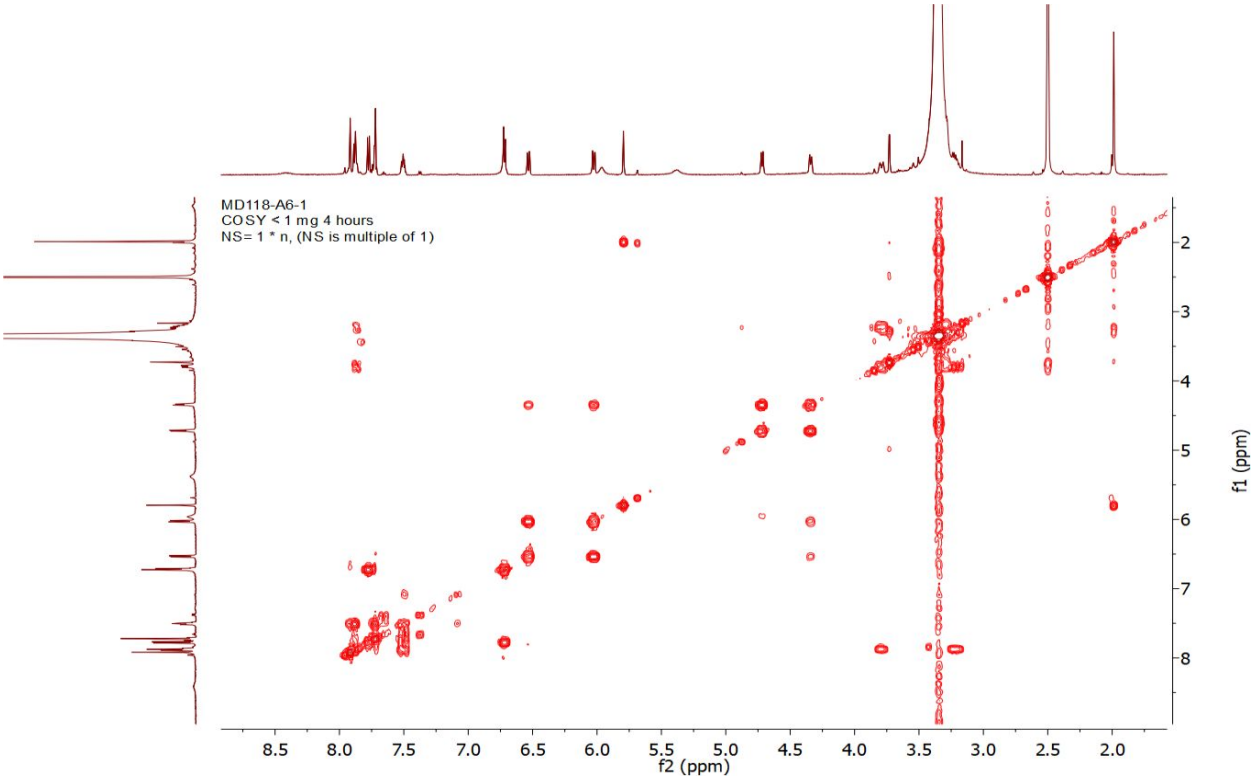

Figure S4-5: HMBC NMR spectrum (600 MHz, in DMSO-d_6) of sungeidine D (**4**)

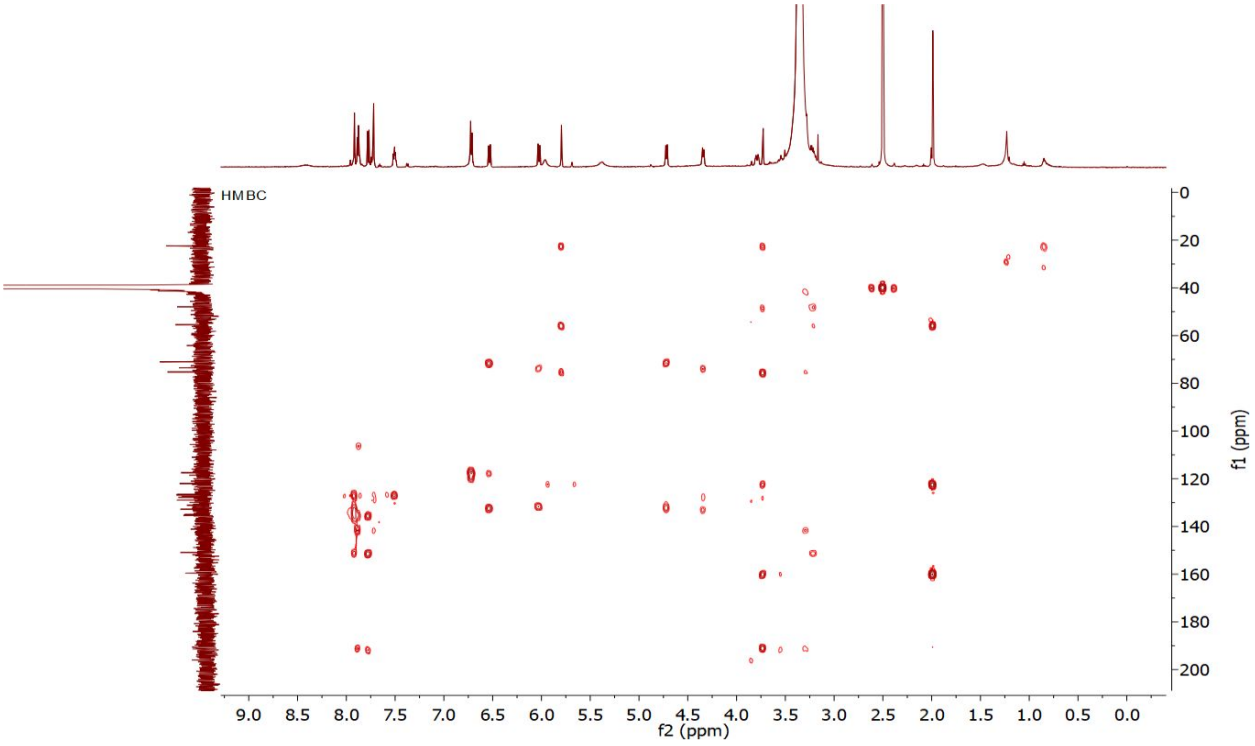

Figure S4-6: NOESY NMR spectrum (600 MHz, in DMSO-d_6) of sungeidine D (**4**)

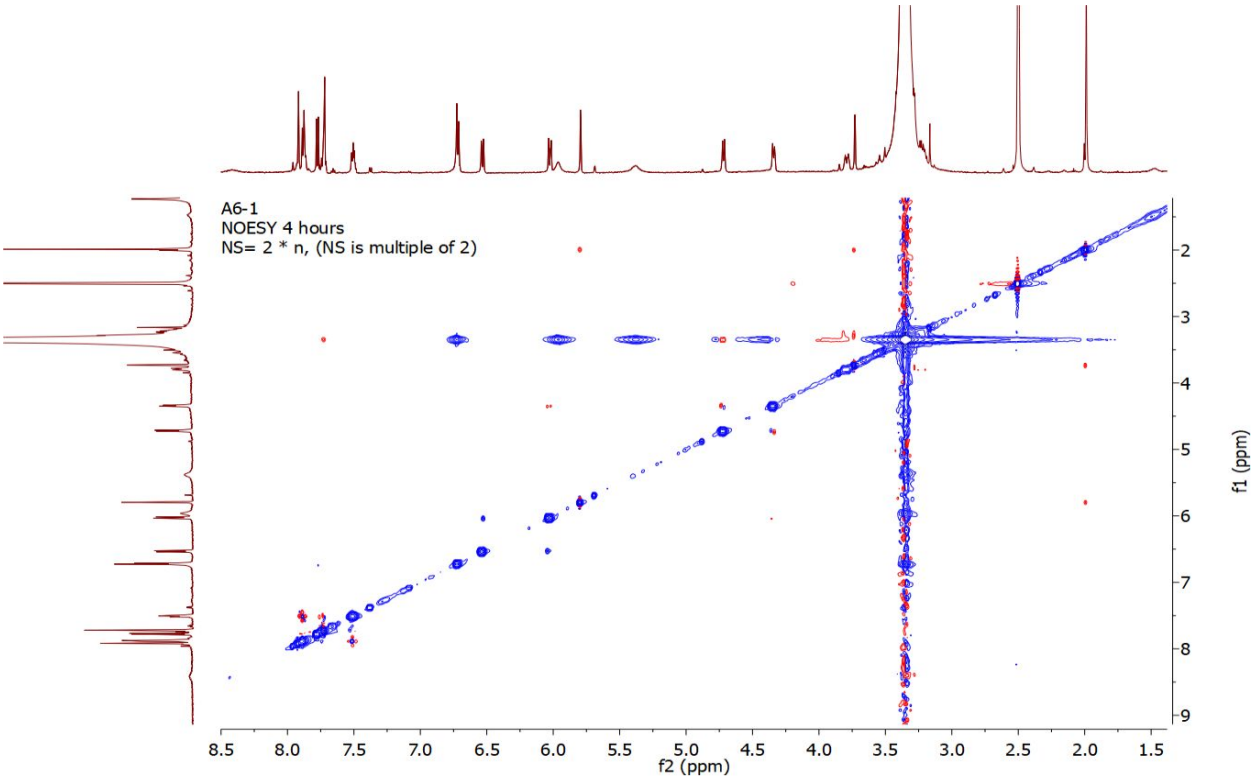

Figure S5-1: ^{1}H NMR spectrum (600 MHz, in DMSO-d_6) of sungeidine E (**5**)

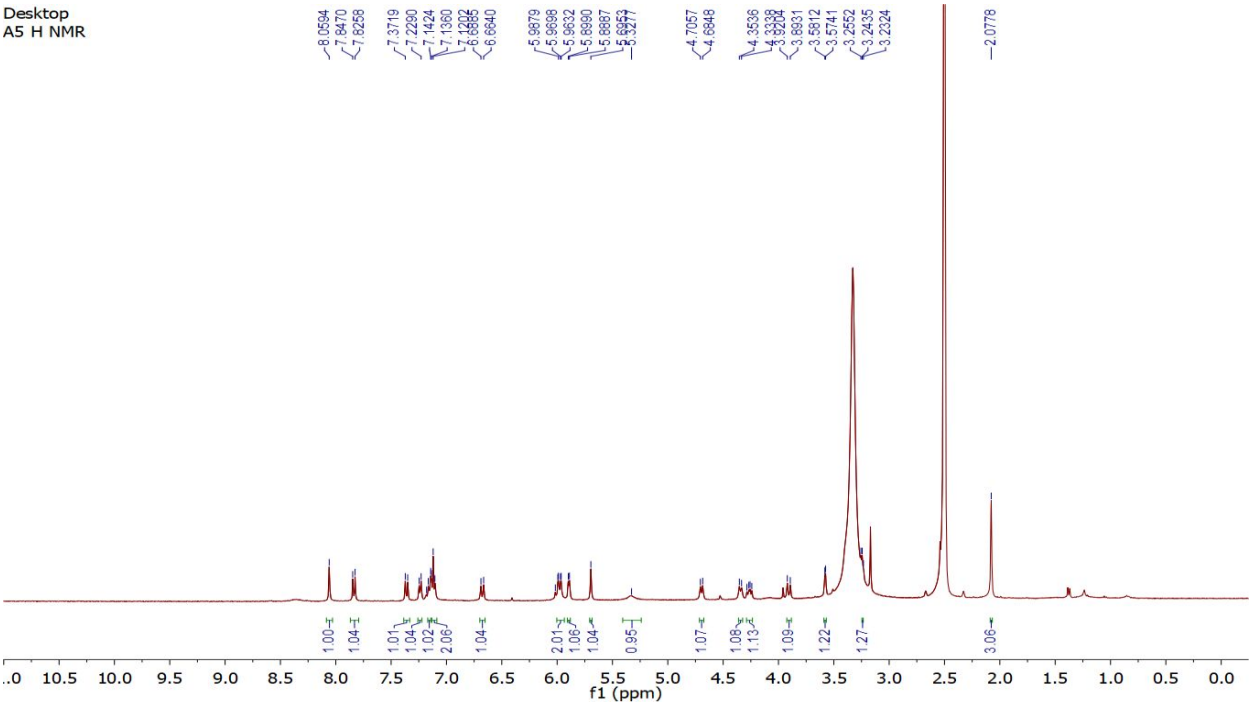

Figure S5-2: ^{13}C NMR spectrum (150 MHz, in DMSO-d_6) of sungeidine E (**5**)

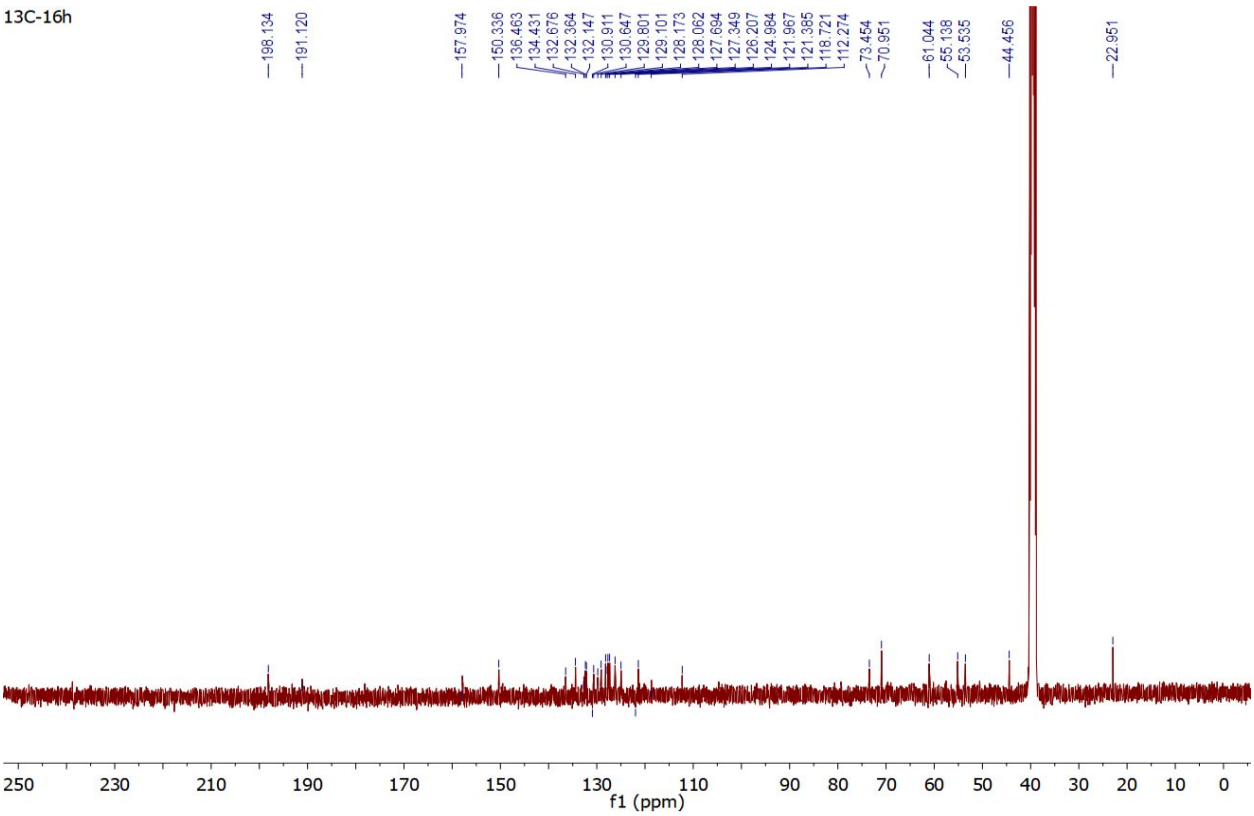

Figure S5-3: HSQC NMR spectrum (600 MHz, in DMSO-d_6) of sungeidine E (**5**)

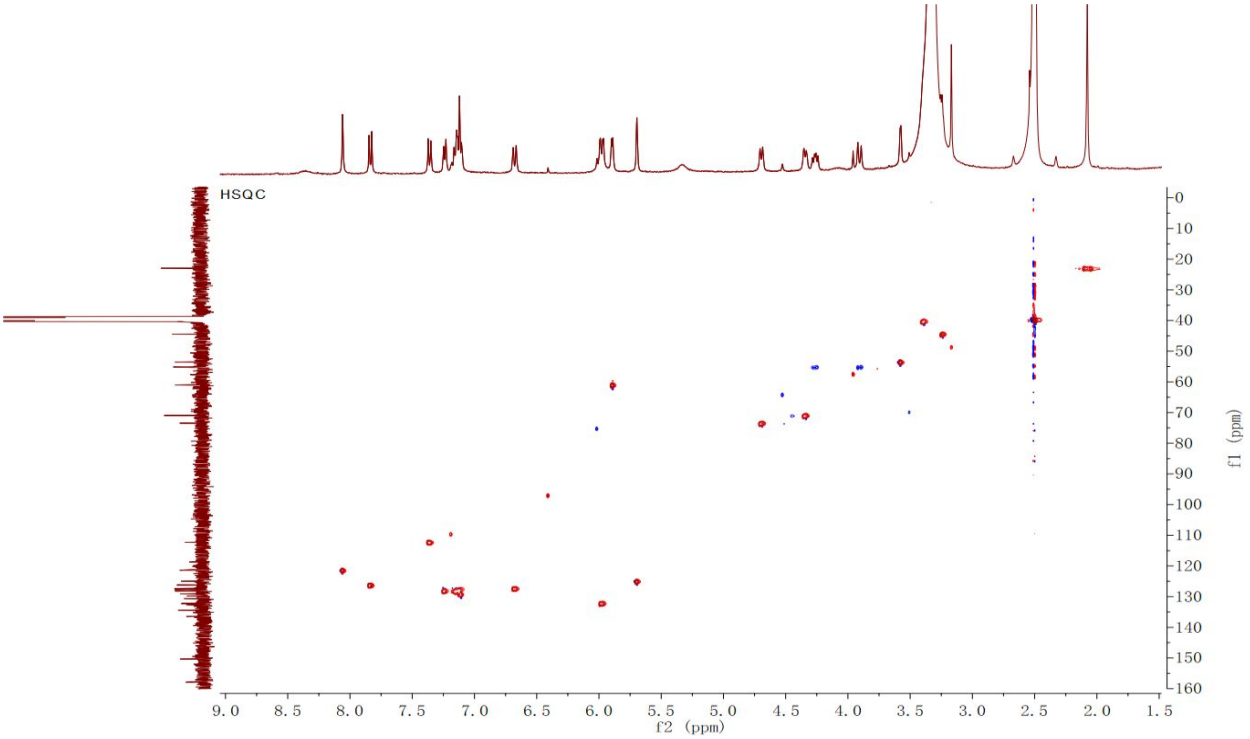

Figure S5-4: ^{1}H-^{1}H COSY NMR spectrum (600 MHz, in DMSO-d_6) of sungeidine E (**5**)

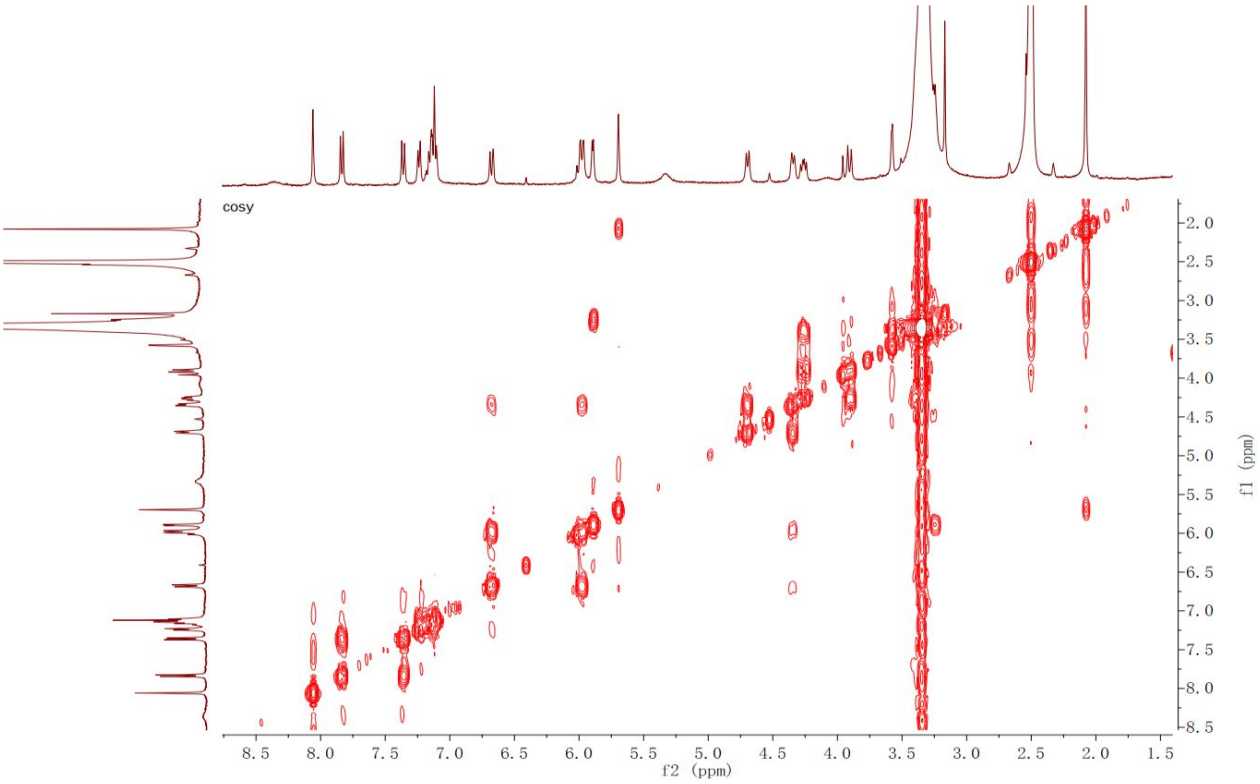

Figure S5-5: HMBC NMR spectrum (600 MHz, in DMSO-d_6) of sungeidine E (**5**)

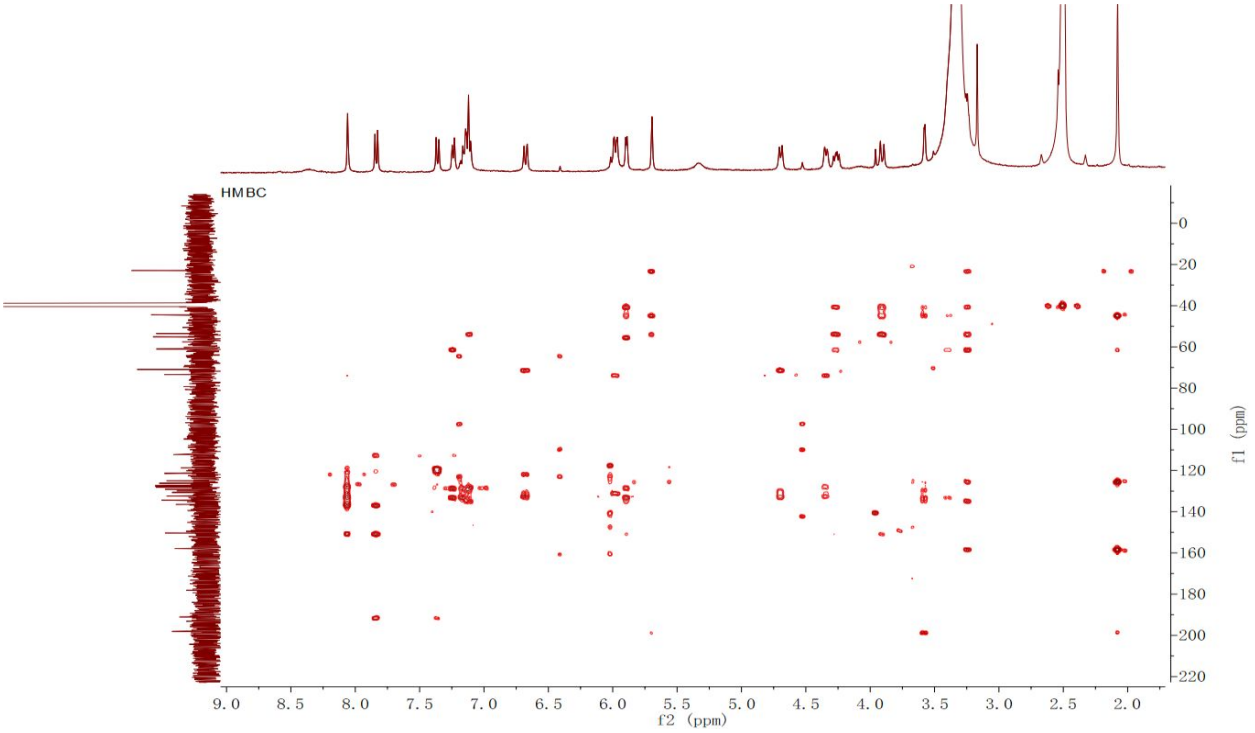

Figure S5-6: NOESY NMR spectrum (600 MHz, in DMSO-d_6) of sungeidine E (**5**)

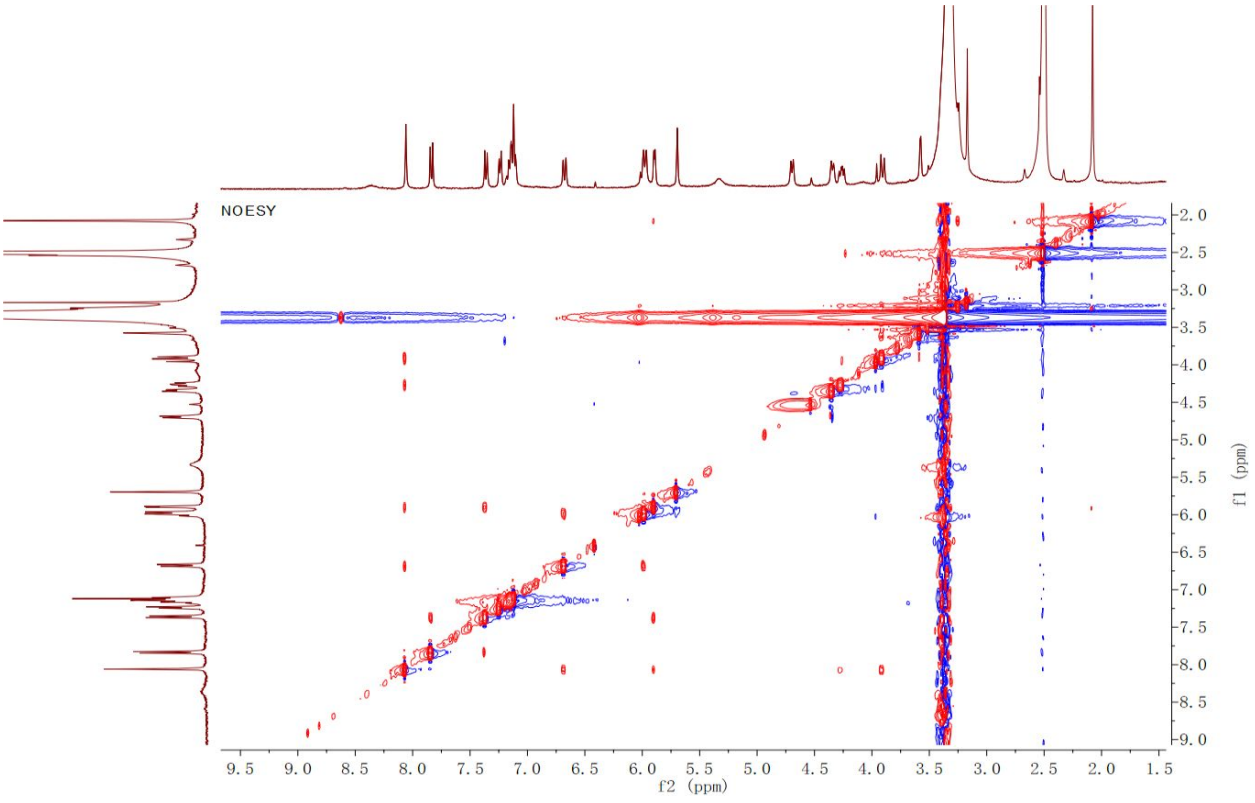

Figure S6-1. ^{1}H NMR spectrum (400 MHz, in DMSO-d_6) of sungeidine F (**6**)

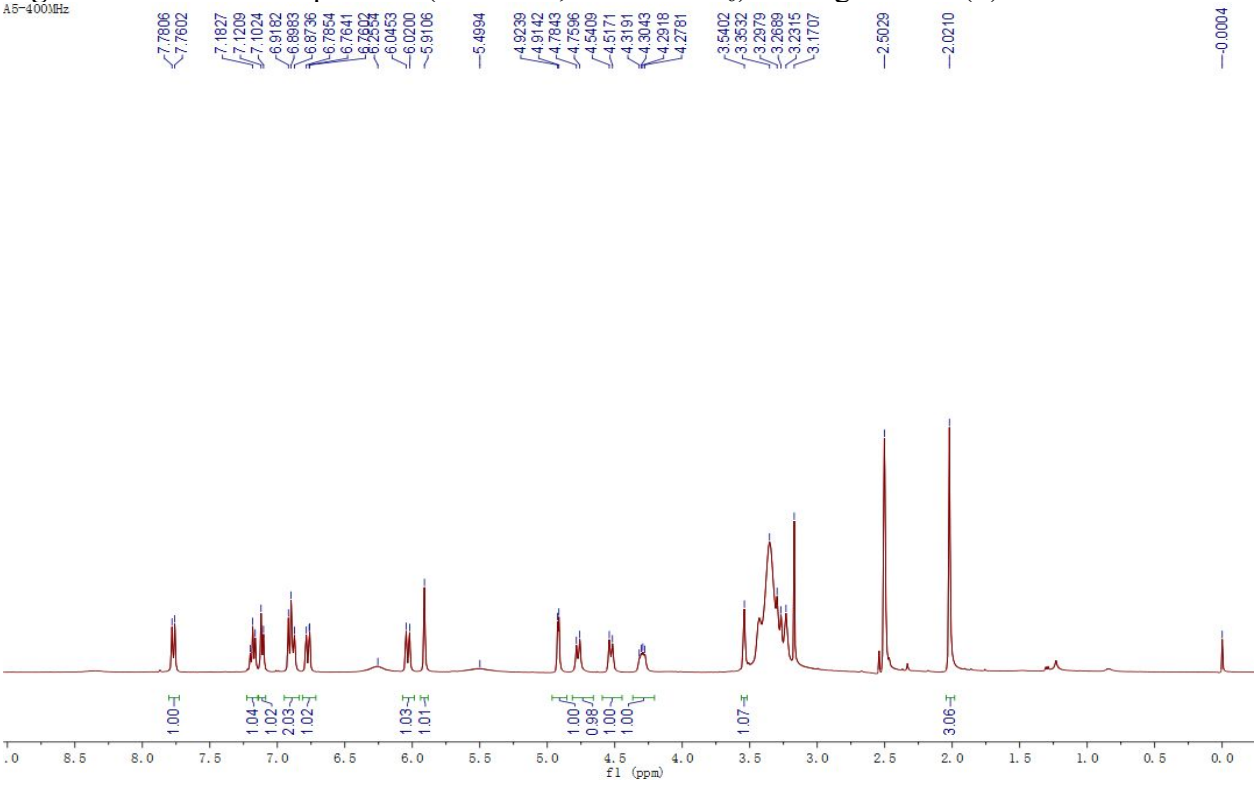

Figure S6-2. ^{13}C NMR spectrum (100 MHz, in DMSO-d_6) of sungeidine F (**6**)

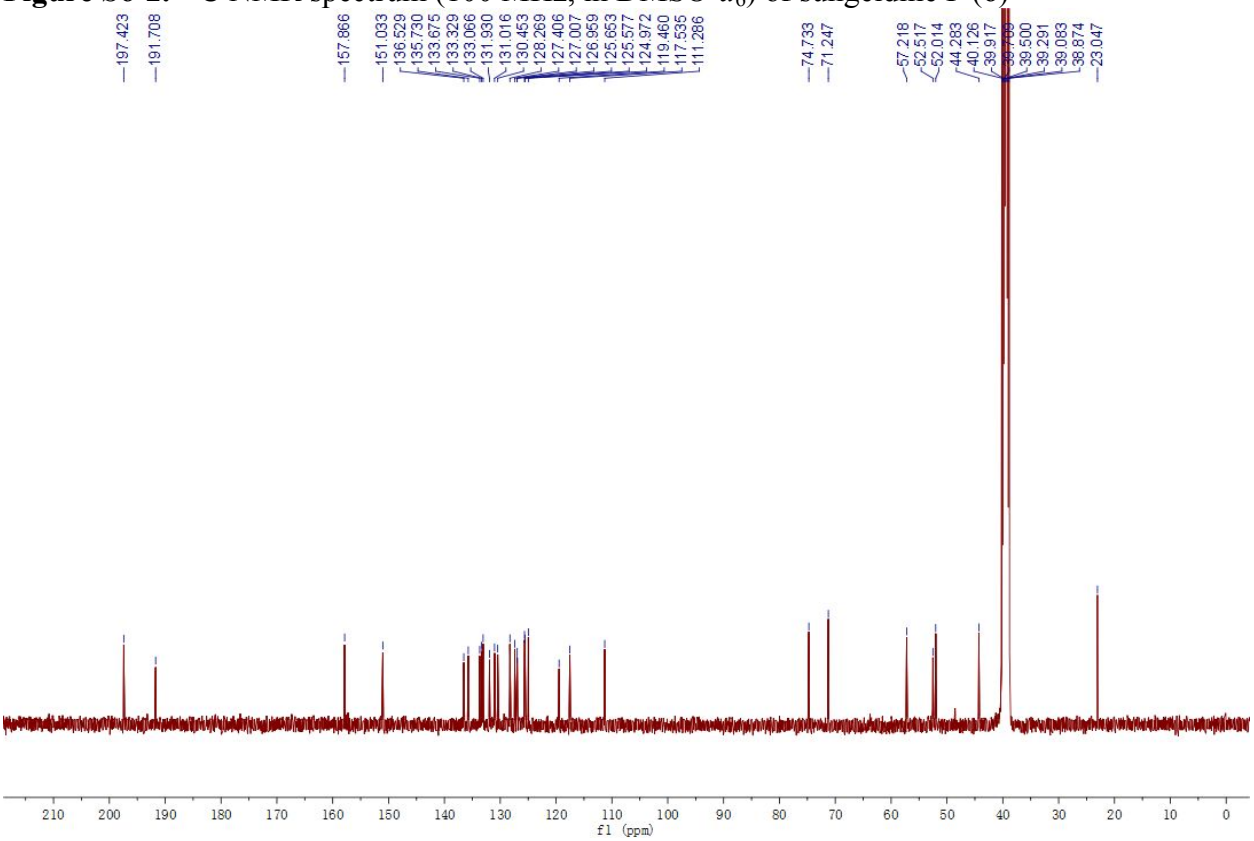

Figure S6-3. HSQC NMR spectrum (400 MHz, in DMSO-d_6) of sungeidine F (**6**)

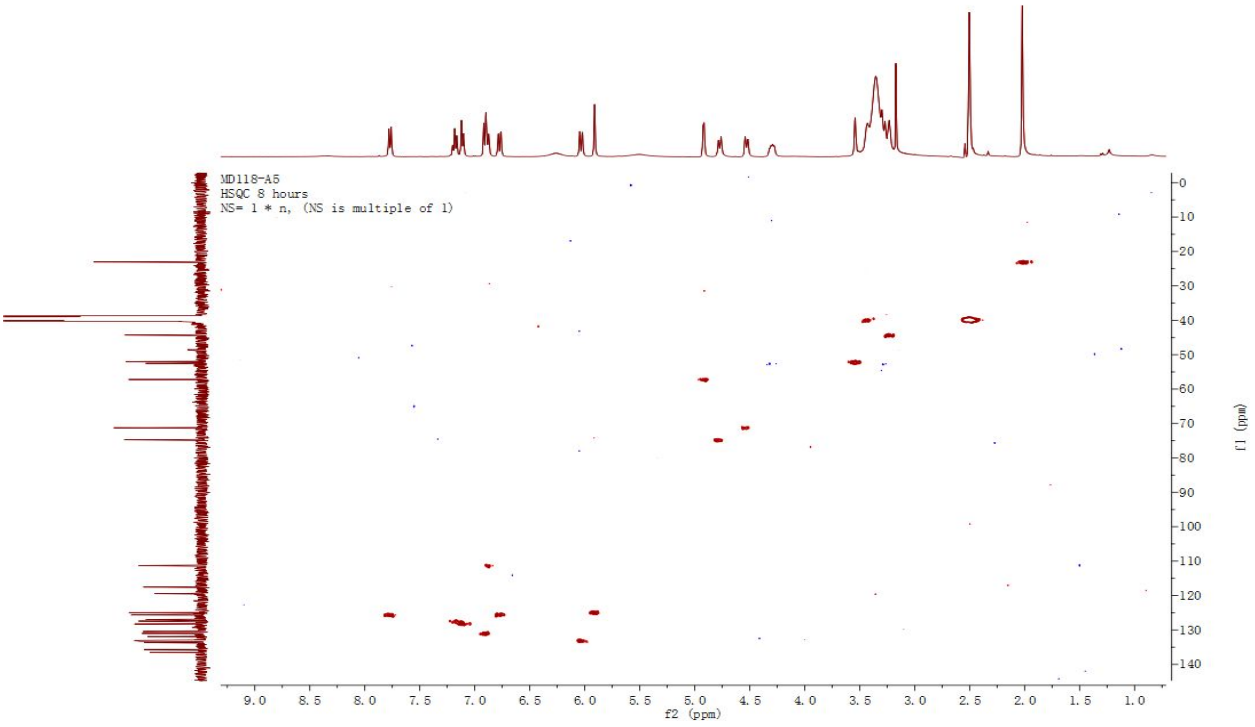

Figure S6-4. ^{1}H-^{1}H COSY NMR spectrum (400 MHz, in DMSO-d_6) of sungeidine F (**6**)

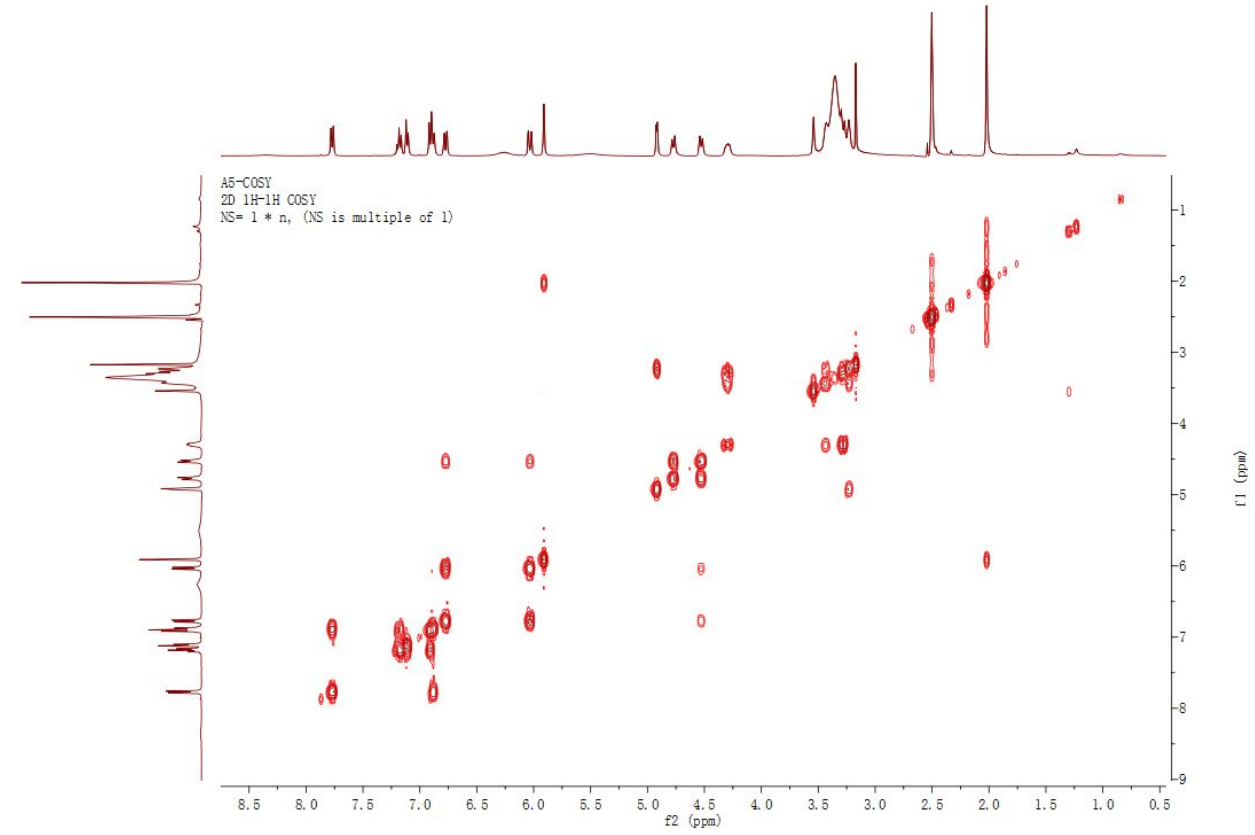

Figure S6-5. HMBC NMR spectrum (400 MHz, in DMSO-d_6) of sungeidine F (**6**)

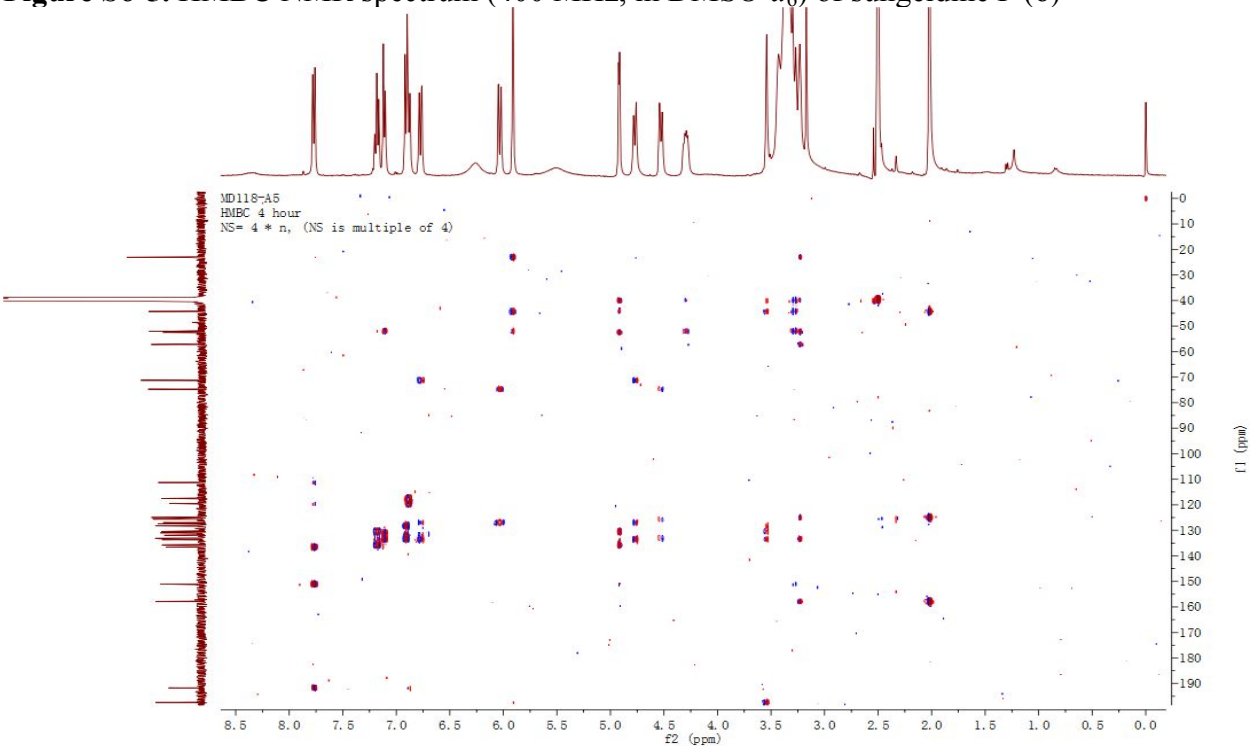

Figure S6-6. NOESY NMR spectrum (400 MHz, in DMSO-d_6) of sungeidine F (**6**)

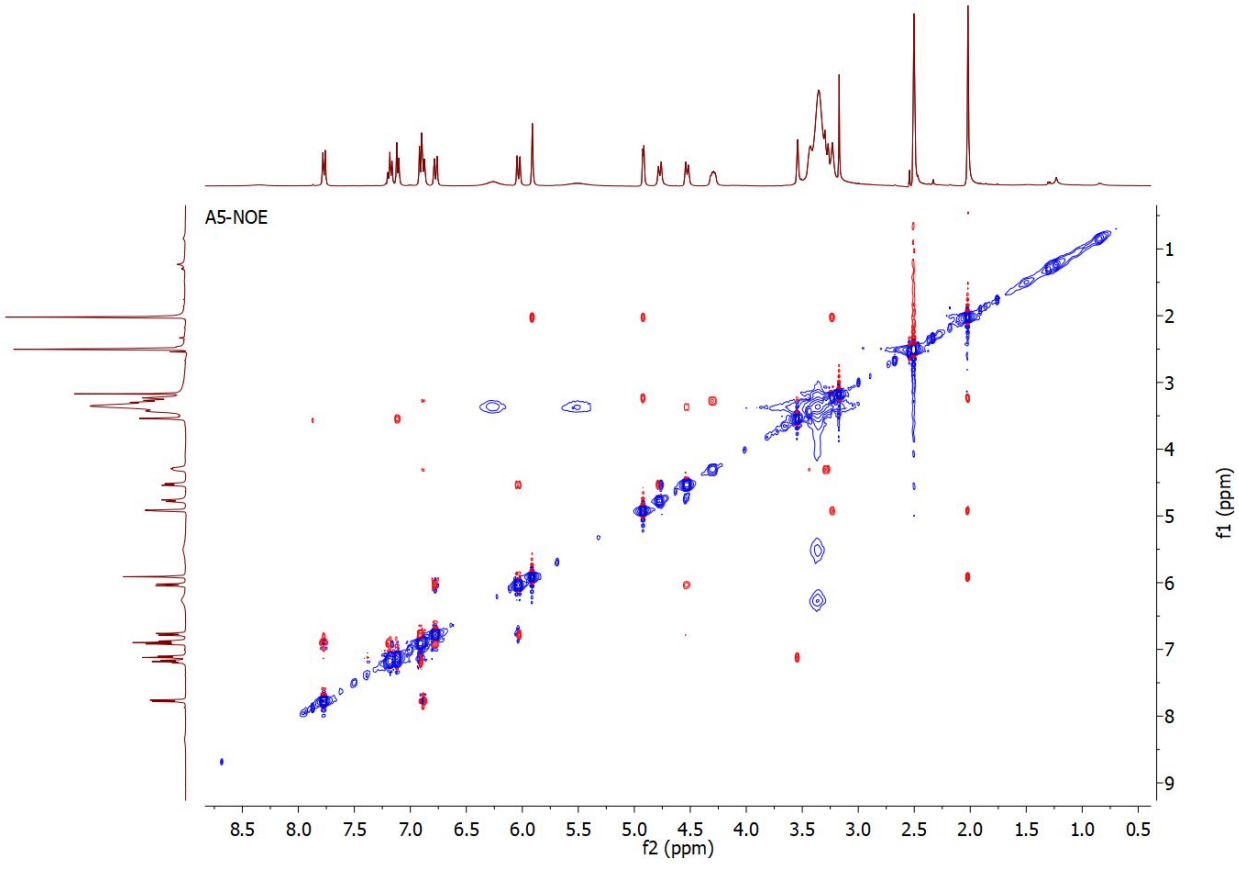

Figure S6-7. ^{1}H NMR spectra (400 MHz, in DMSO-d_6) of sungeidine F (**6**) labelled from [1-^{13}C]- and [2-^{13}C]-sodium acetate.

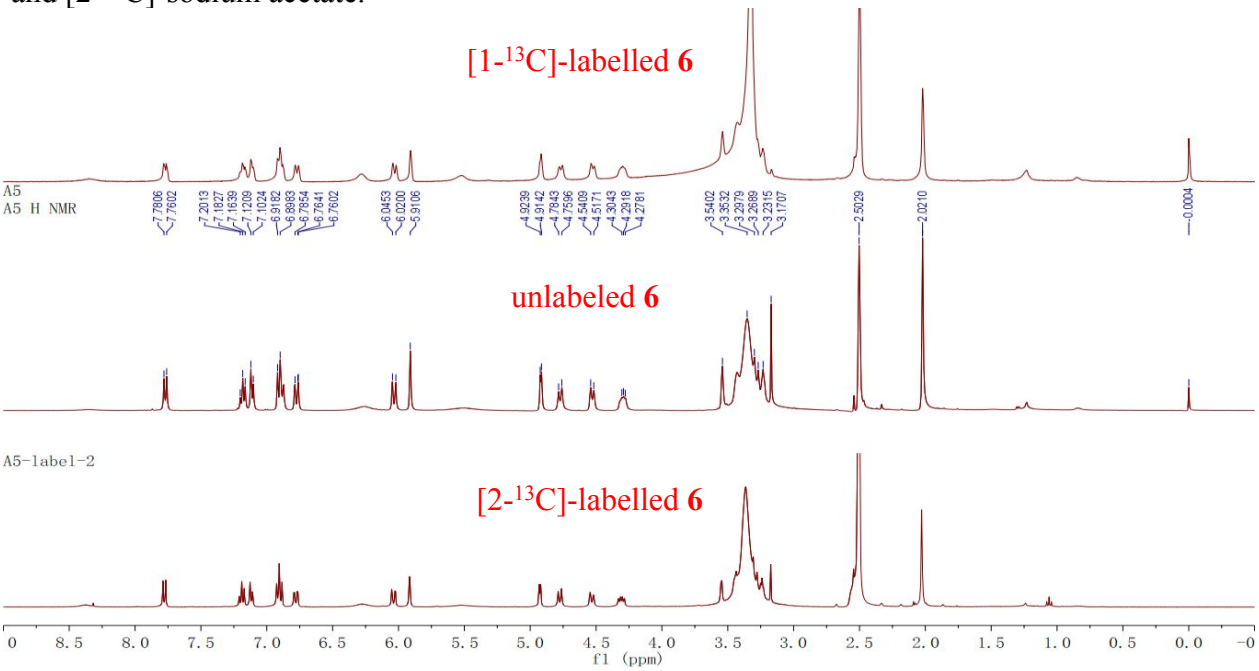

Figure S6-8. ^{13}C NMR spectra (100 MHz, in DMSO-d_6) of sungeidine F (**6**) labelled from [1-^{13}C]- and [2-^{13}C]-sodium acetate.

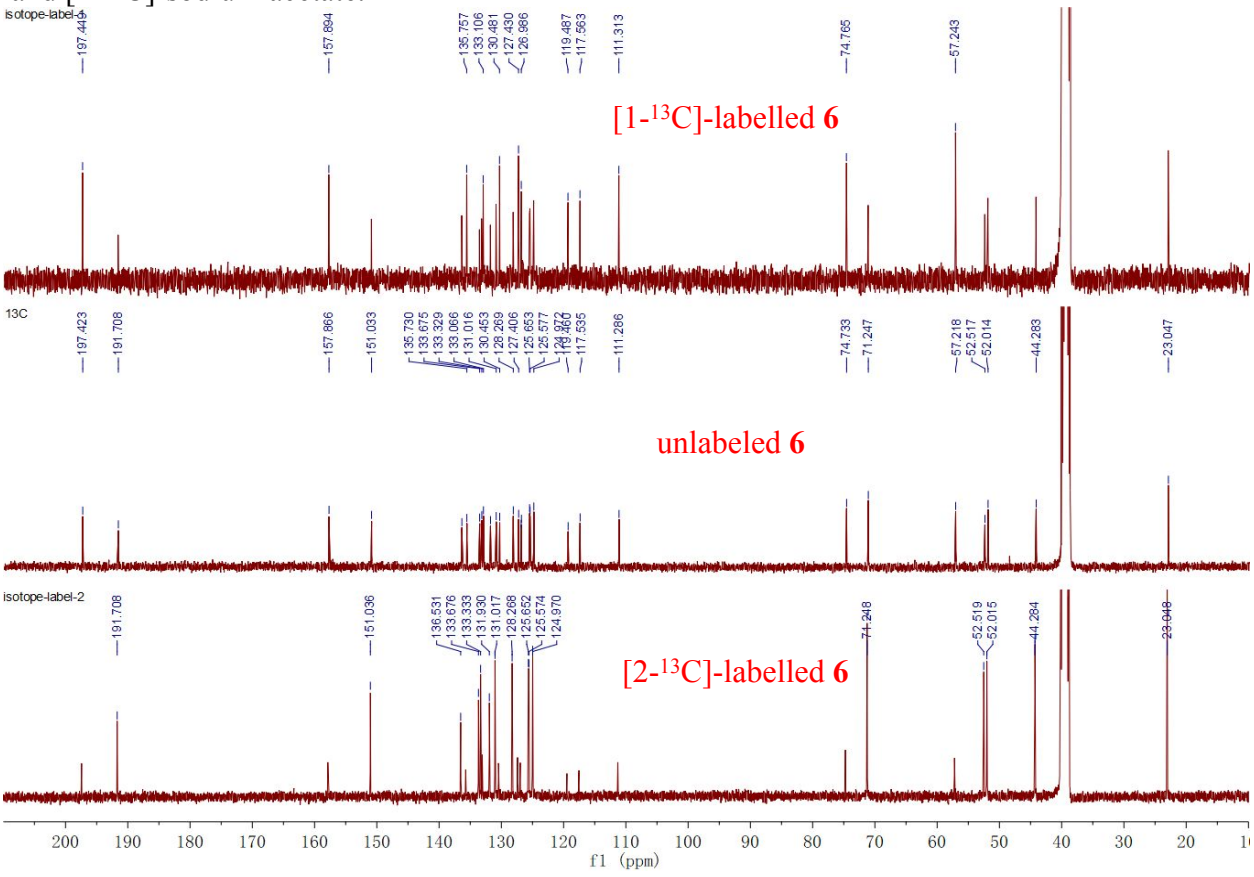

Figure S6-9. ^{1}H NMR spectrum (400 MHz, in DMSO-d_6) of sungeidine F (**6**) labelled from [1,2-$^{13}C_2$]-sodium acetate.

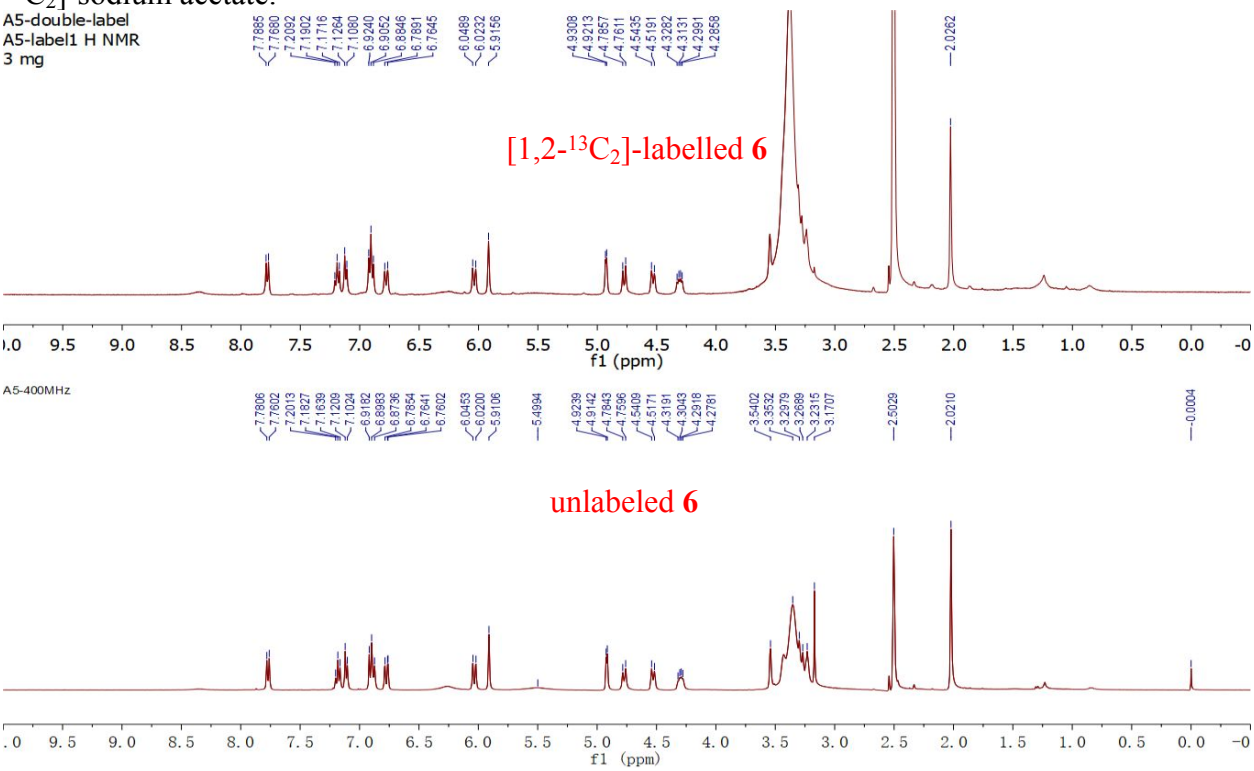

Figure S6-10. ^{13}C NMR spectrum (100 MHz, in DMSO-d_6) of sungeidine F (**6**) labelled from [1,2-$^{13}C_2$]-sodium acetate.

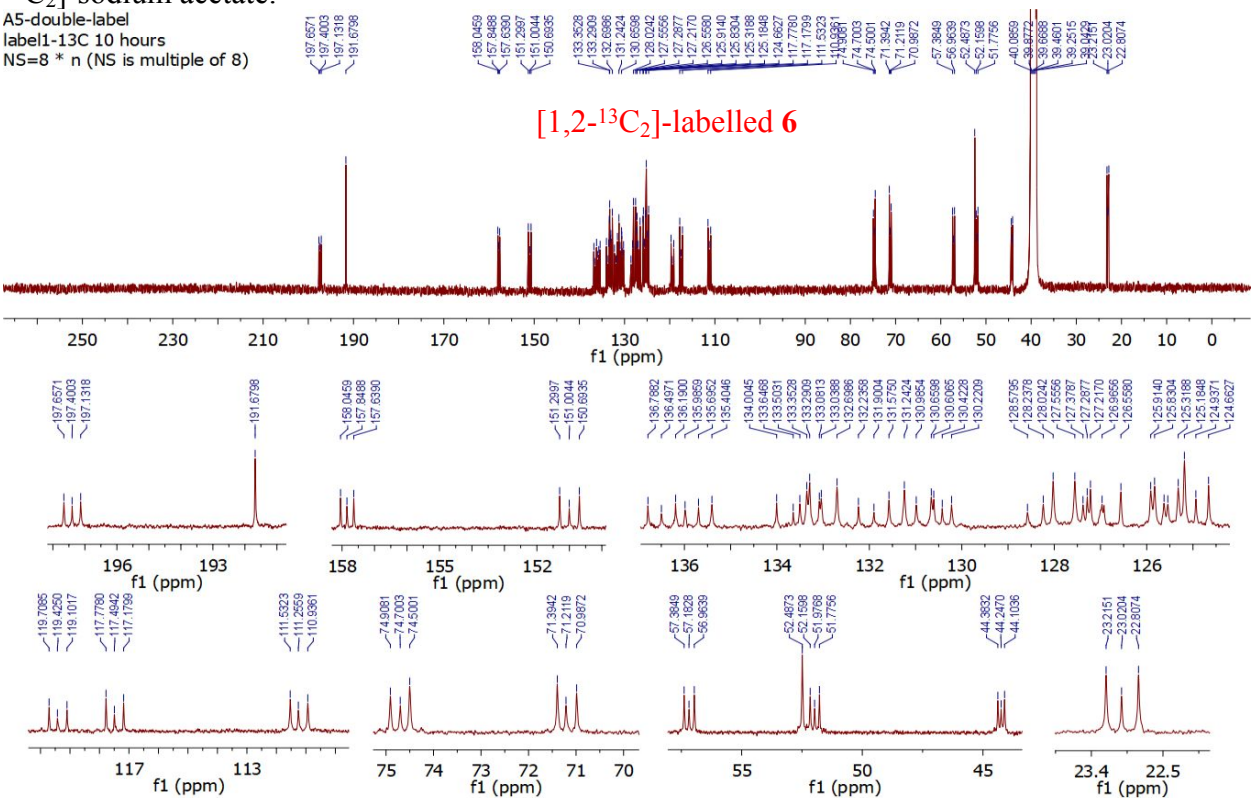

Figure S7-1. ^{1}H NMR spectrum (600 MHz, in DMSO-d_6) of sungeidine G (**7**)

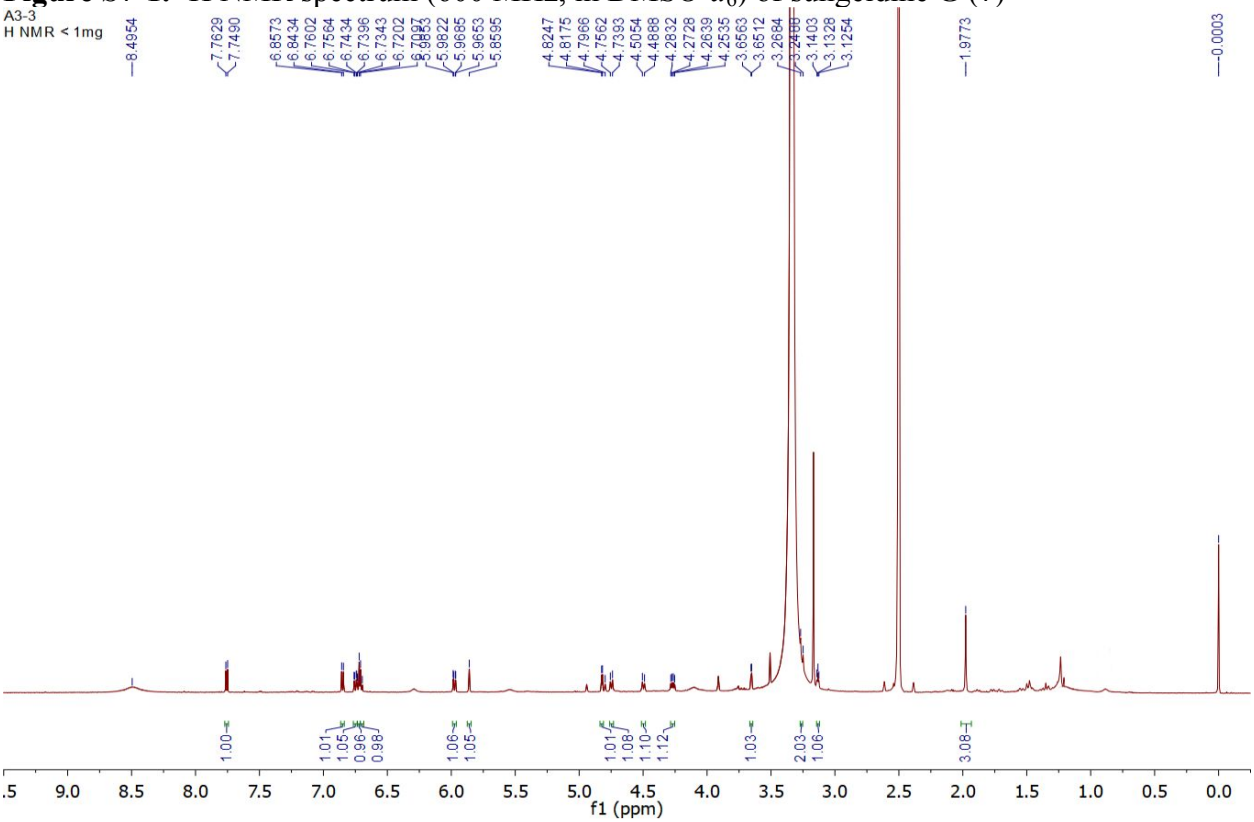

Figure S7-2. ^{13}C NMR spectrum (150 MHz, in DMSO-d_6) of sungeidine G (**7**)

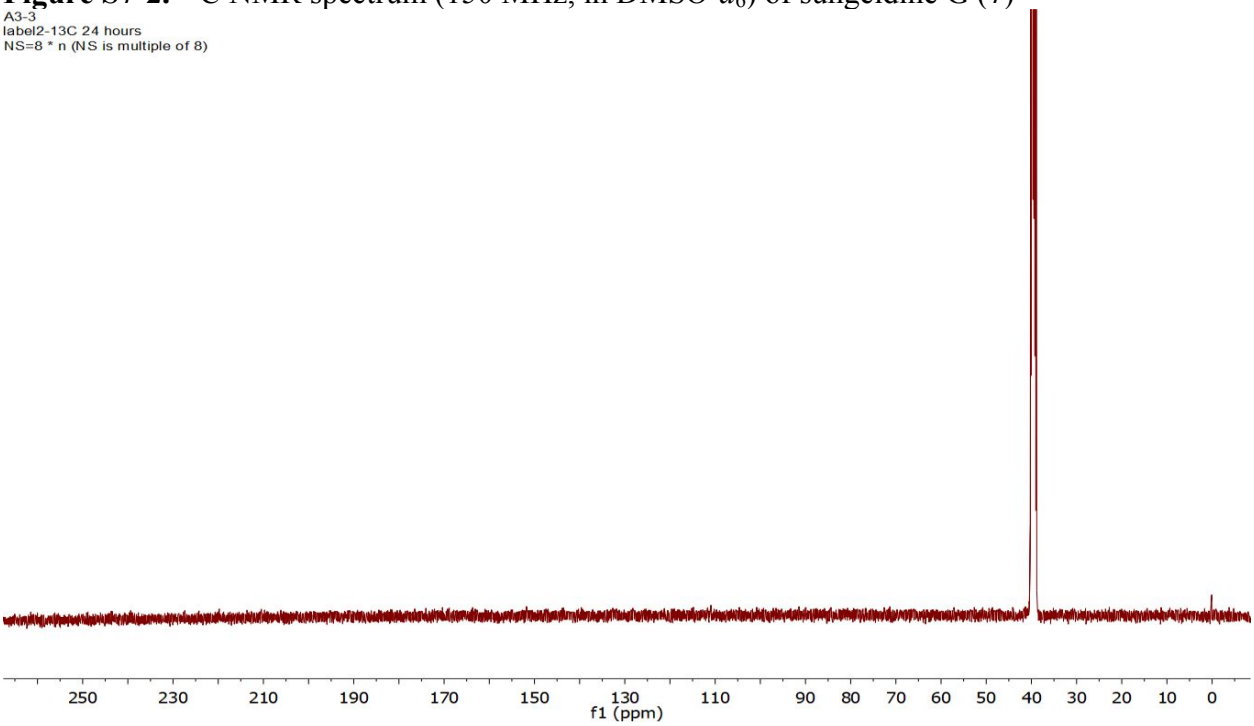

The ^{13}C NMR assignment of tiny amount **7** (0.4 mg) was achieved mainly based on the HSQC and HMBC data analyses, since the acquired ^{13}C signals (24 hr) were extremely weak.

Figure S7-3. HSQC NMR spectrum (600 MHz, in DMSO-d_6) of sungeidine G (**7**)

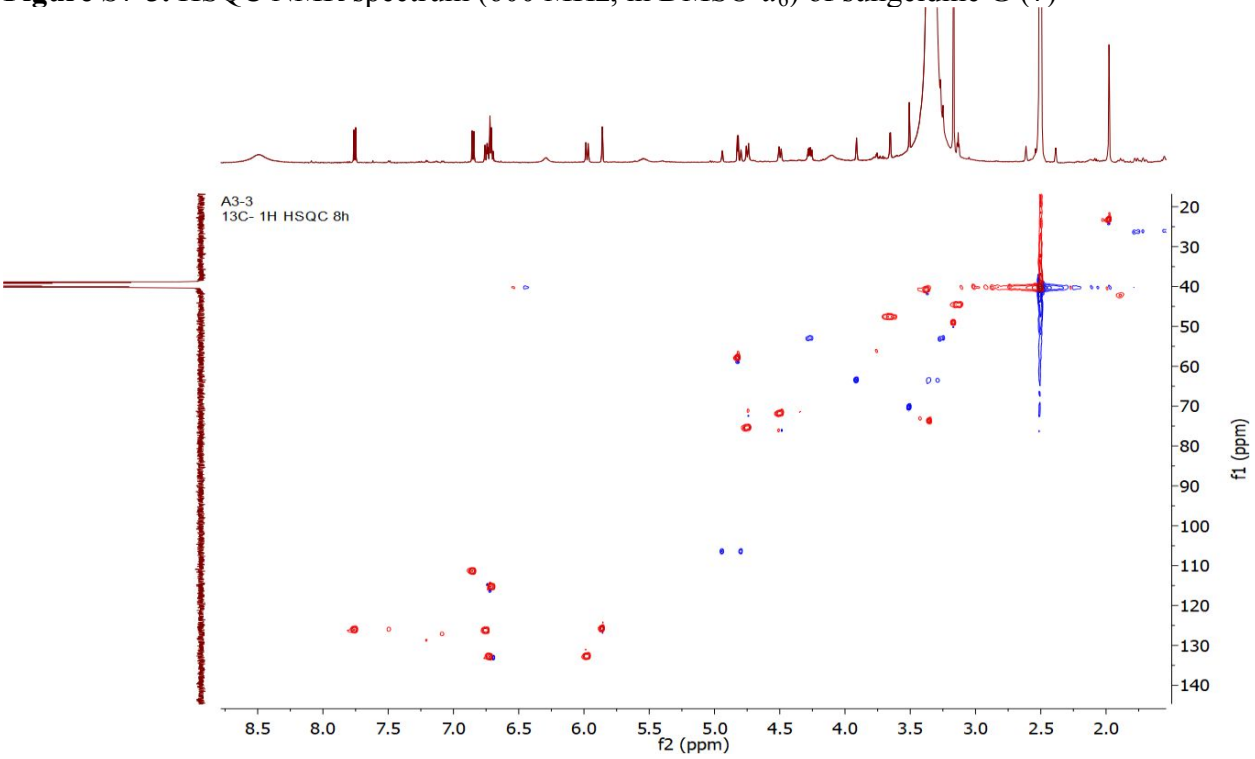

Figure S7-4. ^{1}H-^{1}H COSY NMR spectrum (600 MHz, in DMSO-d_6) of sungeidine G (**7**)

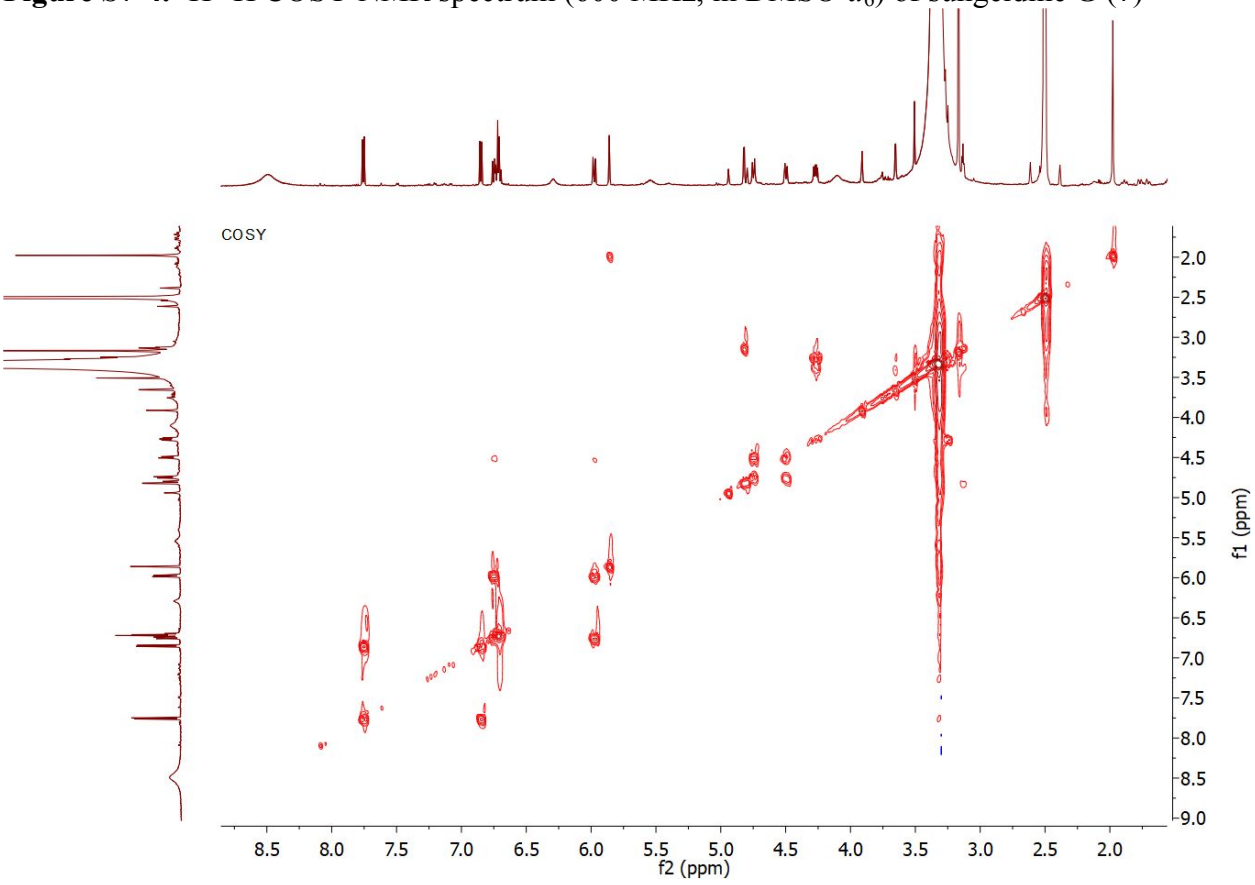

Figure S7-5. HMBC NMR spectrum (600 MHz, in DMSO-d_6) of sungeidine G (**7**)

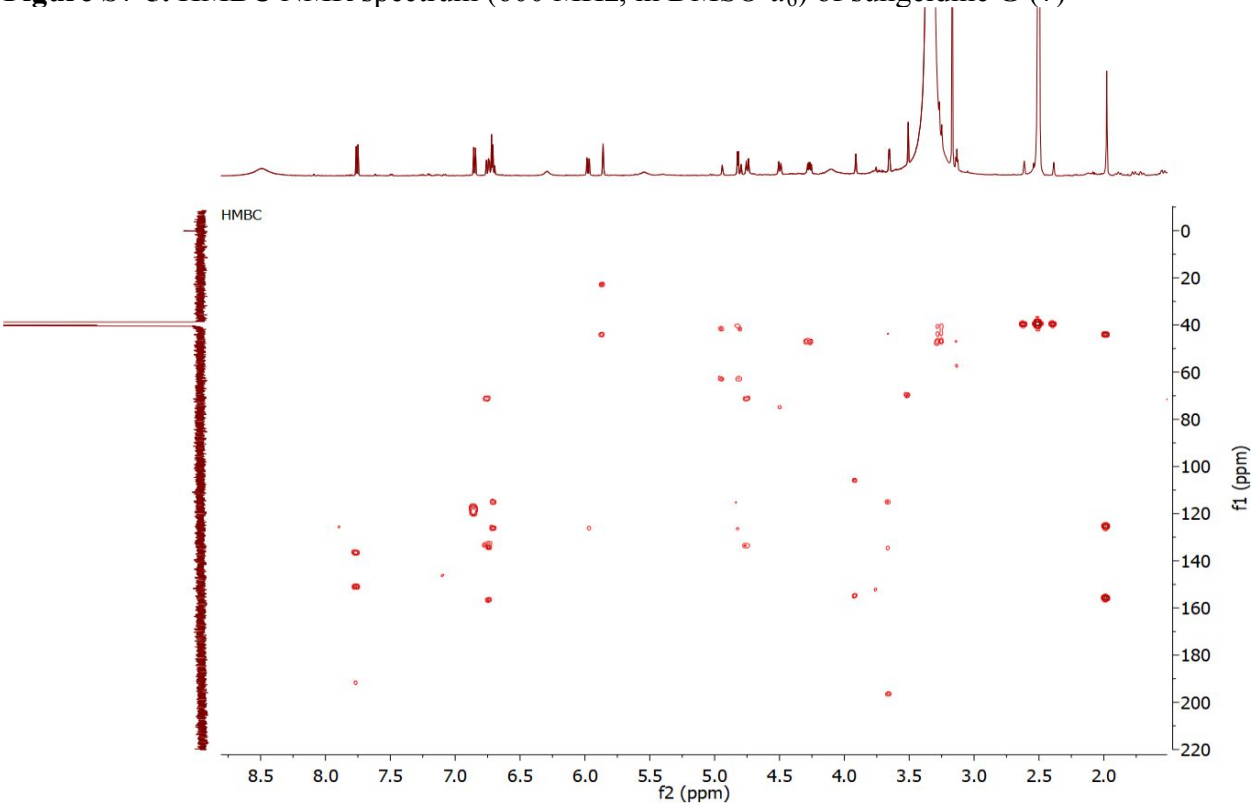

Figure S7-6. NOESY NMR spectrum (600 MHz, in DMSO-d_6) of sungeidine G (**7**)

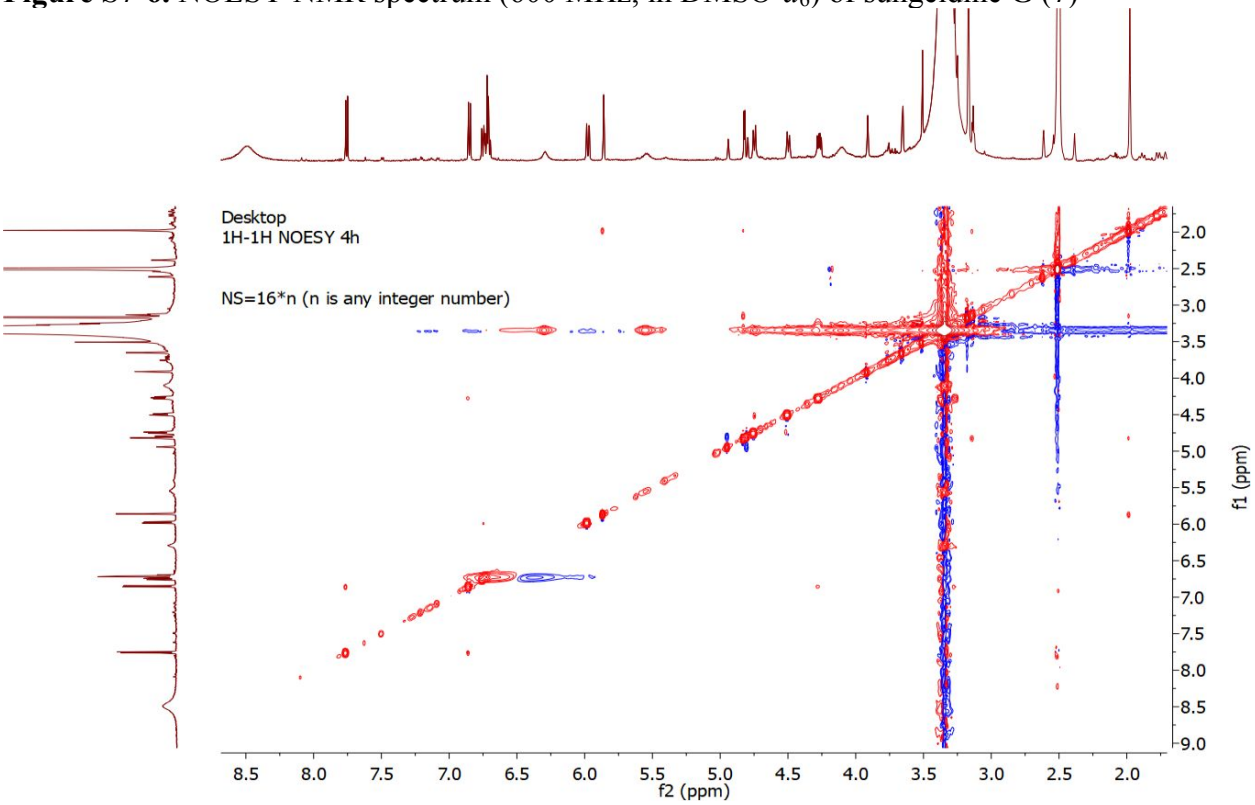

Figure S8-1: ^{1}H NMR spectrum (400 MHz, in DMSO-d_6) of sungeidine H (**8**)

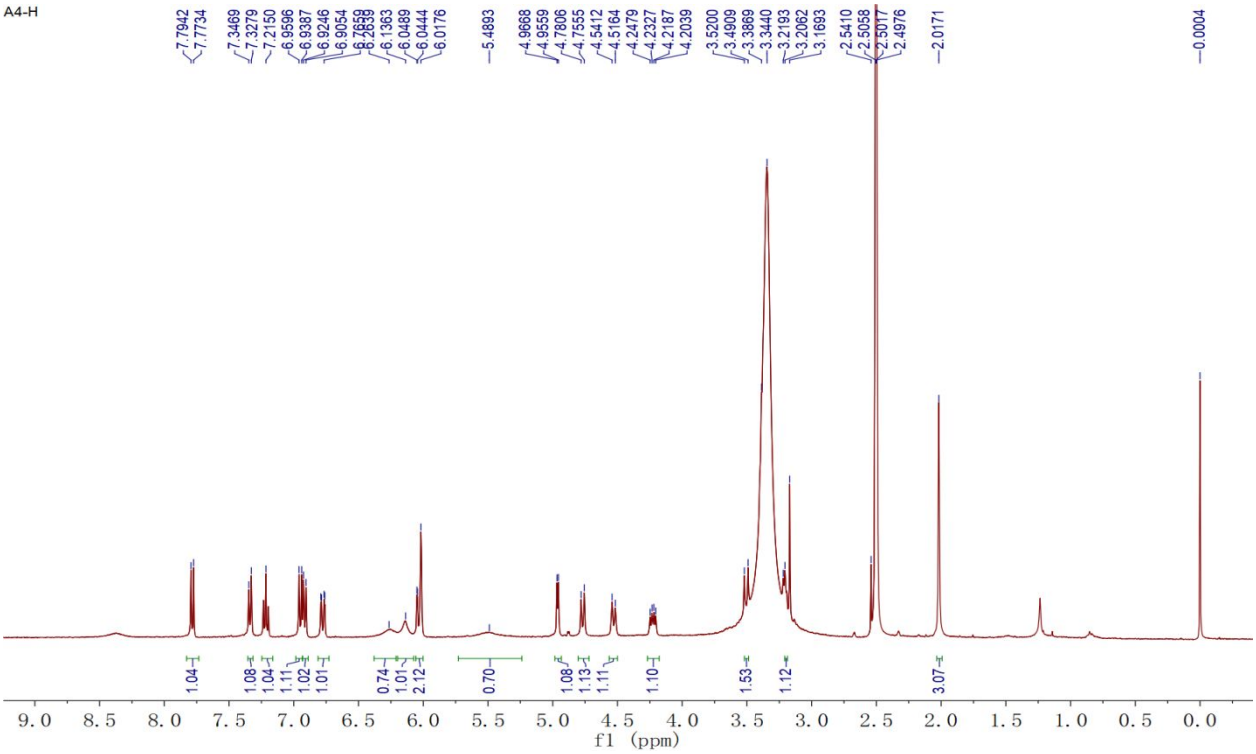

Figure S8-2: ^{13}C NMR spectrum (100 MHz, in DMSO-d_6) of sungeidine H (**8**)

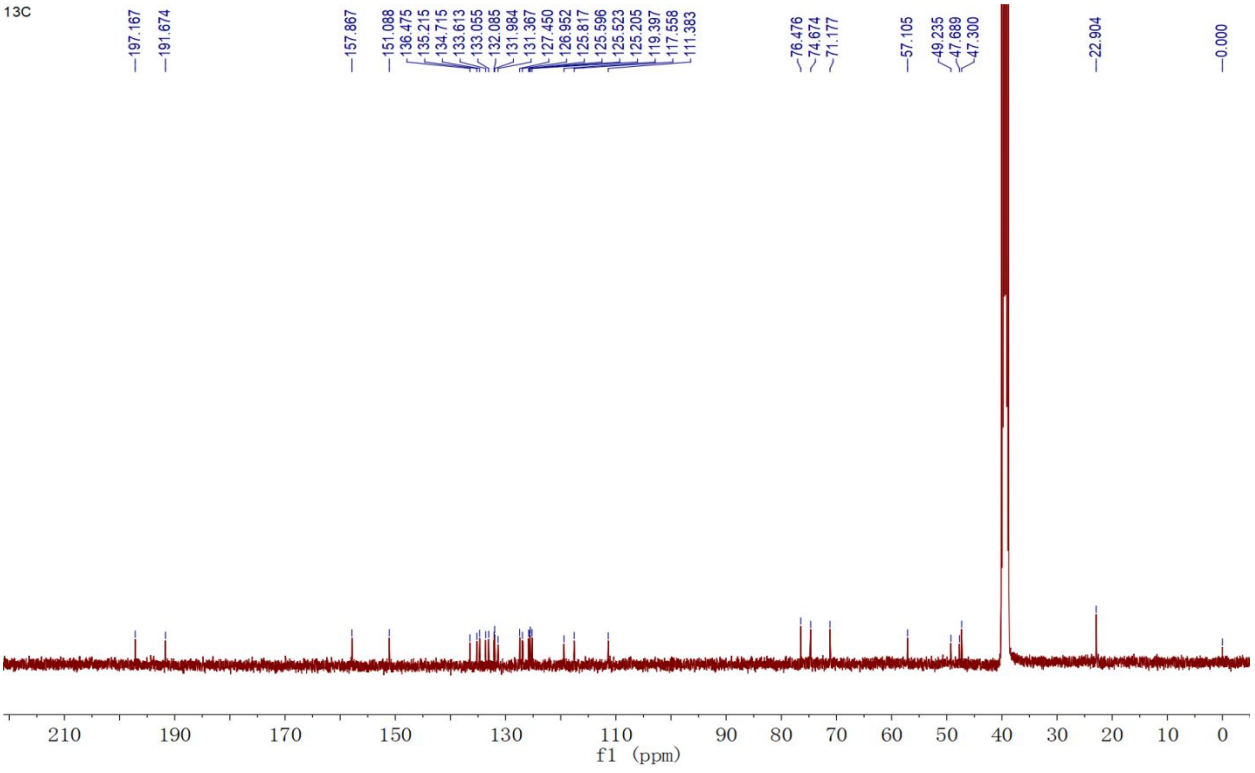

Figure S8-3: HSQC NMR spectrum (400 MHz, in DMSO-d_6) of sungeidine H (**8**)

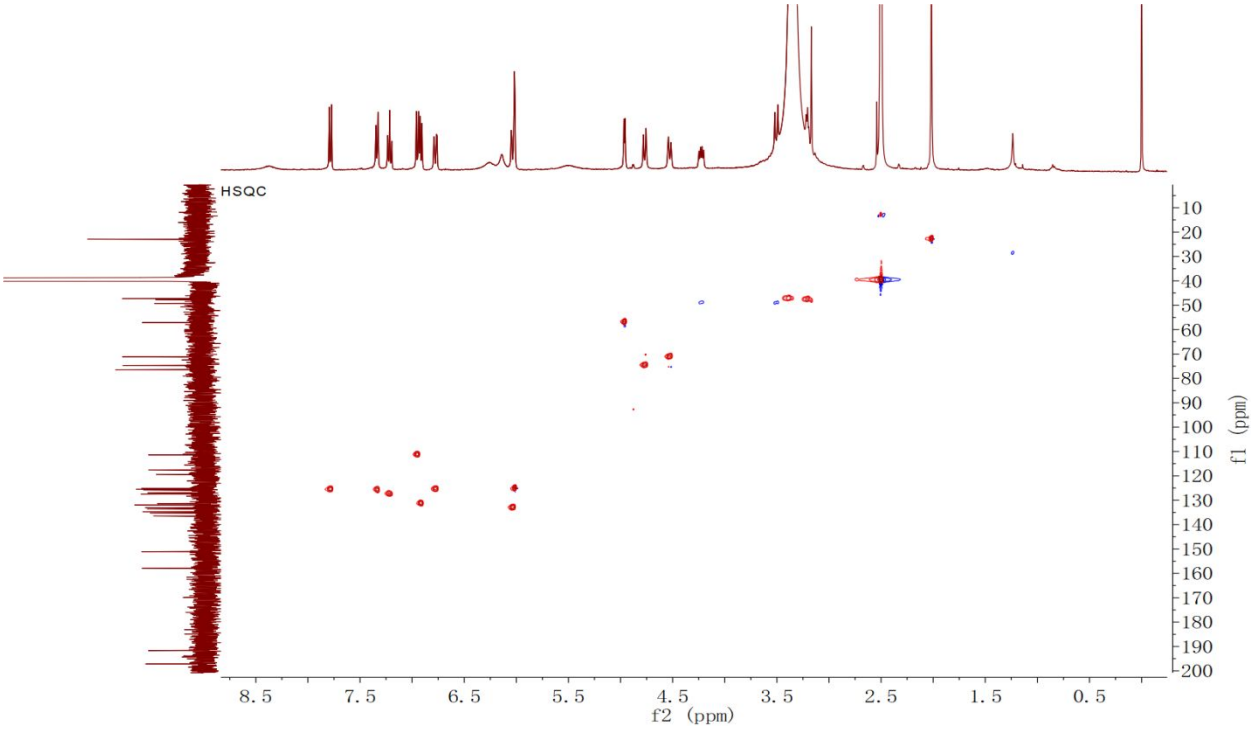

Figure S8-4: ^{1}H-^{1}H COSY NMR spectrum (400 MHz, in DMSO-d_6) of sungeidine H (**8**)

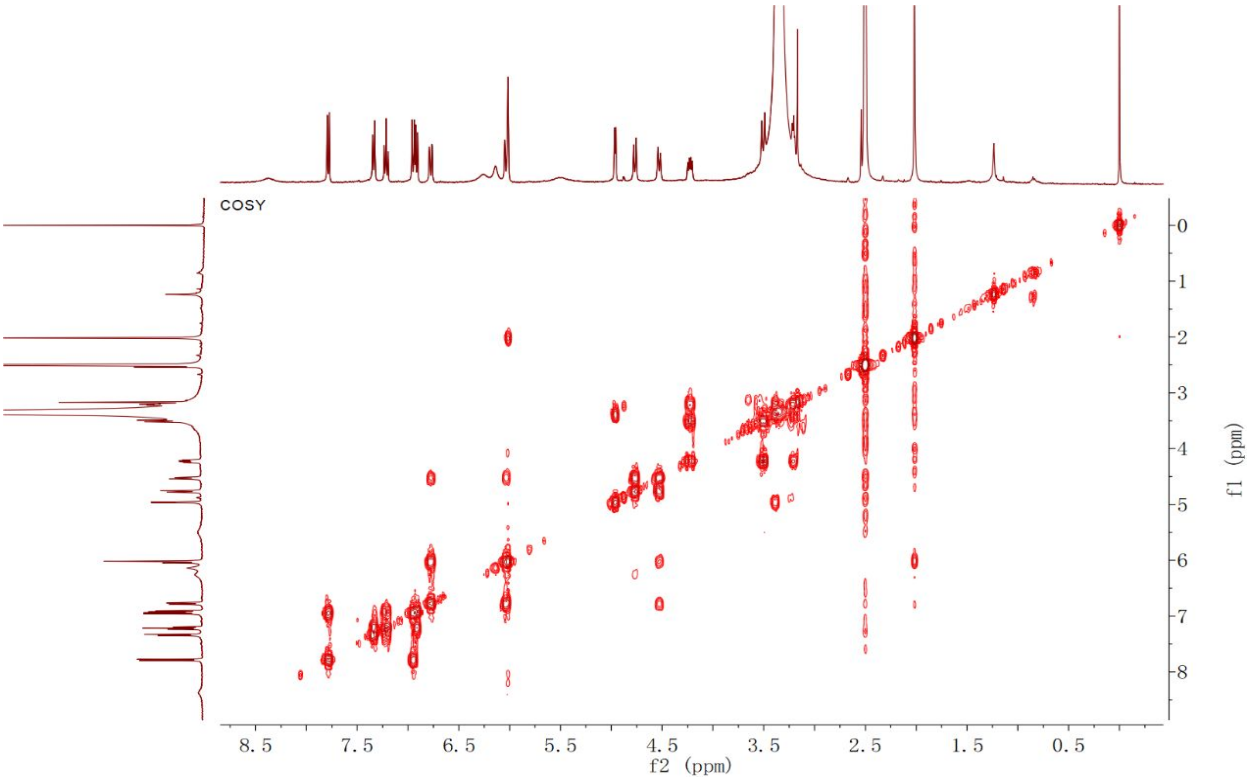

Figure S8-5: HMBC NMR spectrum (400 MHz, in DMSO-d_6) of sungeidine H (**8**)

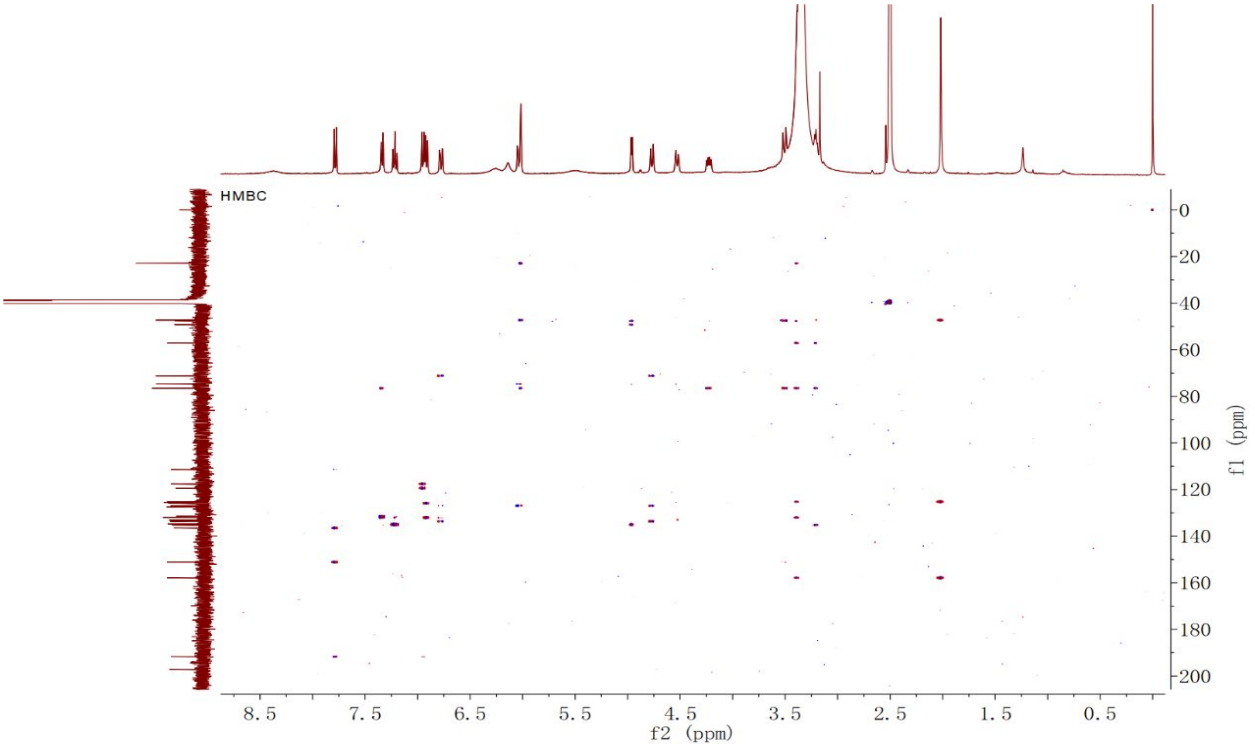

Figure S8-6: NOESY NMR spectrum (400 MHz, in DMSO-d_6) of sungeidine H (**8**)

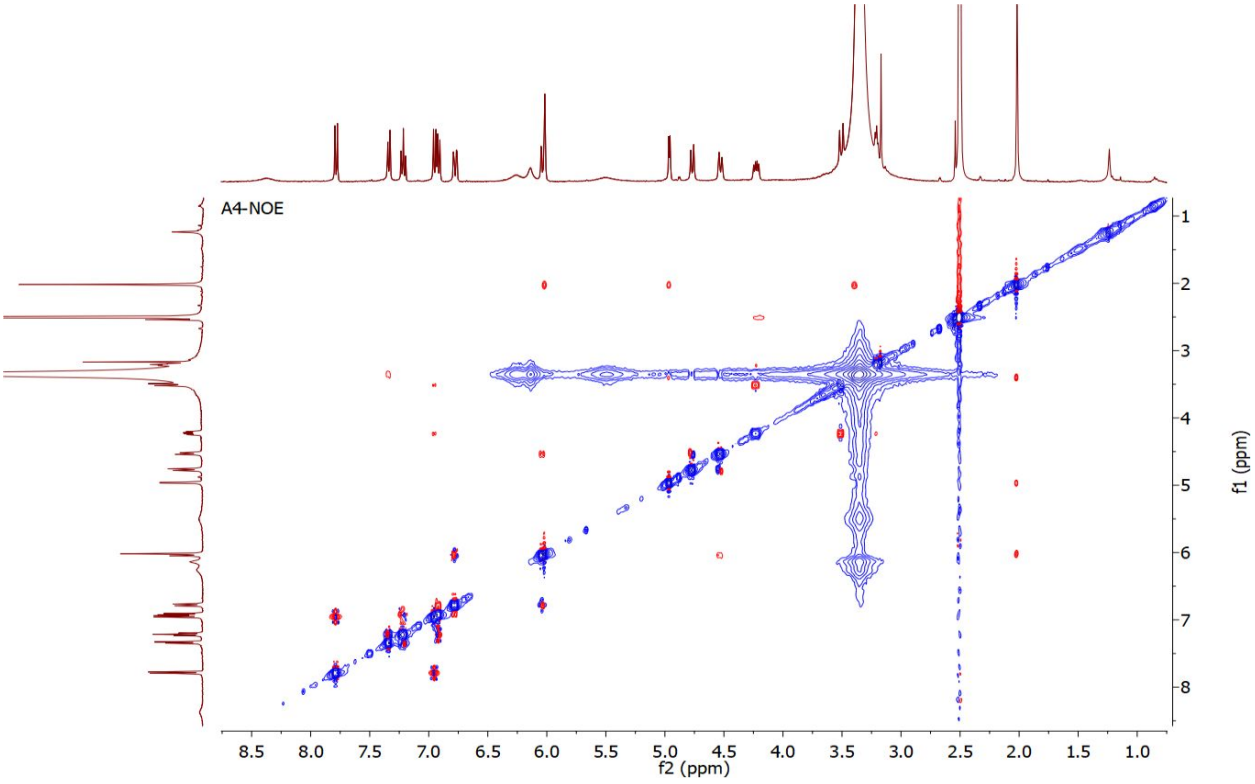

Figure S9-1: ^{1}H NMR spectrum (400 MHz, in DMSO-d_6) of anthramicin (**9**)

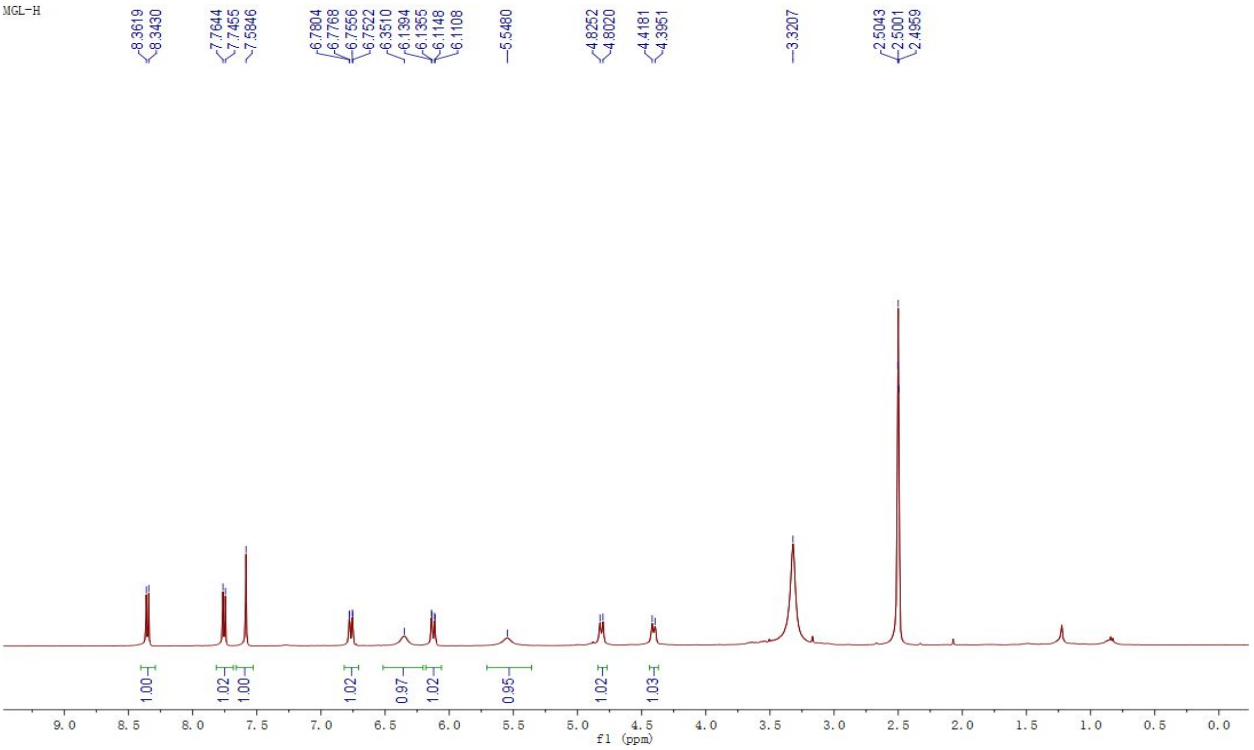

Figure S9-2: ^{13}C NMR spectrum (100 MHz, in DMSO-d_6) of anthramicin (**9**)

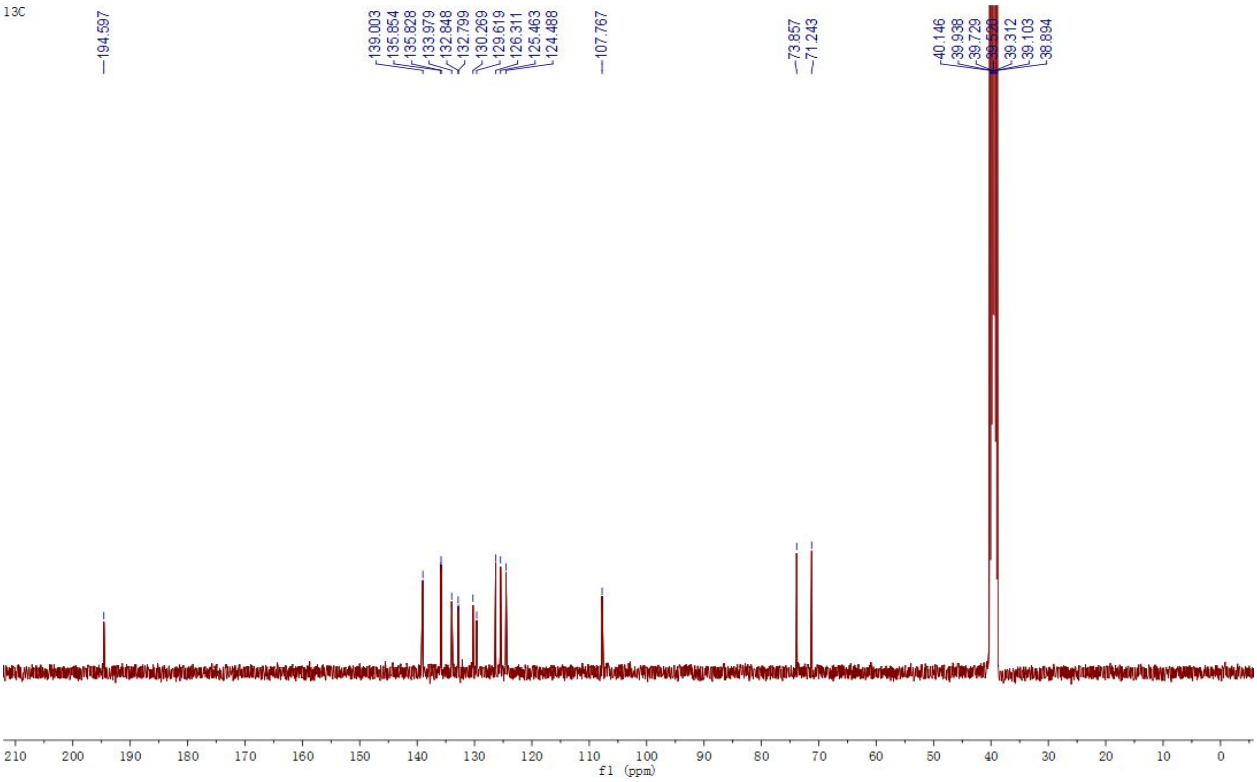

Figure S9-3: HSQC NMR spectrum (400 MHz, in DMSO-d_6) of anthramicin (**9**)

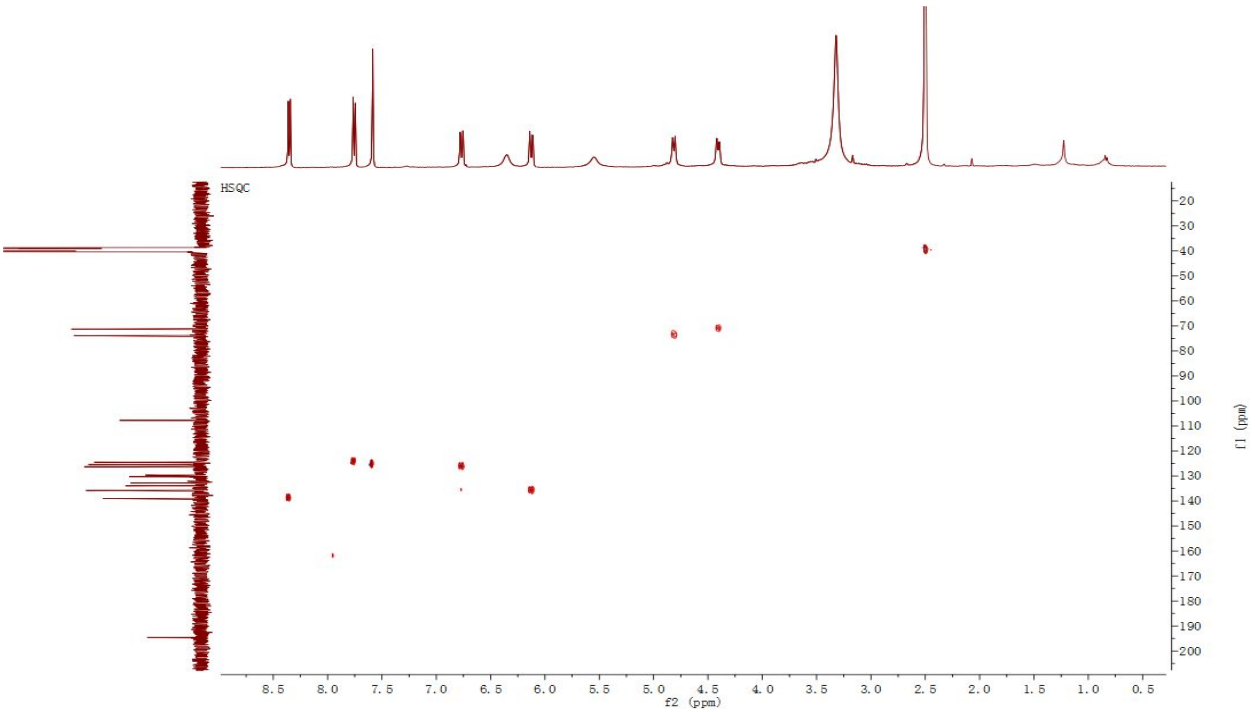

Figure S9-4: ^{1}H-^{1}H COSY NMR spectrum (400 MHz, in DMSO-d_6) of anthramicin (**9**)

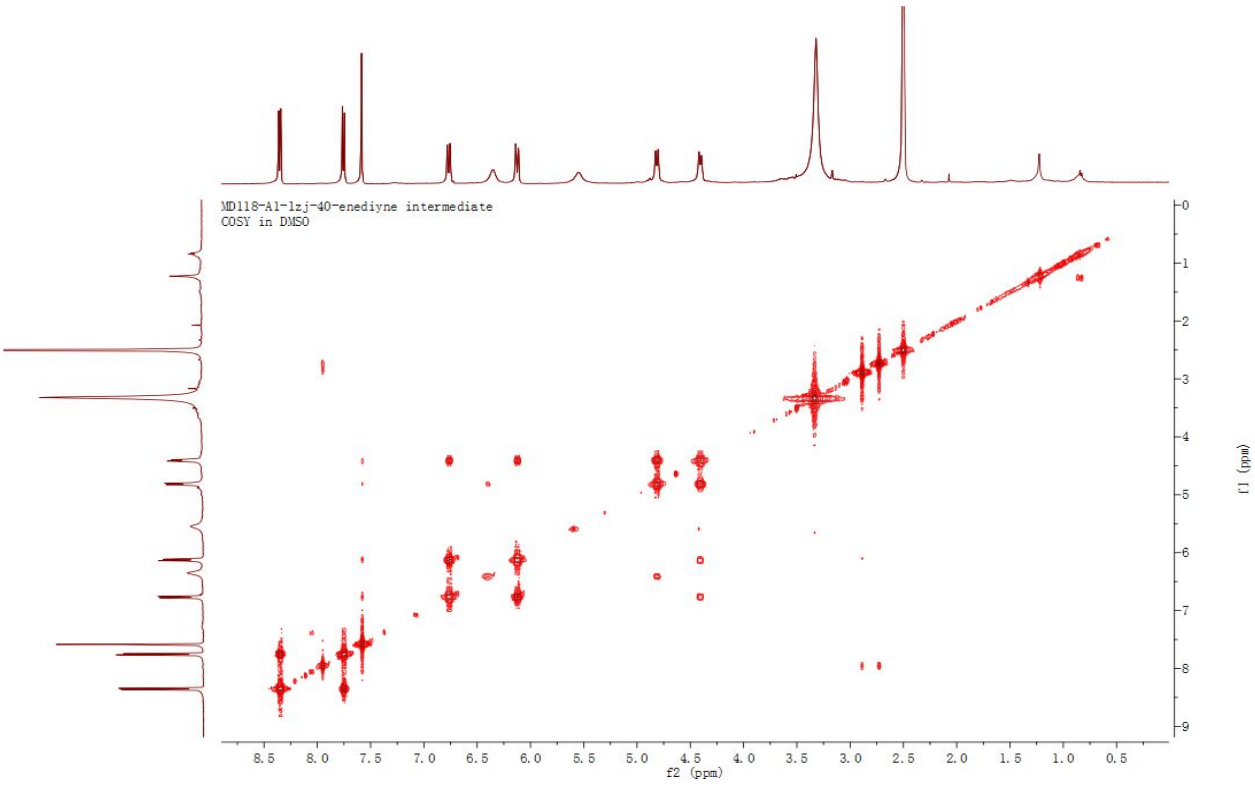

Figure S9-5: HMBC NMR spectrum (400 MHz, in DMSO-d_6) of anthramicin (**9**)

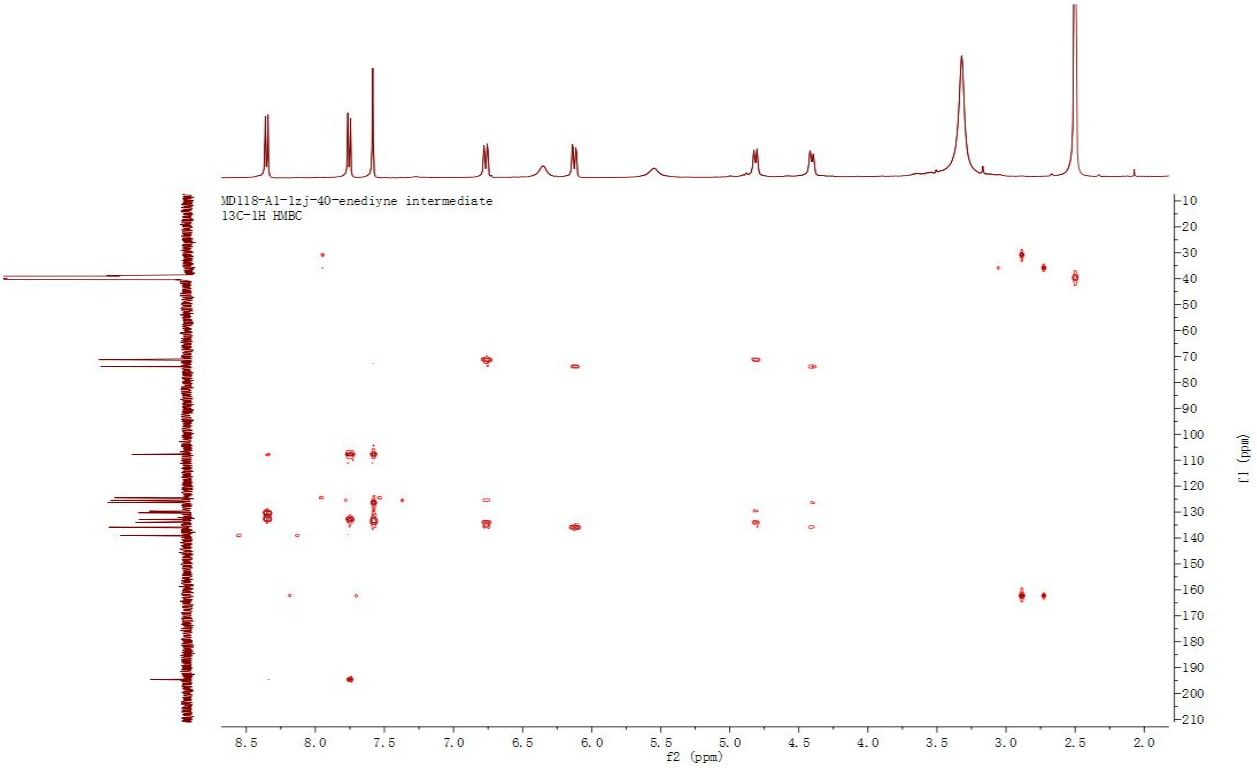

Figure S9-6: NOESY NMR spectrum (400 MHz, in DMSO-d_6) of anthramicin (**9**)

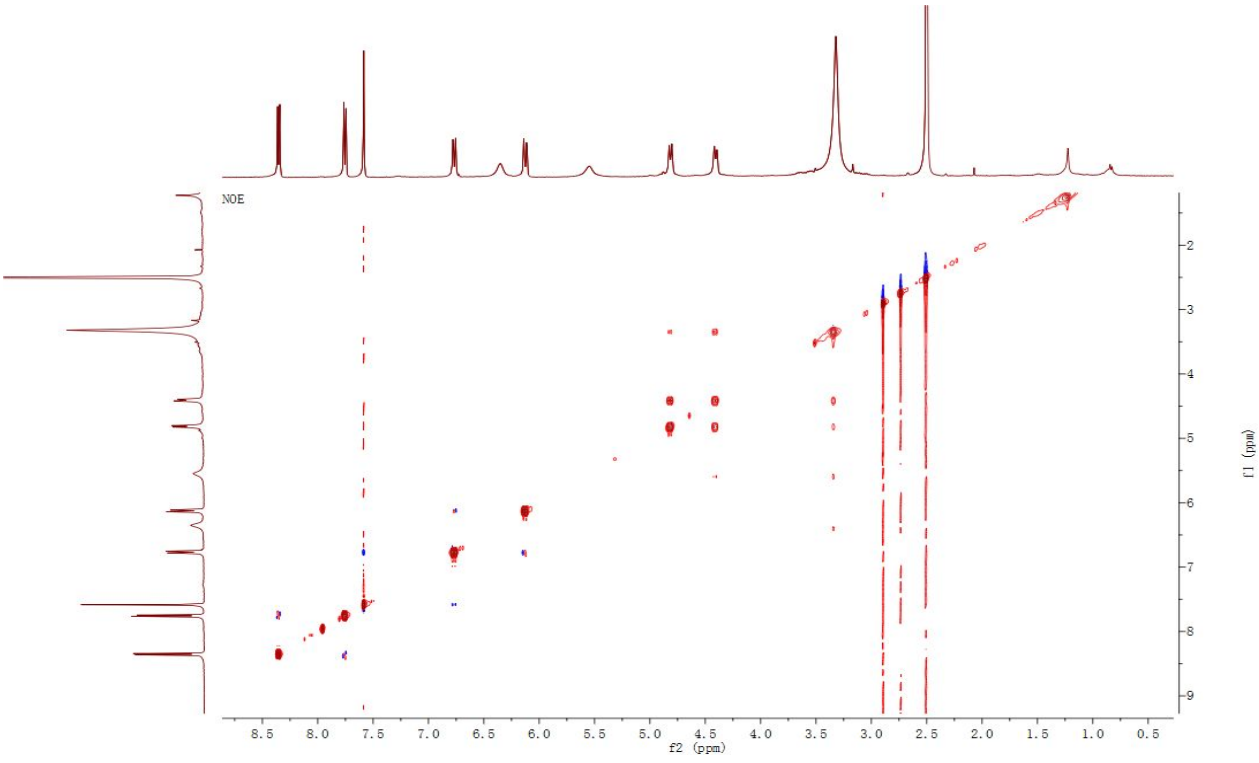

Figure S9-7. ^{13}C NMR spectrum (100 MHz, in DMSO-d_6) of anthramicin (**9**) labelled from [1-^{13}C]- and [2-^{13}C]-sodium acetate.

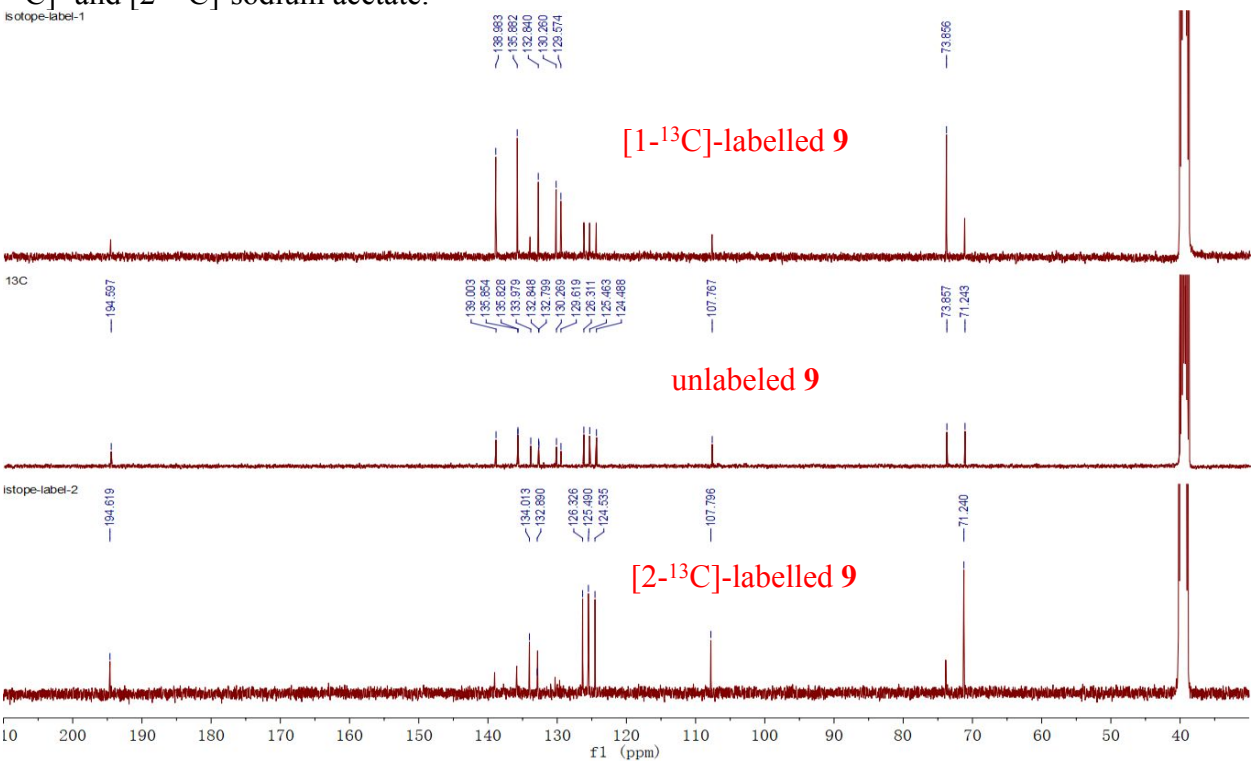

Figure S9-8. HRESIMS and MS/MS spectra of anthramicin (**9**).

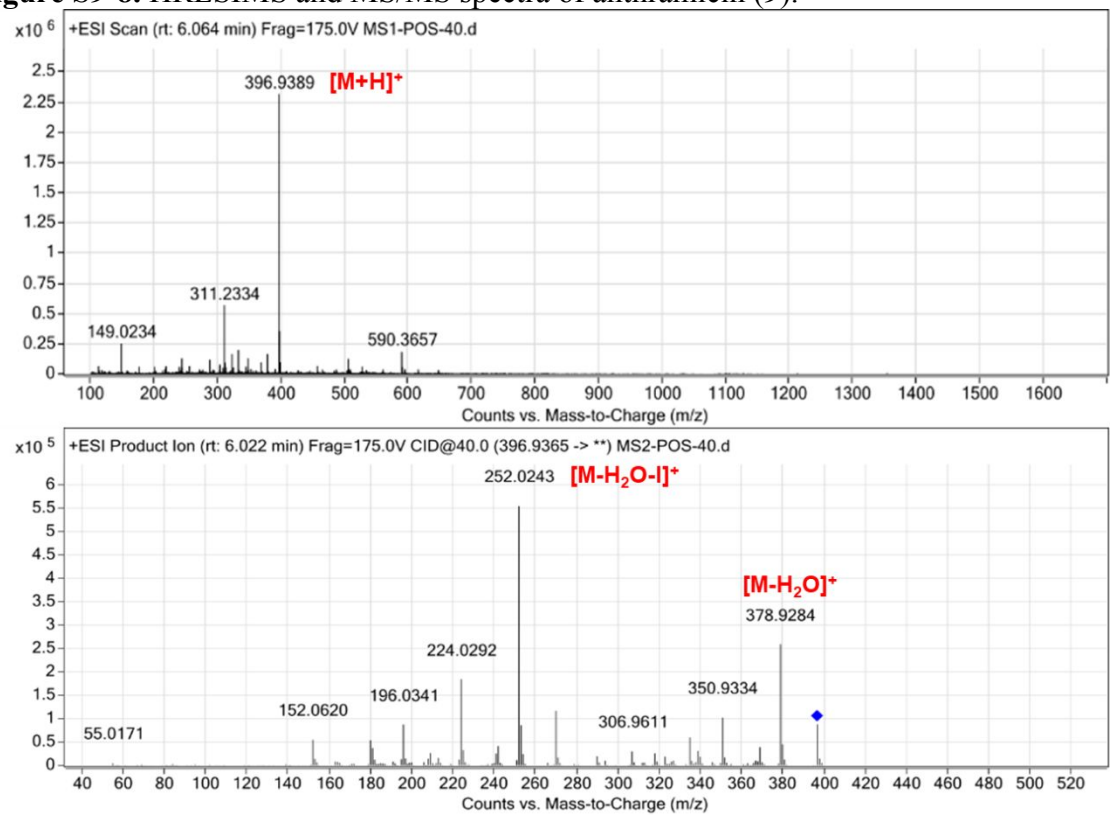

Figure S10: UV-vis spectra of **1**−**9**.

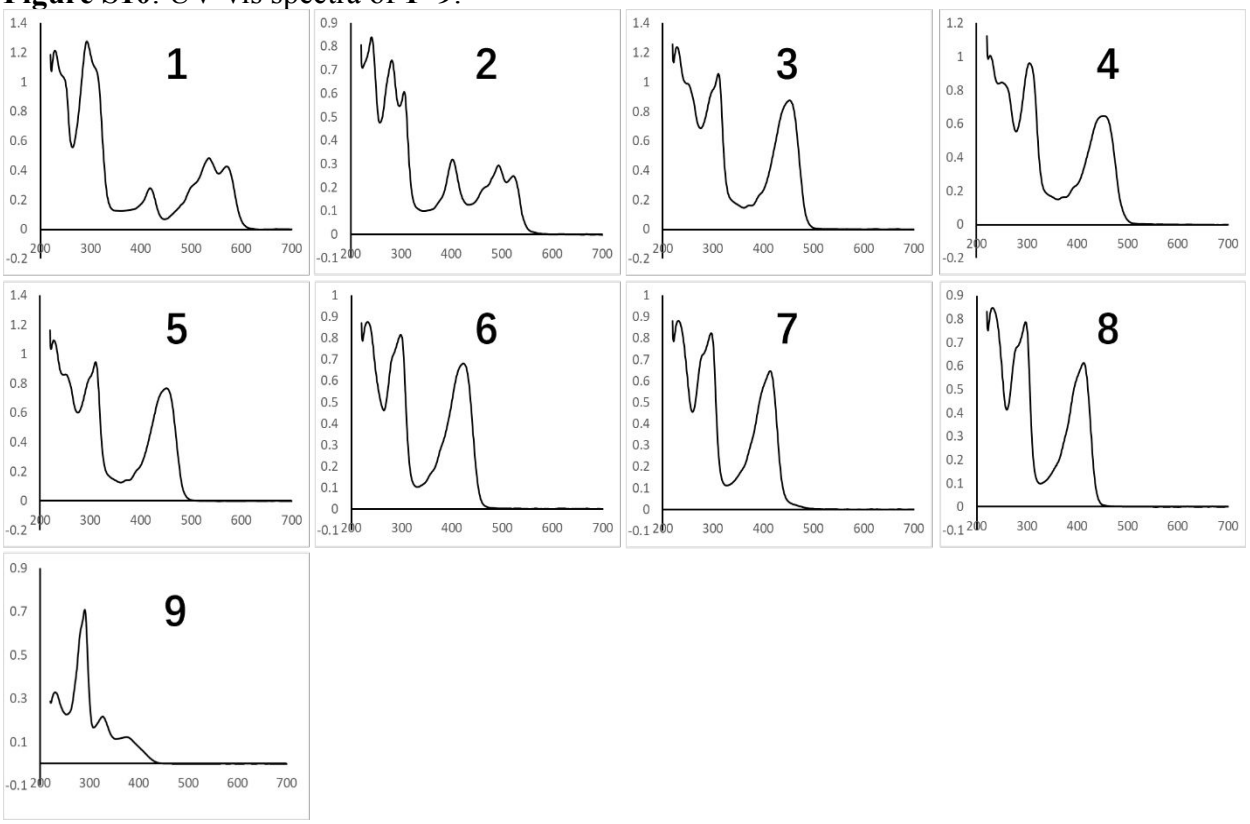

Figure S11: HRESIMS of **2**−**8**, and **6a**.

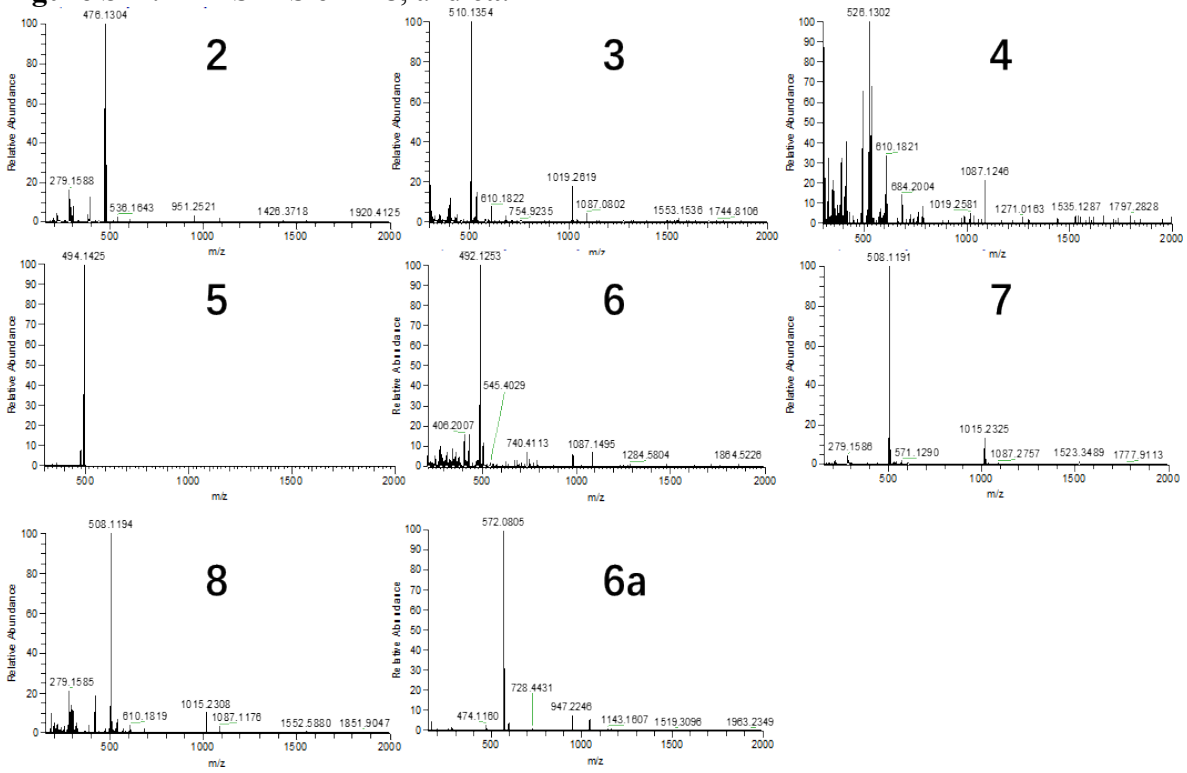

Figure S12. Experimental ECD spectra of **1**−**9.**

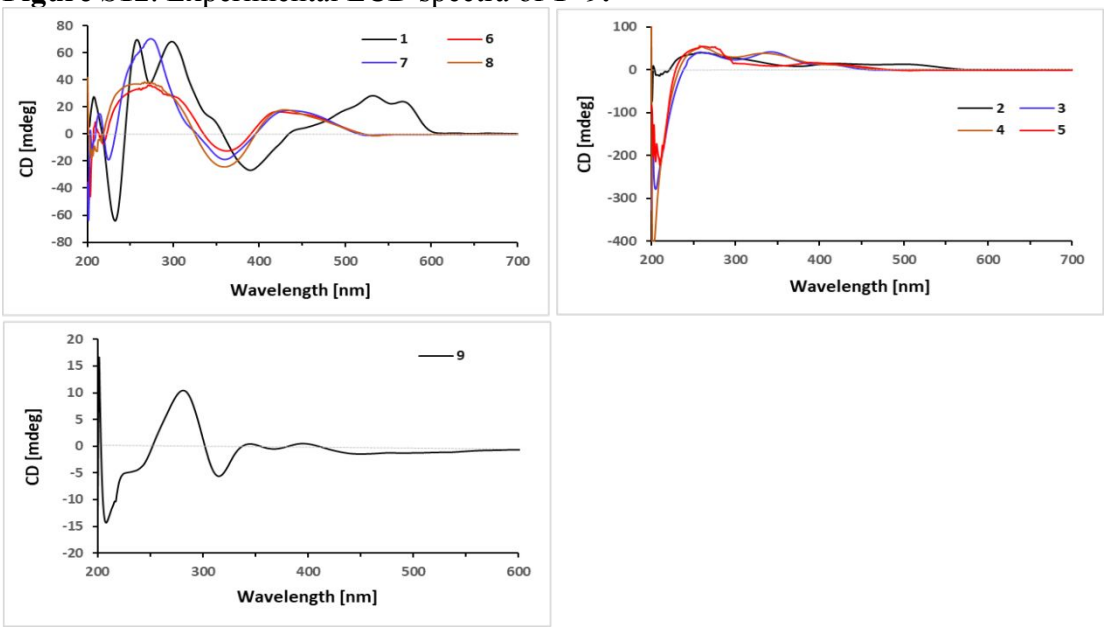

Figure S13: DFT optimized low energy conformations of **1** and **9**.

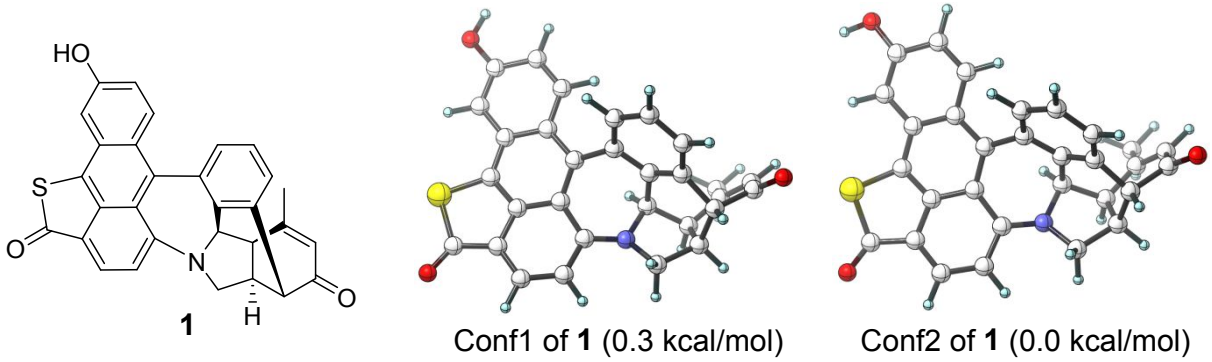

At M06-2X/6-311++G(2d,p)/SMD(MeOH)//M06-2X/6-31G(d) /SMD(MeOH) level

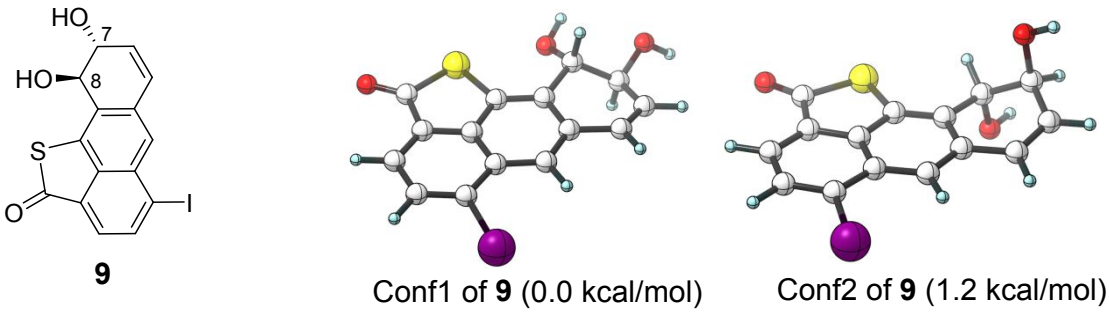

At M06-2X/SDD for iodine and 6-311++G(2d,p) for others/SMD(water) //ωB97X-D/def2tzvp/SMD(water) level

Two conformations of **9** were generated via envelop conformational interconversion of the six-membered ring containing C7 and C8. As a result, O7 and O8 were either both in the equatorial positions (conf.1) or both in the axial positions (conf.2)

Figure S14. Experimental and calculated ECD spectra of **1** (at B3LYP/def2tzvp/SMD(MeOH) level) and **9** (at B3LYP/def2tzvp/SMD(water) level).

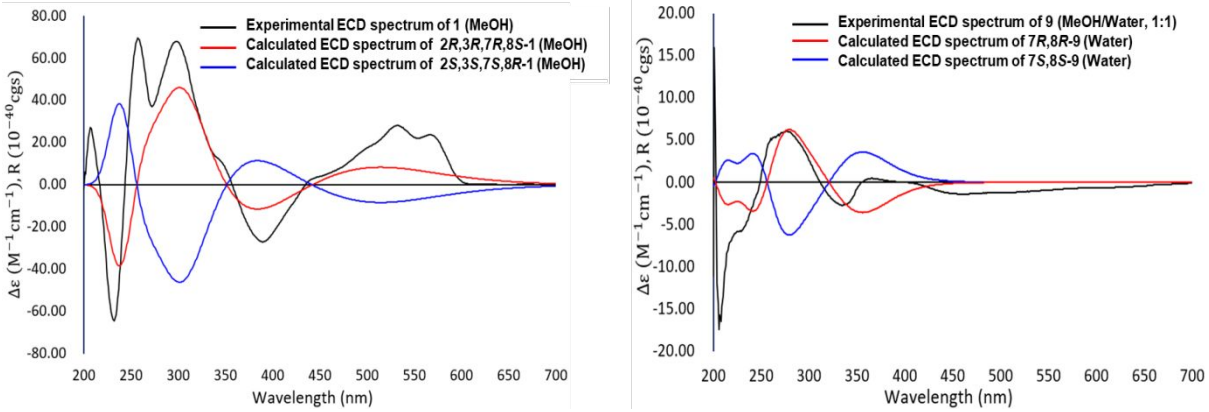

Figure S15: XYZ coordinates of the optimized structures of **1** and **9**.

1-Conf1	X	Y	Z	**1**-Conf2	X	Y	Z
C	3.778952	3.385762	0.414396	C	3.781209	3.385061	0.412511
H	5.113849	1.739455	0.557491	H	5.113638	1.728953	0.555279
C	4.083942	2.050440	0.406919	C	4.085026	2.050189	0.408675
C	1.439193	2.912707	0.038040	C	1.439649	2.917384	0.047012
C	3.060635	1.082679	0.215965	C	3.058271	1.082686	0.221109
C	2.434157	3.823226	0.237610	C	2.435999	3.825635	0.241477
C	1.697572	1.505284	0.014124	C	1.695916	1.507613	0.021960
C	3.317855	-0.292245	0.156371	C	3.315009	-0.291102	0.159177
H	2.214424	4.886938	0.277589	H	2.230040	4.890455	0.283117
C	2.278458	-1.211854	0.034737	C	2.274989	-1.210670	0.034874
C	2.687994	-2.560225	-0.126417	C	2.684461	-2.558319	-0.129963
C	0.912833	-0.817900	-0.018722	C	0.910272	-0.815677	-0.017553
C	0.644275	0.571542	-0.170505	C	0.642610	0.575525	-0.164292
C	1.740661	-3.544249	-0.380692	C	1.737065	-3.541502	-0.387841
H	2.054623	-4.569545	-0.558575	H	2.050775	-4.566272	-0.569045
C	0.387952	-3.226724	-0.355354	C	0.384792	-3.223200	-0.362081
H	-0.351898	-4.013278	-0.457310	H	-0.355498	-4.008907	-0.467321
C	-0.049296	-1.922537	-0.037636	C	-0.052100	-1.919602	-0.040582
S	4.891291	-1.090167	0.157144	S	4.888297	-1.089768	0.157926
C	4.121962	-2.732527	-0.089422	C	4.118383	-2.731168	-0.093325
O	4.789671	-3.745794	-0.202142	O	4.785865	-3.744104	-0.208850
O	4.780560	4.280353	0.605390	O	4.703215	4.363384	0.585690
H	4.423824	5.184622	0.603660	H	5.585616	3.970385	0.700452
C	-0.647017	1.004757	-0.776920	C	-0.648455	1.010628	-0.770420
C	-2.982661	1.176142	-2.325607	C	-2.982471	1.187058	-2.321235
C	-0.664511	1.765167	-1.956851	C	-0.664821	1.774927	-1.947852
C	-1.846992	0.440117	-0.339950	C	-1.848887	0.444270	-0.336846
C	-2.977267	0.412497	-1.161169	C	-2.978192	0.419268	-1.159519
C	-1.837718	1.883347	-2.696107	C	-1.837234	1.895693	-2.687954
H	0.254003	2.212078	-2.326087	H	0.253984	2.223228	-2.314658
H	-1.838537	2.471250	-3.608811	H	-1.837091	2.486904	-3.598523
H	-3.866767	1.188276	-2.958493	H	-3.865906	1.201334	-2.955025
N	-1.334460	-1.721756	0.323639	N	-1.337596	-1.720080	0.320286

C	-1.782906	-0.443312	0.869256	C	-1.786511	-0.443313	0.869381
H	-1.078507	-0.076606	1.618665	H	-1.083046	-0.079260	1.620988
C	-2.510430	-2.469975	-0.176950	C	-2.512830	-2.466818	-0.184009
H	-2.432935	-2.616724	-1.260014	H	-2.433996	-2.610471	-1.267395
H	-2.571802	-3.448949	0.307582	H	-2.574865	-3.447213	0.297596
C	-3.710022	-1.584473	0.233484	C	-3.712842	-1.582528	0.227440
H	-4.574543	-2.201616	0.490368	H	-4.577811	-2.200363	0.481163
C	-3.154334	-0.824574	1.441520	C	-3.158788	-0.826389	1.438606
H	-2.975910	-1.510612	2.278208	H	-2.981460	-1.515124	2.273311
C	-4.009950	0.314338	1.933729	C	-4.015443	0.310690	1.933246
C	-4.134178	-0.514717	-0.795742	C	-4.135436	-0.509492	-0.799021
C	-5.222826	0.370715	-0.201107	C	-5.225403	0.373392	-0.203081
C	-5.003523	0.818443	1.181279	C	-5.008170	0.816823	1.181037
H	-5.658045	1.601743	1.555449	H	-5.663616	1.598543	1.556877
H	-4.531763	-0.970508	-1.707247	H	-4.531311	-0.962457	-1.712682
O	-6.165347	0.762129	-0.875338	O	-6.167451	0.766092	-0.877222
C	-3.706049	0.821020	3.308293	C	-3.713954	0.812870	3.310007
H	-4.360842	1.649163	3.588359	H	-4.369429	1.639924	3.591681
H	-2.664236	1.161596	3.359893	H	-2.672335	1.153563	3.364565
H	-3.811388	0.015106	4.043955	H	-3.820434	0.004484	4.042789
H	0.417376	3.261834	-0.067175	H	0.417466	3.266569	-0.054566

9-Conf1	X	Y	Z	**9**-Conf2	X	Y	Z
C	-2.018968	-0.377437	-0.122105	C	2.076261	-0.378165	-0.142022
C	-1.514390	0.888675	-0.060101	C	1.580795	0.886717	-0.057759
C	0.262935	-1.267313	-0.086102	C	-0.206978	-1.248104	-0.127432
C	-0.114470	1.100281	-0.009194	C	0.189811	1.117066	0.000124
C	-1.091018	-1.471134	-0.128326	C	1.147751	-1.463914	-0.171319
C	0.801363	0.038504	-0.023777	C	-0.733009	0.062164	-0.037627
C	0.293323	2.437107	0.030626	C	-0.194500	2.457993	0.090050
H	0.923607	-2.124302	-0.096362	H	-0.877057	-2.097602	-0.152750
C	1.626088	2.757430	0.069432	C	-1.522494	2.793239	0.146037
H	1.953756	3.788663	0.097490	H	-1.839909	3.825681	0.214552
C	2.567629	1.719021	0.067587	C	-2.475634	1.763693	0.111967
H	3.619617	1.966261	0.099352	H	-3.524209	2.023271	0.156057
C	2.173649	0.398706	0.020510	C	-2.101407	0.439918	0.024170
I	3.667290	-1.066870	0.013707	I	-3.612321	-1.005606	-0.009401
C	-0.842760	3.367056	0.005749	C	0.957049	3.371956	0.110259
S	-2.365207	2.438885	-0.062764	S	2.470003	2.406838	-0.012089
O	-0.811667	4.578020	0.028317	O	0.955055	4.575868	0.190239
C	-3.483557	-0.696213	-0.289830	C	3.548459	-0.662758	-0.283062
H	-3.657152	-0.836854	-1.367056	H	4.124364	0.106391	0.242084
C	-3.874985	-1.999693	0.393087	C	3.947699	-2.010995	0.314466
H	-3.879559	-1.830193	1.478016	H	4.930801	-2.267261	-0.094469
C	-1.621551	-2.835740	-0.167113	C	1.676754	-2.828287	-0.220763
H	-0.915895	-3.637077	-0.351719	H	0.965624	-3.625444	-0.404834
C	-2.903469	-3.093916	0.067049	C	2.962087	-3.096957	-0.011207
H	-3.280103	-4.110300	0.078242	H	3.322276	-4.118669	-0.020362
O	-4.263382	0.379079	0.184328	O	3.836032	-0.622014	-1.674555
H	-5.163562	0.255117	-0.129251	H	4.789820	-0.688542	-1.785571
O	-5.191064	-2.301918	-0.045545	O	4.052222	-1.818248	1.724586
H	-5.553785	-2.982836	0.527279	H	4.178951	-2.676356	2.139487

Figure S16: Feeding of compound **9** into the MD118A and Δ*sgdX2* culture did not result in the production of sungeidines. The experimental conditions are described in the methods section.

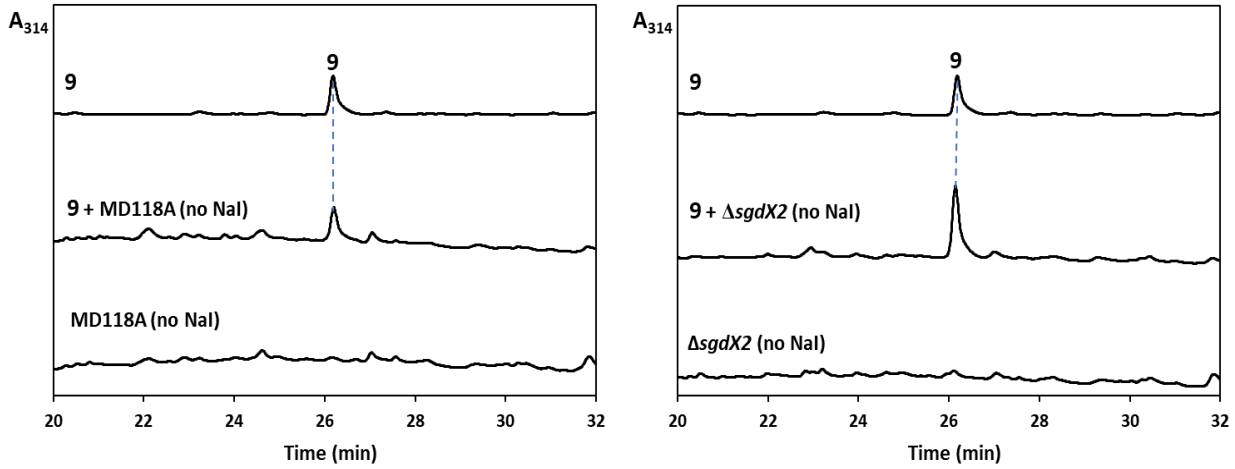

Figure S17: SDS-PAGE analysis the expression and purification of SgdX2 using *E. coli* Rosetta (DE3). The DNA Marker is Thermo Scientific PageRuler Plus Prestained Protein Ladder #26619.

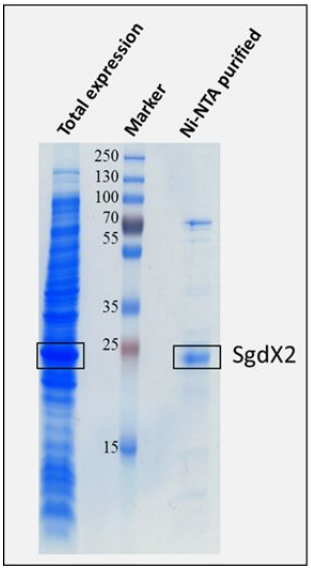

References

1. Low, Z. J.; Pang, L. M.; Ding, Y.; Cheang, Q. W.; Le Mai Hoang, K.; Thi Tran, H.; Li, J.; Liu, X.-W.; Kanagasundaram, Y.; Yang, L.; Liang, Z.-X., Identification of a biosynthetic gene cluster for the polyene macrolactam sceliphrolactam in a *Streptomyces* strain isolated from mangrove sediment. *Sci. Rep.* **2018**, *8*, 1594.
2. Muth, G.; Farr, M.; Hartmann, V.; Wohlleben, W., *Streptomyces ghanaensis* plasmid pSG5: nucleotide sequence analysis of the self-transmissible minimal replicon and characterization of the replication mode. *Plasmid* **1995**, *33*, 113−126.
3. Mahan, S. D.; Ireton, G. C.; Stoddard, B. L.; Black, M. E., Alanine-Scanning Mutagenesis Reveals a Cytosine Deaminase Mutant with Altered Substrate Preference. *Biochemistry* **2004**, *43*, 8957−8964.
4. Dubeau, M.-P.; Ghinet, M. G.; Jacques, P.-É.; Clermont, N.; Beaulieu, C.; Brzezinski, R., Cytosine Deaminase as a Negative Selection Marker for Gene Disruption and Replacement in the Genus Streptomyces and Other Actinobacteria. *Appl. Environ. Microbiol.* **2009**, *75*, 1211−1214.
5. Zeng, H.; Wen, S.; Xu, W.; He, Z.; Zhai, G.; Liu, Y.; Deng, Z.; Sun, Y., Highly efficient editing of the actinorhodin polyketide chain length factor gene in Streptomyces coelicolor M145 using CRISPR/Cas9-CodA(sm) combined system. *Appl. Microbiol. Biotechnol.* **2015**, 1−11.
6. Lamb, S. S.; Patel, T.; Koteva, K. P.; Wright, G. D., Biosynthesis of sulfated glycopeptide antibiotics by using the sulfotransferase StaL. *Chem. biol.* **2006**, *13*, 171−181.
7. Cohen, D. R.; Townsend, C. A., Characterization of an Anthracene Intermediate in Dynemicin Biosynthesis. *Angew. Chem. Int. Edi.* **2018**, *57*, 5650−5654.
8. Xiong, J.; Meng, W.-J.; Zhang, H.-Y.; Zou, Y.; Wang, W.-W.; Wang, X.-Y.; Yang, Q.-L.; Osman, E. E. A.; Hu, J.-F., Lycofargesiines A-F, further *Lycopodium* alkaloids from the club moss *Huperzia fargesii*. *Phytochemistry* **2019**, *162*, 183−192.
9. Tang, Y.; Li, N.; Zou, Y.; Ai, Y.; Ma, G.-L.; Osman, E. E. A.; Xiong, J.; Li, J.; Jin, Z.-X.; Hu, J.-F., LC-MS guided isolation and dereplication of *Lycopodium* alkaloids from *Lycopodium cernuum* var. *sikkimense* of different geographical origins. *Phytochemistry* **2019**, *160*, 25−30.
10. Hensens, O. D.; Giner, J. L.; Goldberg, I. H., Biosynthesis of NCS Chrom A, the chromophore of the antitumor antibiotic neocarzinostatin. *J. Am. Chem. Soc.* **1989**, 111, (9), 3295−3299.
11. Tokiwa, Y.; Miyoshi-Saitoh, M.; Kobayashi, H.; Sunaga, R.; Konishi, M.; Oki, T.; Iwasaki, S., Biosynthesis of dynemicin A, a 3-ene-1,5-diyne antitumor antibiotic. *J. Am. Chem. Soc.* **1992**, *114*, 4107−4110.
12. Lam, K. S.; Veitch, J. A.; Golik, J.; Krishnan, B.; Klohr, S. E.; Volk, K. J.; Forenza, S.; Doyle, T. W., Biosynthesis of esperamicin A1, an enediyne antitumor antibiotic. *J. Am. Chem. Soc.* **1993**, *115*, 12340−12345.
13. Cohen, D. R.; Townsend, C. A., A dual role for a polyketide synthase in dynemicin enediyne and anthraquinone biosynthesis. *Nat. Chem.* **2018**, *10*, 231−236.
14. Gaussian 09, Revision A.02, Frisch, M. J.; Trucks, G. W.; Schlegel, H. B.; Scuseria, G. E.; Robb, M. A.; Cheeseman, J. R.; Scalmani, G.; Barone, V.; Petersson, G. A.; Nakatsuji, H.; Li, X.; Caricato, M.; Marenich, A., Bloino, J.; Janesko, B. G.; Gomperts, R.; Mennucci, B.; Hratchian, H. P.; Ortiz, J. V.; Izmaylov, A. F.; Sonnenberg, J. L.; Williams-Young, D.; Ding, F.; Lipparini, F.; Egidi, F.; Goings, J.; Peng, B.; Petrone, A.; Henderson, T.; Ranasinghe, D.; Zakrzewski, V. G.; Gao, J.; Rega, N.; Zheng, G.; Liang, W.; Hada, M.; Ehara, M.; Toyota, K.; Fukuda, R.; Hasegawa, J.; Ishida, M.; Nakajima, T.; Honda, Y.; Kitao, O.; Nakai, H.; Vreven, T.; Throssell, K.; Montgomery, J. A.; Jr., Peralta, J. E.; Ogliaro, F.; Bearpark, M.; Heyd, J. J.; Brothers, E.; Kudin, K. N.; Staroverov, V. N.; Keith, T.; Kobayashi, R.; Normand, J.; Raghavachari, K.; Rendell, A.; Burant, J. C.; Iyengar, S. S.; Tomasi, J.; Cossi, M.; Millam, J. M.; Klene, M.; Adamo, C.; Cammi, R.; Ochterski, J. W.; Martin, R. L.; Morokuma, K.; Farkas, O.; Foresman, J. B., Fox, D. J. Gaussian, Inc., Wallingford CT, 2016.